Screening and characterization of novel genes involved in the embryogenesis of *Xenopus laevis*

Inaugural-Dissertation

zur
Erlangung des Doktorgrades
Dr.rer.nat.

des Fachbereiches
Bio- und Geowissenschaften,
Landschaftsarchitektur

an der
Universität Essen

vorgelegt von

Ying Cao
aus Jiangsu, China

April 2002

Dedicated to the memory of my mother

Die der vorliegenden Arbeit zugrundeliegenden Experimente wurden in der Abteilung für Zoophysiologie der Universität Essen durchgeführt.

1. Gutachter: Prof. Dr. H. Grunz,
FB9 (Biology), Universität Essen

2. Gutachter: Prof. Dr. G. Ryffel,
Uniklinikum Essen

3. Gutachter:

Vorsitzender des Prüfungsausschusses: Prof. Dr. H. Esche,
Uniklinikum Essen

Tag der mündlichen Prüfung: 02/07/2002

CONTENTS

ABBREVIATIONS

The amino acids

A;(Ala)	Alanine
C;(Cys)	Cysteine
D;(Asp)	Aspartic acid
E;(Glu)	Glutemate
F;(Phe)	Phenylalanine
G;(Gly)	Glycine
H;(His)	Histidine
I;(Ile)	Isoleucine
K;(Lys)	Lysine
L;(Leu)	Leucine
M;(Met)	Methionine
N;(Asn)	Asparagine
P;(Pro)	Proline
Q;(Gln)	Glutamine
R;(Arg)	Arginine
S;(Ser)	Serine
T;(Thr)	Threonine
V;(Val)	Valine
W;(Trp)	Tryptophan
Y;(Try)	Tyrosine

Other abbreviations

A	adenosine
APS	ammonium peroxydisulphate
ATP	adenosine 5’-triphosphate
BCIP	5-bromo-4-chloro-3-indolyl phosphate
bp	base pair
BSA	bovine serum albumin
C	cytidine
°C	degree Celsius

cat.no.	catalogue number
cDNA	complementary DNA
CHAPS	3-[(-cholamidopropyl)dimethylammonio]-1-propansulphate
CTP	cytidine 5'-triphosphate
Da	Dalton
dATP	deoxyadenosine 5'-triphosphate
dCTP	deoxycytidine 5'-triphosphate
DEPC	diethyl pyrocarbonate
dGTP	deoxyguanosine 5'-triphosphate
DMSO	dimethyl sulfoxide
DNA	deoxyribonucleic acid
DNase	deoxyribonuclease
dNTP	deoxynucleotide 5'-triphosphate
ds	double strand
DTT	dithiothreitol
dTTP	deoxythymidine 5'-triphosphate
EDTA	ethylene-diamine tetra-acetate
EGTA	ethylene-glycol-bis(2-aminoethylether)-N,N'-tetra-acetate
EtBr	ethidium bromide
FA	formaldehyde
g	gram
G	guanosine
GTP	guanosine 5'-triphosphate
h, hr, hrs	hour, hours
HEPES	N-(2-hyhroxyethyl)piperazine-N'-2-ethane sulfonic acid
IU	international unit
k	kilo
l	liter
LB	Luria-Bertani culture medium
m	milli
M	molar
mg	milligram
min	minute

mm	millimeter
ml	milliliter
MOPS	3-(N-morpholino)propanesulfonic acid
mRNA	messenger ribonucleic acid
μg	microgram
μl	microliter
NBT	nitro-blue-tetrazolium
ng	nanogram
nl	nanoliter
OD	optical density
PBS	phosphate buffered saline solution
PCR	polymerase chain reaction
pg	picogram
poly(A)$^+$	polyadenylated
PVP	polyvinylpyrrolidone
RACE	rapid amplification of cDNA ends
RE	restriction endonuclease
RNA	ribonucleic acid
RNAse	ribonuclease
rpm	round per minute
rRNA	ribosomal ribonucleic acid
RT	room temperature, reverse transcription
RT-PCR	reverse transcription-polymerase chain reaction
sec	second
ss	single stranded
SDS	sodium dodecylsulphate
T	thymine
Tet	tetracycline
Tris	trishydroxymethylaminomethane
U	unit of enzymatic activity
UV	ultraviolet light
X-gal	5-bromo-4-chloro-3-indolyl-β-D-galactopyranoside

1. INTRODUCTION

The study on developmental biology is largely dependent on a feasible model system. For the study on embryonic development of vertebrates, the African clawed frog (*Xenopus laevis*) is favored because of a few reasons. Large number of eggs (around 1,500 per female) can be obtained and *in vitro* fertilization can be easily conducted without seasonal limitation. The large size (1-2 mm in diameter) of embryos facilitates delicate embryological manipulations, such as preparation of explants. Another attractive trait is rapid embryonic development (Fig.1.1). However, as a working model its advantage is also compromised because about 2-3 years is generally required for the frogs to reach sexual maturity, which is too long for genetic study. The allotetraploidy of *Xenopus laevis* makes another disadvantage, as gene knockout is difficult to perform in tetraploid organisms. For these reasons, *Xenopus tropicalis* has been selected recently as an alternative for genetic manipulations.

1.1 A molecular sketch of *Xenopus* early embryonic development

1.1.1 β-catenin and the establishment of early dorsal axis

Embryonic development involves astonishingly complex biochemical procedures. Great progress has been achieved towards disentangling these procedures. The unfertilized egg of *Xenopus laevis* is polarized along its animal-vegetal axis, though radially symmetrical. Such a radial symmetry along animal-vegetal axis, however, is broken upon fertilization because cortical cytoplasm is driven by microtubules to rotate an average of 30 degree during the first cell cycle (Vincent and Gerhart, 1987). As a consequence, the dorsal side of the embryo forms in the animal region approximately opposite to the random point of sperm entry (Fig.1.1). And the so-called Nieuwkoop signaling center is also

formed in the dorsal side of the vegetal region (Nieuwkoop, 1952; Nieuwkoop, 1973). Molecular events for early dorsal axis establishment have been proposed

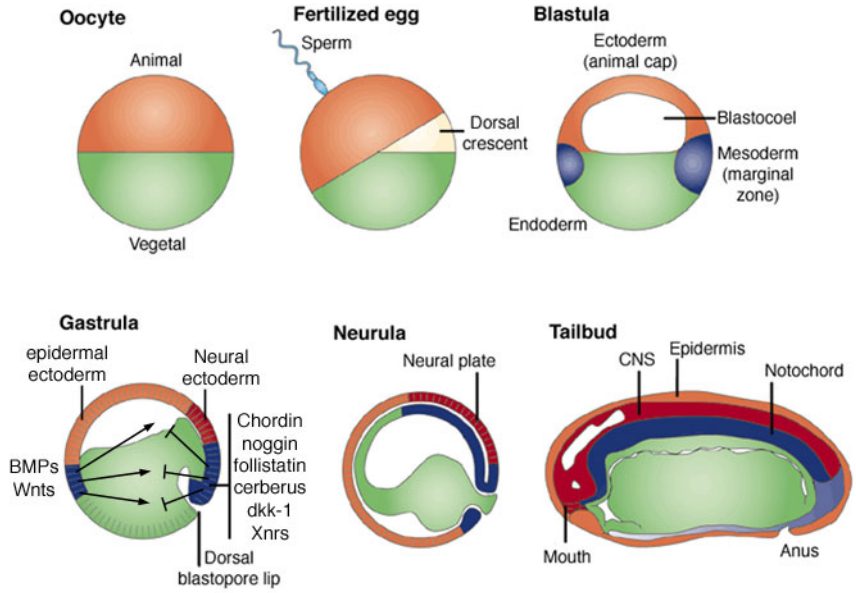

Fig.1.1 The development of *Xenopus*. The ovarian oocyte is radially symmetrical and is divided into an animal and a vegetal domain. One hour after fertilization, an unpigmented dorsal crescent is formed in the fertilized egg opposite the sperm entry point. As the embryo rapidly di-vides into smaller and smaller cells, without intervening growth (cleavage), a cavity called the blastocoel is formed, which defines the blastula stage. By the late blastula stage (9h of development), the three germ layers become defined. The ectoderm, or animal cap, forms the roof of the blastocoel. The mesoderm is formed in a ring of cells in the marginal zone, located between the ectoderm and endoderm. At the gastrula stage (10 h), involution of the mesoderm towards the inside of the embryo starts at the dorsal blastopore lip. The morphogenetic movements of gastrulation lead to the formation of the vertebrate body plan, patterning the ectoderm, mesoderm and endoderm. At the neurula stage (14 h), the neural plate, or future central nervous system (CNS), becomes visible in dorsal ectoderm. By the tailbud stage (24-42 h), a larva with a neural tube located between the epidermis and the notochord has formed. The blastopore gives rise to the anus, and the mouth is generated by secondary perforation (modified from De Robertis et al., 2000). CNS, central nervous system.

(Moon and Kimelman, 1998; De Robertis et al., 2000), in which β-catenin seems to play the key role. β-catenin is present in the eggs of *Xenopus* and early embryos (DeMarais and Moon, 1992; Fagotto and Gumbiner, 1994). The importance of β-catenin in dorsal axis determination resides in that its overexpression mimics the dorsal inducing activity and thus induces a complete secondary axis (Guger and Gumbiner, 1995; Kelly et al., 1995), while loss-of-function analyses reveal that the formation of embryonic endogenous axis is blocked (Heasman et al., 1994; Heasman et al., 2000). In addition, immunostaining studies show that β-catenin is enriched in nuclei on the dorsal side of the embryos during cleavage and blastula stages (Schneider et al., 1996; Larabell et al., 1997). These lines of evidence indicate that β-catenin is the first

component of a signaling pathway shown to be required for endogenous dorsal axis formation and dorsalizes the three germ layers.

Dorsal accumulation and nuclear localization of β-catenin protein is correlated with the activation of maternal Wnt signaling pathway on the dorsal side. In the absence of Wnt, β-catenin is phosphorylated, by glycogen synthase kinase 3β (GSK-3) via formation of complex with adenomatous polyposis coli (APC) tumor suppressor protein, resulting in the degradation of β-catenin (Yost et al., 1996). While when Wnt binds to the frizzled receptor, disheveled (Dsh) is activated. Activation of Dsh results in the inhibition of GSK-3, hence the stabilization and enrichment of β-catenin. As β-catenin accumulates, it is translocated to the nuclei and forms complexes with transcription factor Lef/Tcf-3, which lead to the regulation of target genes such as *siamois*, *twin* and *Xnr3* (Moon and Kimelman, 1998). Subsequently, these genes activate transcription of early genes in the Spemann-Mangold organizer.

1.1.2 The three germ layers

The basic body plan in almost all metazoans is derived from the three germ layers, endoderm, mesoderm and ectoderm. Induction and patterning of the germ layers have also been described in somewhat details in *Xenopus*. The endoderm arises from blastomeres in the vegetal region during early cleavage stages (Fig.1.1). The organs such as gastrointestinal and respiratory tracts, liver, and pancreas originate from this germ layer (Wells and Melton, 1999; Chalmers and Slack, 2000). A two-step molecular model was proposed for endoderm formation (Yasuo and Lemaire, 1999; Yasuo and Lemaire, 2001). First, maternal factors, primarily VegT (Lustig et al., 1996; Zhang and King, 1996; Horb and Thomsen, 1997; Xanthos et al., 2001; Engleka et al., 2001) activate cell-autonomous expression of endoderm-specific genes encoding transcription factors such as Xsox17α (Hudson et al., 1997; Clements and Woodland, 2000) and Mix.1 (Rosa, 1989; Lemaire et al., 1998) and other proteins of TGF-β family, such as Xnr-1, 2, and 4, Activin B and Derriere (Clements et al., 1999; Yasuo and Lemaire, 1999; Sun et al., 1999). Second, zygotically expressed Xnr-1, Xnr-2, Derriere, and possibly other TGF-β factors subsequently activate the zygotic expression of *Mixer* (Henry and Melton, 1998) and *GATA-4*. Further,

expression of *Xsox17α*, *Mix.1*, *Xnr-1* and *Xnr-2*, which involve in the formation of endoderm, are upregulated (Yasuo and Lemaire, 1999).

Mesoderm is formed in the equatorial marginal zone of *Xenopus* blastula (Fig.1.1), and fated to form head mesoderm, notochord, somites in the dorsal side, and blood cells and also somites in the ventral side. It is believed that three signals (Dale and Jones, 1999; Chan and Etkin, 2001) or sometimes called two signals (De Robertis et al., 2000) work sequentially to execute the task. The first signal emits from the ventral endoderm to induce ventral mesoderm. While a small dorsal part of endoderm, i.e., the Nieuwkoop center, releases a second signal to induce dorsal mesoderm, i.e., the Spemann-Mangold organizer tissue. Finally, the organizer gives out the third signal to pattern the initial mesoderm. The organizer itself differentiates into notochord, prechordal mesoderm, floorplate and dorsal endoderm. Growth factors of the TGF-β or FGF families, including activins A, B, and D, Vg1, Xnr-1, 2, and 4, and BMP2, 4, and 7, mimic the mesoderm-inducing signals and therefore are able to induce mesoderm in animal cap explant experiments (Kimelman et al., 1992; Harland and Gerhart, 1997). Amongst these factors, only Vg1 is considered a suitable candidate for mesoderm inducer, because it is maternally encoded and localized to the vegetal region. A processed form of Vg1 induces mesoderm and endoderm in animal cap assays. When it is inhibited by dominant-negative ligands, both dorsal mesoderm and endoderm formation are disrupted, suggesting the role of Vg1 in mesoderm induction (Dale et al., 1993; Thomsen and Melton, 1993; Kessler and Melton, 1995; Joseph and Melton, 1998). However, it is not completely convincing since the wild type Vg1 has no mesoderm inducing activity. The idea that TGF-β and FGF factors are responsible for mesoderm induction has been partially revised recently by the observation that mesoderm induction is dependent on the T-box transcription activator VegT (Zhang et al., 1998; Kimelman and Griffin, 1998). *VegT* is also maternally transcribed and the translated products are localized to vegetal hemisphere of cleaving embryos (Stennard et al., 1999). Convincing evidence has shown the central role of VegT in forming mesoderm and endoderm germ layers (Zhang et al., 1998; Kofron et al., 1999).

Ectoderm is derived from the cells in the animal region. Dorsal ectoderm

close to the organizer develops into neural folds, from which the central nervous system is derived, while ventral ectoderm develops into epidermis (Fig.1.1). At the boundary between neural folds and epidermis, cement gland, various placodes and neural crest are formed. It has been shown that, by ectoderm dissociation experiments, the default state of ectoderm is neural (Grunz and Tacke, 1989; Grunz and Tacke, 1990; Hemmati-Brivanlou and Melton, 1997). Further evidence shows that BMP-4 plays the key role to prevent neural development in the ectoderm (Wilson and Hemmati-Brivanlou, 1995). Dorsal ectoderm is induced to adopt a neural fate by dorsalizing activities of factors in the organizer, such as Chordin, noggin, follistatin, Xnr-3, Cerberus and dkk-1. Chordin, noggin, follistatin and Xnr-3 are antagonists of BMP-4 (Piccolo et al., 1996; Zimmerman et al., 1996; Iemura et al., 1998; Hansen et al., 1997), while Cerberus and dkk-1 are antagonists of Wnt (Piccolo et al., 1999; Glinka et al., 1998). Therefore, repression of BMP or Wnt signaling leads to neural induction in the ectoderm. It is also shown that FGF signaling is involved in anterior neural induction (Hongo et al., 1999). Briefly, the dorsal ectoderm absent of BMP and Wnt pathway adopts a neural fate, while the ventral ectoderm with active BMP and Wnt signaling differentiates into epidermis.

1.1.3 Spemann-Mangold organizer

The most significant event in developmental biology is of course the discovery of the “organizer” by Spemann and Mangold. A small piece of tissue in gastrulae, the dorsal lip of blastopore, is able to pattern an early embryo with distinct anterior-posterior, dorsal-ventral and left-right axes. When transplanted to a heterotopic location of a recipient embryo, the dorsal lip can induce a complete secondary body axis, hence the name “organizer”. Formation of the organizer has been extensively reviewed (Harland and Gerhart, 1997; Nieto, 1999; De Robertis et al., 2000; Bouwmeester, 2001). It can be traced back to the dorsal stabilization of β-catenin during early cleavage. Subsequently after midblastula transition (MBT), the β-catenin signal, in combination with other maternal genes including *Vg1* and *VegT*, activates a dorsal-ventral gradient of Nodal related signals (Xnr) in the endoderm. In turn, this gradient induces the formation of mesoderm: low doses of Xnrs in ventral side induce ventral

mesoderm, while high doses in the dorsal side lead to the formation of organizer.

The axis inducing activities by the organizer have been elucidated at the molecular level. It has been revealed by molecular studies that the organizer is indeed an enrichment of secreted antagonists of growth factors, including Chordin, noggin, follistatin, ADMP, Crescent, shh, Xnrs, cerberus, Lefty, Antivin, Frzb-1 and dkk-1 (De Robertis et al., 2000). It also harbors many nuclear factors, such as Gsc, Xlim-1, HNF-3β, Xnot, Xanf-1, Otx-2, Siamois, Xtwn, Iro3, and *bozozok* (De Robertis et al., 2001). Amongst these secreted proteins, Chordin, noggin and follistatin act as antagonists against BMP4 by direct binding (Piccolo et al., 1996; Zimmerman et al., 1996; Fainsod et al., 1997). Crescent, Frzb-1 and dkk-1 antagonize Wnt (Wang et al., 1997; Pera and De Robertis, 2000; Glinka et al., 1998). Cerberus is a multivalent antagonist for Wnt-8, Xnrs and BMPs (Bouwmeester et al., 1996; Piccolo et al., 1999; Fig.1.1). Lefty/Antivin blocks nodal signaling by binding to TGF-β/Nodal receptor (Meno et al., 1996; Thisse and Thisse, 1999).

In addition to self-differentiation of the organizer as aforementioned, the principal proposed functions are body axis patterning, neural induction of the ectoderm, and morphogenesis (Harland and Gerhart, 1997; Bouwmeester, 2001). First, the organizer reveals a function in dorsal-ventral patterning. Ventral overexpression of mRNAs for Chordin, noggin and follistatin results in the formation of twinned axes, an effect reminiscent of organizer grafting experiments. These factors function as agonists of ventral cell fates, which are specified by BMP4. Such a dorsalization of ventral mesoderm by these proteins has led to the proposal that BMP antagonism is the main inductive activity of the "trunk organizer". Second, the "head organizer" patterns the anterior-posterior axis as it expresses secreted factors, Cerberus, dkk-1 and Frzb-1. These factors are expressed in the dorsoanterior endoderm and prechordal plate, and antagonize Wnt glycoproteins. Combinatorial expression of Wnt antagonists together with BMP antagonists leads to secondary axis with head structures (Glinka et al., 1997; Glinka et al., 1998; Piccolo et al., 1999). Third, in addition to the function as dorsalizing factors, Chordin, noggin and follistatin also act as neural inducers. Based on the neural default model, the ectoderm has a natural

tendency to differentiate into neural tissue (Hemmati-Brivanlou and Melton, 1997). This tendency is inhibited, however, by BMP signaling. The ectoderm with active BMP signaling differentiates into epidermis. Chordin, noggin and follistatin can disable BMP signaling via direct ligand binding. Therefore, the ectoderm free of BMP signaling will be neural, from which future nervous system will be derived. Finally, the organizer also controls some of the complex morphogenetic movements (Harland and Gerhard, 1997; Bouwmeester, 2001). The first reason should be that extensive morphogenesis is necessary to bring the organizer to the vicinity of other tissue so that the organizer's inducers can reach the distant targets. Some, nevertheless not all, morphogenetic movements are dependent on the organizer, i.e., the movement of the organizer itself and thus induced movement of neighboring tissues, in particular the somitic mesoderm. Anterior organizer cells perform a spreading migration. The posterior organizer cells, and the somites which are induced from lateral-ventral mesoderm by organizer signals, engage in convergent extension.

Once the germlayers are formed and body axes are established, embryos will proceed to organogenesis, thus a free-swimming larva of *Xenopus laevis* comes into entity.

1.2 The objective of this research

Last year the most celebrated event in biology was the announcement of the completion of human genome sequencing. The deciphering of genomic genetic codes of human and many other organisms makes some think that it is time to understand how an organism is built. This is apparently a great leap towards this goal but still far from it. Because the single words in the tome of genome are recognized, and herculean efforts are required to compile words into meaningful sentences and paragraphs, that is to say, to probe gene functions and crossregulation between genes during life cycles. If for embryogenesis, it is exactly the objective of modern developmental biology. In the case of amphibians including *Xenopus laevis*, some 50,000 genes are estimated to participate in embryonic development (Wolpert et al., 1998). Albeit many key molecules in *Xenopus* development have been characterized and to some extent the framework of early embryogenesis has been established as outlined above,

the major part of the genes have yet to be discovered and functionally analyzed. To achieve this goal, a variety of approaches have been developed. One simple way is to identify genes in homology with those well described in the embryogenesis of other organisms, such as *Drosophila* and mice. This is a valuable approach to investigate whether or not the functions of these genes are conserved through invertebrate to vertebrate. Or in most other cases, genes are identified from cDNA libraries constructed from specific stages or tissues, for example oocytes (I. Dawid, D. Melton) (names indicating group leaders), eggs (M. King), embryos at different stages (I. Dawid, M. King, P. Lemaire, C. Kintner, T. Pieler), LiCl-dorsalized embryos (P. Lemaire, C. Niehrs), dorsal blastopore lip (E.M. De Robertis), or induced pronephros (M. Asashima), etc. Research works with these libraries have been leading to the identification of many genes that improve profoundly our knowledge of embryogenesis. The highlighted events may be the discovery of genes in the Spemann-Mangold organizer from a dorsal blastopore lip library (Bouwmeester et al., 1996) and a LiCl-treated stage 13 embryo library (Glinka et al., 1998). Some strategies were also developed specifically for the isolation of genes for secreted proteins (Klein et al., 1996; Jacobs et al., 1997; Pera and De Robertis, 2000; Matsui et al., 2000; Tsuda et al., 2002), as they play key roles in cell-cell signaling. In addition, there is a strategy particularly developed for isolating genes for DNA-binding proteins (Mead et al., 1998).

A few years ago, Professor Dr. Horst Grunz proposed an idea to isolate endoderm inducing or neural inducing genes by constructing endoderm- or notochord-specific cDNA library. In order to obtain adequate amount of endoderm or notochord tissue for library construction, an *in vitro* system that was well established on the basis of earlier results was employed (Grunz, 1969; Minuth and Grunz, 1980; Grunz, 1983; Grunz and Tacke, 1989). The principle is that disaggregated animal cap cells at stage 8-9 treated with high concentration of activin will differentiate into homogeneous endoderm-like tissue or into homogeneous notochord tissue when treated with lower concentration of activin. The homogeneity of these induced tissues was confirmed with histological sections or markers, such as endoderm-specific gene *endodermin* (Sasai et al., 1996). The libraries were constructed successfully.

These led to the identification of the transcription factor XER81, which interferes with activin-mediated induction of Xegr-1 and Gsc (Chen et al., 1999), and the retinoic acid hydroxylase XCYP26, which helps to establish boundaries of retinoic acid signaling during embryogenesis (Hollemann et al, 1998). Here what will be described is the screening and characterization of three genes *XODC2*, *XCL-2* and *XETOR* from the endoderm-like cDNA library.

1.3 Calpains, XCL-2 and convergent extension movements

Calpains are intracellular nonlysosomal cysteine protease that absolutely requires Ca^{2+} for activity. There are three forms of Calpains, μ-Calpain requiring Ca^{2+} in micromole for activity *in vitro*, m-Calpain requiring Ca^{2+} in millimole, and an intermediate form identified in chicken. Both μ-Calpain and m-Calpain are heterodimers consisting of an 80 kDa large subunit and a common 30 kDa small subunit (Sorimachi et al., 1994; Arthur et al., 1995; Suzuki and Sorimachi, 1998). Calpains play a role in various pathological states, including degenerative diseases of muscle and nerve, apoptosis, hypertension, cataract formation, rheumatoid arthritis, and Alzheimer's disease. Calpain was originally discovered as an activator of phosphorylase *b* kinase (Huston and Krebs, 1968) and later identified as an activator of protein kinase C (Takai et al., 1977). Actually Calpains cleave many membrane proteins and membrane-associated proteins. There are typical Calpains with four complete domain structures and atypical Calpains generally with only protease domain. Moreover, some typical Calpains are ubiquitous while others are tissue-specific (Sorimachi et al., 1994). Calpains have been discovered in a wide spectrum of organisms from Aspergillus, yeast, nematode, *Drosophila* to chicken and human, though, their functions in embryonic development are very poorly known. The Calpain identified here, XCL-2, is a typical tissue-specific m-type Calpain large subunit. It will be shown here some lines of evidence for its role in convergent extension movements during embryonic development of *Xenopus laevis*.

Convergent extension movements are the major driving force for the process of gastrulation, neurulation and formation of body axis in *Xenopus laevis* (Keller, 1986). During gastrulation, mesoderm at the blastopore lip involutes, converges toward the dorsal midline (convergence), and at the same time

elongates along the future anterior-posterior axis (extension), thus the axial mesoderm, paraxial mesoderm as well as neural tissues are formed symmetrically (Keller and Tibbetts, 1989). Moreover, the movement is also the driving force for the closure of blastopore (Keller and Tibbetts, 1989).

Cellular basis for convergent extension movements have been more comprehensively investigated as compared to the molecular mechanism. However, there have been increasing evidences that some molecules are involved in this procedure. Among them known in somewhat more details are the second group of Xwnts, i.e., Xwnt4, Xwnt5 and Xwnt11 (Moon et al., 1993; Tada and Smith, 2000), the receptors frizzled-7 (Djiane et al., 2000), frizzled-8 (Deardorf et al., 1998) and frizzled-11 (Tada and Smith, 2000). Some Ca^{2+}-dependent proteins, such as C-cadherin, were also shown to take part in morphogenetic movements by interfering cell adhesion (Lee and Gumbiner, 1995). More recently, Disheveled signaling was shown to regulate both neural and mesodermal convergent extension (Wallingford and Harland, 2001).

In the following, it will be presented that overexpression of wild-type *XCL-2* disrupted gastrulation movement and convergent extension during gastrulation and neurulation. Moreover, overexpression of a dominant-negative mutant caused a phenotype morphologically similar to, but histologically different from, that caused by overexpression of wild-type *XCL-2*. The mutant phenotype can be rescued by injection of wild-type *XCL-2*. These data suggest that XCL-2 plays an important role in convergent extension movements during embryogenesis in *Xenopus laevis*.

1.4 ETO/MTG8/CDR, XETOR and primary neurogenesis

The proto-oncogene *ETO* (for *E*ight-*T*wenty *O*ne, also known as *MTG8* or *CDR*) encodes a protein with potent activity of transcriptional repression. *ETO* on chromosome 8 in human is often translocated to *AML1* on chromosome 21 to make a fusion transcript in acute myeloid leukemias (Feinstein et al., 1995; Melnick et al., 2000; Wang et al., 1998). AML1 contains a “Runt domain” named after the *Drosophila* gene *runt*, and its *Xenopus* homologue Xaml has been identified to play a significant role in primitive hematopoiesis, albeit it is also expressed in the sensory neurons during neural plate stage (Tracey et al.,

1998; Koyano-Nakagawa et al., 2000). So far the *ETO* coding sequence has also been revealed to be conservative through *Drosophila* to human (Feinstein et al., 1995; Kitabayashi et al., 1998). One attractive feature of these genes is that they are mainly expressed in the nervous system in different species (Feinstein et al., 1995; Wolford and Prochazka, 1998), suggesting they should be functionally conservative. But so far no functional analyses have been made for these genes during the development of nervous systems.

In *Xenopus laevis*, a primary nervous system is formed in the neural plate stage from neuroectoderm, which is induced by neuralizing signals such as noggin, Chordin and follistatin from the organizer (Saxen, 1989; Harland and Gerhart, 1997; Streit and Stern, 1999). These inducers function to induce and pattern the neural plate by antagonizing the BMPs, Wnts, and the newly identified Tiarin (Tsuda et al., 2002; Wessely and De Robertis, 2002). The neural inducers of organizer activate neuralizing genes in the *Sox* and *Zic* families, such as *SoxD*, *Zic-r1*, *Zic3*, *Sox2* and *geminin*, which subsequently activate proneural genes (Mizuseki et al., 1998a; Mizuseki et al., 1998b; Nakata et al., 1997; Kroll et al., 1998). Expression of these *Sox* and *Zic* genes is localized to the dorsal ectoderm during early gastrula. They are promoted by Chordin but inhibited by BMP signaling. Overexpression of these genes leads to an increase of proneural genes such as *Xngnr-1*, *Xash-3*, and *XNeuroD*, and consequently, the promotion of primary neuronal differentiation. These neuralizing genes, therefore, may act to link neural inducers to activate proneural genes.

Primary neurogenesis is promoted by proneural genes both in *Drosophila* and *Xenopus* (Fig.1.2). The basic Helix-Loop-Helix (bHLH) transcription factors encoded by the *achaete-scute complex* (*AS-C*) and *atonal* genes in *Drosophila* provide cells with the potential to adopt a neural fate, therefore they are termed “proneural genes”. A few of such transcription factors have also been characterized in *Xenopus*. When embryos are still at early gastrula (stage 10.5), a bHLH transcription factor gene *Xngnr-1* starts to express, and defines the three prospective patches of primary neurons in the neural plate. Overexpression of this gene will lead to strong ectopic neuron formation (Ma et al., 1996). Expression of *Xngnr-1* precedes that of *Xash-3* and *Xath3*, which begin to

express since stage 11 and 12 (Zimmerman et al., 1993; Takebayashi et al., 1997), respectively. *Xash-3* is an *AS-C* homologue, too. Overexpression of *Xash-3* promotes neuron formation within neuronal domains in lower concentration while inhibits neuron formation in higher concentration due to the activation of lateral inhibition (Ferreiro et al., 1994; Chitnis and Kintner, 1996). When overexpressed in concert with a zinc-finger transcription factor gene *XMyT1*, however, it induces ectopic neurons in naïve ectoderm (Bellefroid et al., 1996). In the case of *Xath3*, a *Drosophila atonal* homologue, overexpression will lead to strong ectopic neuron formation, too (Takebayashi et al., 1997; Perron et al., 1999). Overexpression showed that Xngnr-1 activates *Xath3* in a unidirectional way (Bellefroid et al., 1996; Perron et al., 1999). Still downstream, a neural differentiation gene *XNeuroD* is activated by Xngnr-1 also in a unidirectional way (Ma et al., 1996). *XNeuroD* is another bHLH transcription factor starting to express since stage 13.5 (Lee et al., 1995). Again, overexpression of this gene induces formation of ectopic neurons in nonneural ectoderm (Lee et al., 1995). More recently, *Xebf3* was identified as a downstream target of XNeuroD (Pozzoli et al., 2001). It is activated at 15.5 and promotes neuronal differentiation, as XNeuroD does. The temporal sequence of expression of these genes and the unidirectional way of activation reflect that they regulate successive stages of primary neurogenesis.

On the other hand, neurogenesis is repressed by neurogenic genes via downregulating proneural proteins. In *Drosophila*, the products of neurogenic genes *Delta* and *Notch* comprise a cell-cell signaling mechanism termed lateral inhibition whereby a cell committed to neural fate forces its neighbors to remain nonneural (for reviews, see Artavanis-Tsakonas et al., 1995; Kopan and Turner, 1996; Beatus and Lendahl, 1998). Neural precursors are first specified by proneural genes in clusters of cells within the neuroepithelium. In the meantime, proneural proteins also enhance the expression of the inhibitory ligand encoded by *Delta* (Kunisch et al., 1994), and in turn they are inhibited by signaling via the receptor encoded by *Notch* in the neighboring cells. By this way, cells expressing proneural genes and hence *Delta* adopt a neural fate while their neighbors remain nonneural. When these genes are mutated in *Drosophila*, massive over-production of neurons will be resulted, hence the name

"neurogenic genes".

The mechanism is also conserved in vertebrates (Fig.1.2). Homologues of *Delta* and *Notch* have been identified in *Xenopus*, namely, *X-Delta-1* and *X-Notch-1*. It was shown that they control the number of primary neurons in very much the same way as in *Drosophila* (Chitnis et al., 1995; for review, see Beatus and Lendahl, 1998). Increased density of primary neurons is observed within the neuronal domains when the signaling is blocked by X-Delta-1^{STU}, a dominant negative form of the ligand. In contrast, when the pathway is activated by a dominant active form of the receptor, X-Notch-1ICD, primary neuron formation is repressed (Chitnis et al., 1995), as a result of inhibition of proneural genes including *Xngnr-1*, *Xash-3*, and *Xath3* (Ma et al., 1996; Chitnis and Kintner, 1996; Perron et al., 1999; Bellefroid et al., 1996). Therefore, lateral inhibition plays an instrumental role in keeping the balance between the number of neuronal precursors and the number of primary neurons.

After these successive waves of neurogenesis, a number of neuroectodermal cells are sorted out to become neurons while others remain epidermal (Lewis, 1996; Lee, 1997; Chitnis, 1999). This primary nervous system is composed symmetrically of lateral, intermediate and medial longitudinal stripes on each side of the dorsal midline, which differentiate into motorneurons, interneurons and sensory neurons, separately.

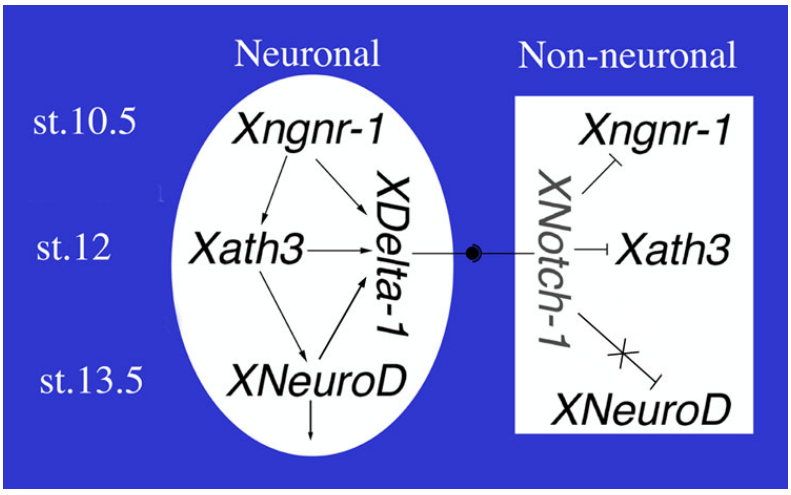

Fig.1.2 A simplified model for primary neurogenesis. It is pro-moted by proneural genes while repressed by lateral inhibition via cell fate selection, as a result of inhibitory effect of lateral inhibi-tion signaling on the function of early pro-neural genes. But late expressed proneural genes are refractory to lateral inhibition. Such a mechanism determines the number but not the localization of primary neurons.

So far, lateral inhibition is known to be the principal inhibitory mechanism for the regulation of primary neurogenesis. Blocking of lateral inhibition will

lead to more densely formation of primary neurons without alteration in the size of neurogenic domains, suggesting that lateral inhibition regulates primary neurogenesis by the way of limiting only the number of primary neurons. It is interesting to notice that *Xngnr-1* defines proneural domains much larger than the area where primary neurons form, as shown by a much larger expression domains of *Xngnr-1* than those of *N-tubulin*. Furthermore, the early proneural genes often have broader expression domains than those of late expressed ones, for example, *Xngnr-1* is expressed in broader domain than is *Xath3*, and the domain of *Xath3* is broader than *XNeuroD* (Ma et al., 1996; Perron et al., 1999; Lee et al., 1995). Such a correlation of temporal and spatial expression is also reported between *XMyT1* and *N-tubulin*, since *XMyT1* is expressed earlier in a broader domain than is *N-tubulin* (Bellefroid et al., 1996). Therefore, there should be a mechanism to regulate proneural genes such that primary neurogenesis can occur at an exact localization. It is known that lateral inhibition is particularly responsible for the regulation of earlier expressed genes, in particular those for neuronal determination (Chitnis and Kintner, 1996), such as *Xngnr-1* and *Xash-3*. While in later stages, neuronal differentiation genes such as *XNeuroD* and its downstream regulator *Xebf3* are proved to be resistant to lateral inhibition, although overexpression of *XNeuroD* itself also activates *X-Delta-1* (Lee et al., 1995; Chitnis and Kintner, 1996; Pozzoli et al., 2001). Then it comes another question how primary neurogenesis is negatively regulated when lateral inhibition is no longer effective for late expressed genes.

In the following it will be shown the molecular cloning of *XETOR*, an *ETO* related gene in *Xenopus*, and its functions during primary neurogenesis. Briefly, it was found that expression of *XETOR* starts from stage 12.5 in symmetrical stripes on either side of dorsal midline. The expression domain overlaps with but is broader than that of *N-tubulin*. By both gain-of-function and loss-of-function analyses, it was found that 1) XETOR is an inhibitory factor for primary neurogenesis in independence of lateral inhibition; 2) XETOR functions via establishing a negative feedback loop with proneural genes, similar to the case of lateral inhibition; 3) XETOR puts into action when lateral inhibition is no longer effective, because proneural genes sensitive to lateral inhibition are not

sensitive to XETOR while those insensitive to lateral inhibition are sensitive to XETOR; 4) XETOR and lateral inhibition antagonizes each other; 5) loss of XETOR function *in vivo* causes expansion of neurogenic domains; and conclusively 6) XETOR and lateral inhibition comprise a dual inhibitory mechanism to refine the number and localization of neurons for primary neurogenesis.

2. MATERIALS AND METHODS

2.1 Preparation of embryos

Eggs of *Xenopus laevis* were obtained by the way of hormone induction. Various doses (250-1,500 IU, depending on the condition of frogs) of chorionic gonadotropin (Sigma, cat.no.: CG-10) dissolved in 0.4% NaCl solution were subcutaneously injected to the dorsal lymph sac of healthy female frogs. In general the injected frogs were kept at room temperature waterbath overnight and began spawning eggs the next morning. In some cases when the frogs wouldn't give eggs the next morning, then an additional dose of around 500 IU was injected.

Testes used for *in vitro* fertilization were dissected out from adult male frogs and maintained in L-15 (Leibovitz, Sigma, cat.no.: L-4386) solution (5 ml L-15, 1 ml calf serum (Sigma, C-6204), 4 ml sterile water and 100 μl penicillin/ streptomycin stock solution (10,000 IU/10,000 μg/ml)) on ice or at 4°C. In this way they can be kept for as long as two weeks, still viable of fertilization.

For *in vitro* fertilization, female frogs were encouraged to lay eggs into a large petri dish by gentle squeezing. Simultaneously a small piece of testis was cut into fine pieces with scissors, suspended in 0.5-1 ml 0.1× MMR (Marc's Modified Ringer's Solution; 1×: 100 mM NaCl, 2 mM KCl, 2 mM $CaCl_2$, 1 mM $MgCl_2$, 5 mM HEPES, pH7.4) and transferred onto the eggs. The eggs were gently mixed well with the sperm suspension, spread to a single layer on the bottom of petri dish. Five minutes later, plenty volume of 0.1× MMR was added to the fertilized eggs so that they could be submerged in the solution. About 30-40 min later, fertilization rates can be determined by observing cortical rotation. Embryos were dejellyed with 2% cysteine (Merck, cat.no.: 1.02839.0100) adjusted to pH8.0, washed intensively and cultured in 0.1× MMR until the desired stages (Nieuwkoop and Faber, 1967).

When used for whole mount *in situ* hybridization, normal or treated embryos at the desired stages were first fixed in HEMFA (0.1 M HEPES, 2 mM EGTA, 1 mM

$MgSO_4$, 4% formaldehyde) for 1 hr at room temperature, then dehydrated in 100% ethanol and stored at –20°C. For RT-PCR, embryos were snap-frozen in liquid nitrogen and stored at –80°C.

2.2 Screening of cDNA library using whole mount *in situ* hybridization

The screening procedure started from a λZAP Express™ cDNA library, which was constructed with endoderm-like tissue induced from disaggregated/ reaggregated *Xenopus* animal caps treated with activin (Cao et al., 2001). A part of the phage cDNA library was converted to plasmid library by *in vivo* excision of the pBK-CMV phagemid vector containing cloned insert from the phage vector, according to the manufacturer's protocol (Stratagene). Single colonies were grown using the phagemid library on LB-kanamycin agar plates (LB agar, Sigma, cat.no.: L-2897). Around 4,000 single colonies were randomly picked out and cultured separately in each well of the 96-well microplate that contained 2× LB medium (LB broth, Sigma, cat.no.: L-3022). The strategy of large-scale whole mount *in situ* hybridization was employed for library screening.

2.2.1 PCR amplification of cDNA inserts

To prepare antisense RNA probes used for *in situ* hybridization, cDNA inserts were amplified using PCR with forward primer CMV-F and reverse primer CMV-R. The amplified products contained the whole inserts and T7 promoter, allowing transcription of antisense RNA using T7 RNA polymerase. Amplification was carried out in a volume of 20 μl.

Preparation of PCR mixture:

sterile millipore H_2O	16.14	μl
10× PCR buffer	2	μl
dATP, dCTP, dGTP, dTTP mix (25 mM each, Roche Molecular Biochemicals, cat.no.:1969064)	0.16	μl
CMV-F (10 mM)	0.3	μl
CMV-R (10 mM)	0.3	μl
single colony culture medium as template	1	μl
Goldstar Taq DNA polymerase (5 U/μl, Eurogentec, cat.no.: L026/E01-7)	0.1	μl
	20	μl

PCR mixture was loaded to each well of a 200 µl Thermal Cycler (thin walled 96 well) Plate (Whatman, cat.no.: 7703-1901). Amplification program was as follow: predenaturation at 95°C for 4 min; then 40 cycles of denaturation at 95°C for 45 sec, annealing at 56°C for 45 sec, and extension at 72°C for 3 min; afterwards an extra extension of 10 min. Five microliters of the amplification products were directly used for transcription.

Primers:

CMV-F (forward): 5'-CGCGCCTGCAGGTCGACACTA-3'

CMV-R (reverse): 5'-GCAAGGCGATTAAGTTGGGTA-3'

2.2.2 Transcription of antisense RNA probes for library screening

For the experiments hereinafter in which RNase was a concern, all solutions were prepared with DEPC (Sigma, cat.no.:D-5758) treated millipore water, and all RNase-free utensils and disposables were used.

Preparation of rNTP mixture:

rATP (10 mM)	50 µl
rCTP (10 mM)	50 µl
rGTP (10 mM)	50 µl
rUTP (10 mM)	32.5 µl
fluorescein-12-UTP (10 mM, Roche Molecular Biochemicals, cat.no.: 1373242)	17.5 µl
	200 µl

Preparation of transcription reaction mixture:

PCR product	5 µl
5× transcription buffer	4 µl
DTT (0.75 M)	0.8 µl
rNTP mix	2 µl
RNase inhibitor (40 U/µl, Strategene, cat.no.: 300151)	0.25 µl
T7 RNA polymerase (50 U/µl, Stratagene, cat.no.: 200340)	0.25 µl
DEPC-H_2O	7.7 µl
	20 µl

Transcription was performed at 37°C for 4 hrs. Probes were purified with Sephadex G-50 (medium, Sigma, cat.no.: G-50-150) in 96-well filter plates. The Sephadex G-50 columns were prepared as follow: 50 g of Sephadex G-50 was

suspended thoroughly in 700 ml of Sephadex G-50 storage solution (0.1% SDS, 0.3 M NaCl, 10 mM Tris-HCl pH8.0) and autoclaved. This suspension was loaded with full volumes to each well of the 96-well filter plates, which were spun at 1,200 rpm for 10 min to condense Sephadex. Afterwards adequate volumes of STE (50 mM NaCl, 10 mM Tris-HCl pH7.5, 2 mM EDTA) buffer were loaded to each well to equilibrate the Sephadex columns for twice. Centrifuge at 1,200 rpm for 5 min. To purify the probes, transcription products were loaded to the columns and centrifuge at 1,200 rpm for 10 min. Probes were subsequently collected and examined with agarose gel electrophoresis without EtBr.

2.2.3 Whole mount *in situ* hybridization

The protocols were essentially as described (Harland, 1991; Oschwald et al., 1991; Jowett, 2001). For single hybridizations, digoxigenin-labeled probes were always used and a purplish dark color was developed with chromagen NBT/BCIP; for double hybridization, a digoxigenin-labeled probe and a fluorescein-labeled probe were used simultaneously.

Whole mount *in situ* hybridization was performed in glass vials with a volume of 5 ml; while large scale hybridization was performed in a special 4×6 well stainless steel plates fitting in 4×6 tissue culture plates (Nalse Nunc International, cat.no.: 146485). The volumes of all solutions used were 4 ml in each glass vial and 500 μl in each well of a plate. All treatments were made at RT unless otherwise indicated in the experimental procedure.

Embryos at three representative stages: gastrula, neurula and tailbud, were used for library screening.

Solutions:

10× PBS: 0.1 M Na_2HPO_4, 20 mM KH_2PO_4, 1.4 M NaCl, 28 mM KCl.

PTw: 1× PBS, 0.1% Tween-20 (Sigma, cat.no.: P-1379).

20× SSC: 3 M NaCl, 0.3 M sodium citrate.

100× Denhart's solution: 2% BSA (Sigma, cat.no.: A-2153), 2% PVP (Sigma, cat.no.: P-5288), 2% Ficoll-400 (Sigma, cat.no.: F-4375).

Hybridization solution: 50% formamide (Sigma, cat.no.: F-7503), 5× SSC, 1

mg/ml Torula RNA (Sigma, cat.no.: R-6625), 100 mg/ml heparin (Sigma, cat.no.: H-9399), 1× Denhart's solution, 0.1% Tween-20, 0.1% CHAPS (Sigma, cat.no.: C-5849), 10 mM EDTA.

5× MAB: 0.5 M maleic acid, 0.75 M NaCl, pH7.5.

10% BMB: 10% Boehringer Mannheim Blocking Reagent (Roche Molecular Biochemicals, cat.no.: 1096176) in 1× MAB, autoclave, aliquot and store at –20°C.

goat serum (Gibcol BRL, cat.no.: 16210-064, or Sigma, cat.no.: G-9023): treat at 55°C for 30 min, aliquot and store at –20°C.

APB: 100 mM Tris-HCl pH9.5, 50 mM $MgCl_2$, 100 mM NaCl, 0.1% Tween-20.

NBT (Roche Molecular Biochemicals, cat.no.: 1087479) stock solution: 75 mg/ml NBT in 70% dimethylformamide, -20°C.

BCIP (Roche Molecular Biochemicals, cat.no.: 1383221) stock solution: 50 mg/ml BCIP in 100% dimethylformamide, -20°C.

NBT/BCIP stock solution (Roche Molecular Biochemicals, cat.no.: 1681451), 4°C.

Magenta phosphate (Molecular Probes, cat.no.: B-8409) stock solution: 50 mg/ml in 100% dimethylformamide, -20°C.

Tetrazolium red (Sigma, cat.no.: T-8877) stock solution: 75 mg/ml in 70% dimethylformamide, -20°C.

Fast Red (Roche Molecular Biochemicals, cat.no.: 1496549) chromagenic solution: 1 Fast Red tablet in 2 ml of 0.1 M Tris-HCl pH8.2.

Day 1

Rehydration of embryos:

100% ethanol	5 min 1×
75% ethanol in H_2O	5 min 1×
50% ethanol in H_2O	5 min 1×
25% ethanol in PTw	5 min 1×
PTw	5 min 4×

proteinase K treatment:

Embryos in each vial were treated with 10 μg/ml proteinase K (Sigma, cat.no.: P-2308) in 2 ml PTw for 15-30 min, depending on different stages. Generally

gastrula or early embryos were treated for about 10-15 min, neurulae for 20 min, while longer treatment was used for later stages. The embryos were immediately subject to subsequent steps.

acetification:

0.1 M triethanolamine (pH7.5) (Sigma, cat.no.: T-1502)	5 min	2×
0.1 M triethanolamine (pH7.5) 4 ml + acetic anhydride 10 μl	5 min	1×
0.1 M triethanolamine (pH7.5) 4 ml + acetic anhydride 20 μl	5 min	1×
PTw	5 min	2×

fixation and washing:

PTw+4%FA	20 min	1×
PTw	5 min	5×

For large-scale hybridization in library screening, a bleaching step was added here to remove the pigments on embryos, so as to facilitate observation of signals immediately after color development. While this bleaching may cause the embryos to be fragile, therefore, in other cases the embryos were only bleached after color development.

bleaching:

5× SSC+50% formamide+1% H_2O_2	light	5-25 min	1×
5× SSC+50% formamide		10 min	5×

hybridization:

First the embryos in each vial were briefly washed with a mixture of 500 μl PTw and 500 μl hybridization solution, then washed once more with 1 ml hybridization solution at 65°C for 10 min. Afterwards prehybridization was performed in 1 ml hybridization solution at 60°C for 6 hrs. Then hybridization was carried out in 1 ml hybridization solution containing antisense RNA probes at 60°C overnight.

Day 2

Probes in hybridization solution were collected and stored at –20°C for future use up to multiple times. Subsequently the embryos were subject to the following steps.

washing:

hybridization solution 500 μl	60°C	10 min	1×

2× SSC	60°C	20 min	3×
RNase treatment:			
20 μg/ml RNase A (Sigma, cat.no.: R-5000) +10 U/ml RNase T1 (Roche Molecular Biochemicals, cat.no.: 109193) in 2× SSC	37°C	1hr	1×
again washing:			
2× SSC		10 min	1×
0.2× SSC	60°C	30 min	2×
then blocking:			
MAB		15 min	2×
MAB+2% BMB		15-60 min	1×
MAB+2% BMB+20% goat serum (Gibcol BRL, cat.no.: 16210-064, or Sigma, cat.no.: G-9023)		60 min	1×
and antibody incubation:			
MAB+2% BMB+20% goat serum+ anti-digoxigenin antidody (1:5000, Roche Molecular Biochemicals, cat.no.: 1093274)		4 hrs	1×
again washing:			
MAB		30 min	2×
MAB	4°C	overnight	

Day 3

chromagenic reaction with NBT/BCIP:			
MAB		1 hr	1×
APB		5 min	2×
2 μl of NBT stock/3.5 μl BCIP stock in 1 ml APB or every 20 μl NBT/BCIP stock in 1 ml APB		5 min-1 week	

After sufficient staining, embryos were treated in absolute methanol for 10 min to make color differentiation. In the case of large scale *in situ* hybridization, now the stained embryos were ready for observation. Otherwise the embryos would be bleached in methanol/10% H_2O_2 for one to two weeks. Then embryos were stored in HEMFA or subject to sectioning.

For double hybridization, the fluorescein-labeled probes, which represent more abundant transcripts, must be viewed first. Also, Fast Red should be the first chromagenic reagent if it is used. If magenta phosphate/tetrazolium red is used for double staining, then either magenta phosphate/tetrazolium or NBT/BCIP can be used first, and chromagenic reaction protocol is exactly the same. Albeit magenta

phosphate generally produces slight or even no background staining, the signal is weak and much longer time is required for color reaction. The concentration of antibody could vary to some extent. For the detection of rare transcripts, such as the genes expressed in the primary neurons, the concentration of anti-fluorescein antibody can be increased to 1:2,000, and the anti-digoxigenin antibody can be 1:1,000. The following is a protocol for double *in situ* hybridization:

Day 1-2

The same as described above.

Day 3

chromagenic reaction with Fast Red:

MAB	1 hr	1×
0.1 M Tris pH8.2	5 min	2×
1 Fast Red tablet in 2 ml 0.1 M Tris (pH8.2)	5 min-48 h	

or **Day 3**

chromagenic reaction with magenta phosphate/tetrazolium red:

MAB	1 hr	1×
APB	5 min	2×
3.5 μl of magenta phos stock/4.5 μl tetrazolium red stock in 1 ml APB	5 min-72 h	

When the first signal reached the desired intensity, the following steps were followed for the second signal development.

Day 1

stop the first chromagenic reaction:

PTw	5 min	2×

inactivation of the first alkaline phosphatase activity (the red signal by Fast Red is unstable in heat and organic solvents, therefore the first alkaline phosphatase activity is killed with low pH instead of heating. While in the case of magenta phosphate, the color precipitate is stable in heat and organic solvents):

0.1M glycine hydrochloride (Sigma, cat.no.: G-2879) pH2.2	30 min	1×

thorough washing:

PTw		5 min	5×

signal fixing:

PTw+4%FA		20 min	1×

again blocking and anti-digoxigenin antibody incubation:

MAB		10 min	3×
MAB+2%BMB		30 min	1×
MAB+2%BMB+20% goat serum		1 hr	1×
MAB+2%BMB+20% goat serum +anti-digoxigenin antibody (1:1000)		4 hrs	1×

washing:

MAB		30 min	2×
MAB	4°C	overnight	

Day 2

chromagenic reaction with NBT/BCIP:

The same as described above.

For rare transcripts, color reaction was performed at RT or 37°C; while for abundant transcripts, it was carried out at 4°C. Chromagenic reaction was stopped with washing in PTw.

After large scale *in situ* hybridization, clones that generated staining patterns of potential interests were singled out and respective plasmids were prepared. Around 300-500 bp of inserts in these plasmids were sequenced and compared with Genbank databases. Finally 3 clones were selected to get full sequences of the inserts.

2.3 Plasmid preparation

2.3.1 Using TELT

At some occasions a mini-preparation of plasmids was performed for sequencing or diagnostic purposes, as described below:

1) Harvest cells from 1.5 ml overnight culture by centrifugation at 6,000 rpm for 5 min, using a conventional table-top microcentrifuge;

2) Remove supernatant completely with vacuum sucking and resuspend the

cells in 150 μl TELT solution (50 mM Tris-HCl pH7.5, 10 mM EDTA, 3.2 M LiCl, 0.5% Triton X-100);

3) Add 15 μl of 50 mg/ml lysozyme (Sigma, cat.no.: L-6876) to the cells, mix well by vortexing, and incubate at RT for 5 min;

4) Incubate the cells in boiling water for 2 min and immediately chill on ice for 5 min;

5) Centrifuge at full speed (13,000 rpm) for 8 min. Remove the pellets of cell debris and genomic DNA with sterile toothpicks;

6) Add 100 μl isopropanol to the supernatant and vortex;

7) Centrifuge at full speed for 15 min. Remove supernatant with pipette and wash pellets with 200 μl 70% ethanol;

8) Centrifuge at full speed for 5 min, remove supernatant carefully and air-dry plasmid pellets;

9) Dissolve the pellets in 30 μl of 10 mM Tris-HCl (pH8.5) containing 10 ng/ml RNase A, incubate first at RT for 2-5 min and then at 65°C for 5 min;

10) Spin down and transfer the solution into a new tube, store at –20°C.

2.3.2 Using QIAGEN Plasmid Midi Kit

For *in vitro* transcription, plasmids were prepared using QIAGEN Plasmid Midi Kit (Qiagen, cat.no.: 12143). The protocol provided with the kit was eventually followed. Concentrations of samples were determined with UV-spectrophotometer.

2.4 Agarose gel electrophoresis

The protocol for agarose gel electrophoresis was essentially as described (Sambrook et al., 1989).

2.5 Preparation of antisense probes for functional analyses

Plasmids were linearized with respective restriction endonucleases and purified using QIAquick PCR purification kit (Qiagen, cat.no.: 28104). The protocol provided with the kit was exactly followed. Every 1 μg of the linearized plasmids was used for antisense probe transcription. Afterwards probes were purified using

Qiagen RNeasy kit (Qiagen, cat.no.: 74104). The protocol of the kit was essentially followed, with only minor modification in that 400 μl of buffer RLT was used instead of 350 μl. Because it was observed that, for purification of *in vitro* transcripts, the yield was quite low when 350 μl of buffer RLT was used as recommended by the kit protocol. While 50 μl more of RLT will increase the yield about two folds.

For each whole mount hybridization, 1/2 of the antisense probes prepared from 1 μg linearized plasmids were used in 1 ml of hybridization solution. While in the case of *N-tubulin*, 1/8 of the antisense probe prepared from 1 μg of linearized plasmid was used in 1 ml of hybridization solution. Empirical experiments showed that higher concentrations of probes brought about heavy background overstaining.

XODC1 (Bassez et al., 1991) was cut with *Bam*HI and transcribed with T3 RNA polymerase, *XODC2* was cut with *Nde*I and transcribed with T7, *XCL-2* was cut with *Eco*RI and transcribed with T7, *Chordin* and *Xsox3* were cut with *Eco*RI and transcribed with T7, *Xbra*, *XNAP* and *Xvent-1* were cut with *Sal*I and transcribed with T7, *XMyoD* was cut with *Bam*HI and transcribed with T7, *Xotx2* was cut with *Bam*HI and transcribed with T3, *XETOR* was cut with *Eco*RI and transcribed with T7, *N-tubulin* and *Xngnr-1* were cut with *Bam*HI and transcribed with T3, *X-Delta-1* was cut with *Xho*I and transcribed with T7, *Xaml1* was cut with *Sal*I and transcribed with T7, *XMyT1* was cut with *Bam*HI and transcribed with T7, *Xath3* was cut with *Not*I and transcribed with T7, *ESR1* was cut with *Eco*RI and transcribed with SP6, *Xash3* was cut with *Not*I and transcribed with T3, and *XNeuroD* was cut with *Xba*I and transcribed with T7 RNA polymerase.

2.6 Histological sections

After whole mount *in situ* hybridization, embryos were embedded in paraffin and sections were prepared as described (Grunz, 1973; Penzel et al., 1997).

2.7 RT-PCR

2.7.1 Total RNA preparation

Total RNA used for RT-PCR was extracted from whole embryos of stages 0-42 or adult tissues, using RNA*Clean*™ (Hybaid-AGS, cat.no.: RC100) solution.

1) Into a 1.5-ml RNase-free Eppendorf tube put 10 embryos or adequate amount of adult tissues pulverized in liquid nitrogen. Stand the tube on dry ice;

2) Add 1 ml RNA*Clean*™ solution to each tube. Homogenize the embryos by pipetting until no cell clumps can be seen;

3) Add 100 μl (0.1 volume) $CHCl_3$ to each tube, mix well by vortexing;

4) Incubate the tubes on ice for 5 min;

5) Precipitate the homogenate at 13,000 rpm at 4°C for 15 min;

6) Carefully transfer the aqueous phase to a new tube, and add 600 μl of isopropanol, mix well;

7) Incubate the tube at –20°C for 15 min;

8) Pellet RNA at 13,000 rpm at 4°C for 15 min;

9) Wash RNA pellet twice: first with 900 μl of 70% ethanol, and then with 500 μl of 70% ethanol;

10) Air-dry the RNA pellet for about 10 min;

11) Dissolve the RNA pellet in 50 μl of DEPC-H_2O, check the purity and concentration with UV-spectrophotometer and the integrity with agarose gel electrophoresis, and store the sample at –80°C.

2.7.2 Reverse transcription

Reverse transcription was carried out in a total volume of 20 μl.

1) Preparation of Mix1:

Total RNA (0.5 μg/μl)	2 μl
Hexamer random primer $p(dN)_6$ (0.1 mM, Roche Molecular Biochemicals, cat.no.:1034731)	1 μl
DEPC-H_2O	9 μl
	12 μl

2) Incubate the mixture at 70°C for 10 min. Immediately chill on ice;

3) Preparation of Mix2:

5× first strand buffer	4 μl
0.1M DTT	2 μl
dNTPs mix (10 mM each)	1 μl
	7 μl

4) Add Mix1 and Mix2 together and mix well gently, precipitate briefly, then incubate at 25°C for 10 min;

5) Add 1 μl (200 units) of SuperScript^{TM}II Reverse Transcriptase (Gibcol BRL, cat.no.: 18064-014) to the above mixture in step 3); for negative control (RT-), add 1 μl DEPC-H_2O instead of reverse transcriptase to make a total volume of 20 μl. Mix well;

6) Incubate the transcription mixture first at 42°C for 50 min, then at 70°C for 15 min. Afterwards store the sample at –20°C.

2.7.3 PCR

Amplification was performed in total volume of 50 μl.

Preparation of PCR mixture:

H_2O	32.9 μl
10× PCR reaction buffer	5 μl
dNTPs mix (1.25 mM each)	8 μl
forward primer (50 mM)	1 μl
reverse primer (50 mM)	1 μl
RT product	2 μl
Goldstar Taq DNA polymerase (5 U/μl)	0.1 μl
	50 μl

The annealing temperatures and numbers of cycles for amplification were dependent on primers used. For *XODC1*, the annealing temperature was 55°C and cycle number was 27; for *XODC2*, 60°C, 29 cycles; *XCL-2,* 60°C, 31 cycles. Because probably the transcripts of *XETOR* are very rare, it had been not possible to obtain enough products for detection in one round of amplification even the cycle numbers were increased to as many as 45, therefore temporal expression of *XETOR* was not analyzed with RT-PCR. For all amplifications, 25 μl of each final product was loaded into 1% agarose gels for electrophoresis detection with EtBr.

2.7.4 Primers used for RT-PCR

XODC1 (product size: 387 bp):

Forward: 5’-GGGCAAAGGAGCTTAATGTG-3’

Reverse: 5’-CATTGGCAGCATCTTCTTCA-3’

XODC2 (product size: 404 bp):

Forward: 5’-AGCTGGGAGCTGGATTTGACTG-3’

Reverse: 5’-GCGTGCATCAGAAATAGCCTGA-3’

XCL-2 (product size: 400 bp):

Forward: 5'-AGAGGTCGCCAGGAGAAGTTGA-3'

Reverse: 5'-TACAGCACGGCTCATTGTTCGT-3'

2.8 Generation of complete coding sequences of *XCL-2* and *XETOR* with RACE

Coding sequences of *XCL-2* and *XETOR* were found to be incomplete at their 5' ends. Therefore 5'RACE (Frohman et al., 1989) was employed to get the complete coding regions from poly(A)$^+$ RNA.

2.8.1 Preparation of poly(A)$^+$ RNA

About 500 μg of total RNA was extracted from 100 embryos at stage 25 for *XCL-2* or stage 30 for *XETOR* using the RNAclean^{TM} protocol. An Oligotex^{TM} mRNA Mini kit (Qiagen, cat.no.: 70022) was used to extract poly(A)$^+$ RNA from 500 μg of total RNA. The midi-preparation protocol in the kit was essentially followed except that the time for secondary structure disruption and for Oligotex:mRNA hybridization was doubled. In addition, the steps from secondary structure disruption to Oligotex:mRNA complex precipitation were repeated once. Finally the poly(A)$^+$ RNA from 500 μg of total RNA was dissolved in 30 μl elution buffer and checked with agarose gel electrophoresis.

2.8.2 Isolation of 5' end coding sequence of *XCL-2*

1) First-strand cDNA synthesis

Preparation of first-strand cDNA synthesis mix:

cDNA synthesis buffer	4 μl
dNTPs mix (10 mM each)	2 μl
gene-specific cDNA synthesis primer 11sp1 (12.5 μM)	1 μl
poly(A)$^+$ RNA	10 μl
AMV reverse transcriptase (20 units/μl, Roche Molecular Biochemicals, cat.no.: 1495062)	1 μl
RNase-free H_2O	2 μl
	20 μl

2) The mixture was incubated at 55°C for 60 min and then at 65°C for 10 min.

3) Purification of cDNA: First-strand cDNA was purified using High Pure PCR

Product Purification Kit (Roche Molecular Biochemicals, cat.no.: 1732668) according to the instruction manual of the kit. Finally the cDNA was eluted with 50 μl of 10 mM Tris-HCl pH8.5 instead of 1 mM Tris-HCl.

4) Tailing reaction of cDNA: A poly dA tail should be added to the 3' end of the cDNA.

Preparation of the following mixture:

purified cDNA	19 μl
10× reaction buffer	2.5 μl
dATP (2 mM)	2.5 μl
	24 μl

5) The above mixture was incubated first at 94°C for 3 min and then immediately chilled on ice. Afterwards 1 μl of terminal transferase (10 units/μl, Roche Molecular Biochemicals, cat.no.: 220582) was added to the mixture and incubated for 30 min at 37°C for tailing and 10 min at 70°C for the inactivation of terminal transferase. This dA-tailed cDNA was directly used as template for PCR.

6) First round of PCR amplification

Preparation of PCR mixture:

H_2O	29.5 μl
10× PCR reaction buffer	5 μl
dNTPs mix (1.25 mM each)	8 μl
dA-tailed cDNA	5 μl
anchor-dT primer (12.5 μM)	1 μl
gene-specific nested primer 11sp2 (12.5 μM)	1 μl
*Pfu*Turbo® DNA polymerase (2.5 units/μl, Stratagene, cat.no.: 600250)	0.5 μl
	50 μl

Reaction mixture was incubated for 2 min at 94°C and followed first by 5 cycles of (94°C, 45 sec; 55°C, 1 min; 72°C, 3 min) and then by 33 cycles of (94°C, 45 sec; 60°C, 1 min; 72°C, 3 min), finally an extra extension at 72°C for 10 min. The first round PCR product was purified and every 2% of it was used as template in the second round of PCR in a total reaction volume of 100 μl. In the second round, the simple anchor primer and a further nested gene-specific primer 11sp3 were used. Thirty cycles of (94°C, 45 sec; 60°C, 1 min; 72°C, 2.5 min) were carried out. The final PCR product was extracted from agarose gel using QIAquick Gel Extraction kit (Qiagen, cat.no.: 28704) and sequenced. A final cDNA sequence

of 2639 bp was obtained. The putative translation initiation codon for ORF is preceded by a stop codon 12 triplets upstream, indicating that the coding region is complete.

2.8.3 Isolation of 5' end coding sequence of *XETOR*

Because *XETOR* is a rare transcript in *Xenopus* embryonic cells, it was not successful to get the correct 5' coding region with the above method, probably due to its low specificity. Therefore the SMART™ RACE cDNA Amplification Kit (Clontech, cat.no.: K1811-1) and the protocol provided by the kit was used instead. cDNA was first reverse transcribed from Poly(A)$^+$ RNA from stage 30 embryos using gene-specific primer GSP-RT and SuperScriptII RNaseH$^-$ Reverse Transcriptase (Gibcol BRL, cat.no.: 18064-014). The first strand cDNA was used as template in the first round of RCR, which was performed first at (94°C, 10 sec; 72°C, 3min) for 5 cycles, then at (94°C, 10 sec; 70°C, 15 sec; 72°C, 3 min) for another 5 cycles, and again at (94°C, 10 sec; 68°C, 15 sec; 72°C, 3 min) for 25 cycles, using a nested gene-specific primer GSP1 and the Universal Primer Mix in the kit. In order to obtain adequate quantity of product, a second round of PCR was performed using the first round PCR product as template and a further nested gene-specific primer NGSP1 and the Nested Universal Primer in the kit. The product was purified again from agarose gel and sequenced. A final cDNA sequence of 2936 bp was obtained. The putative translation initiation codon for ORF is also preceded by a stop codon 11 triplets upstream, indicating that the coding region is complete.

2.8.4 Primers used for 5'RACE

Anchor-d(T) primer: 5'-GACCACGCGTATCGATGTCGACT_{17}-3'
Simple anchor primer: 5'-GACCACGCGTATCGATGTCGAC-3'
11sp1: 5'-CGAGGTGGGCATCTGTATGGTC-3'
11sp2: 5'-TACAGCACGGCTCATTGTTCGT-3'
11sp3: 5'-TGGTGAGGGTGTCAGGAGACAG-3'
GSP-RT: 5'-TGTTCTGCTCCCAAAGTCACGA-3'
GSP1: 5'-TATCCACTTCCTGACAGCGACGCAGCAC-3'

NGSP1: 5'-TCTAACGTCCCGGTGTTCGCCGATCTTG-3'

2.9 Constructs

In order to investigate the functions of *XODC2*, *XCL-2* and *XETOR* for embryogenesis, expression constructs and a series of mutants were made for these genes.

2.9.1 *XODC2* constructs

The open reading frame of *XODC2* was amplified from plasmid pBK-CMV-*XODC2* using PCR with primers 4Forf and 4Rorf, and subcloned to *Eco*RI-*Xba*I sites of pCS2+ to make pCS2+*XODC2*. It was previously shown that a mutant of human ODC in which the active site K69 and C360 were both changed to A works in a dominant negative manner *in vivo*, therefore, these two corresponding sites, K68 and C357, in XODC2 were also mutated to make a similar mutant by the way of PCR. First, three fragments P1, P2 and P3 were PCR amplified from pBK-CMV-*XODC2* with primer pairs 4Forf and K68A-R, K68A-F and C357A-R, and C357A-F and 4Rorf, separately. Fragments P1 and P2 were then joined together to make P12 with primers 4Forf and C357A-R, and finally P12 was joined with P3 to make a full sequence of ORF using primers 4Forf and 4Rorf but K68 and C357 were changed to A, separately. This mutated ORF was again subcloned to *Eco*RI-*Xba*I sites of pCS2+ to make pCS2+*dnXODC2*. Both constructs were confirmed by sequencing.

Primers:

4Forf (forward): 5'-CCGG**GAATTC**AAAATGCAAGGGTATATCCA-3'

4Rorf (reverse): 5'-GC**TCTAGA**GCTCAAATGATGCTGGTGGCTG-3'

K68A-F (forward): 5'-TTCTATGCAGTGGCGTGTAACAGC-3' (mutated codon underlined, AAG→GCG)

K68A-R (reverse): 5'-GCTGTTACACGCCACTGCATAGAA-3'

C357A-F (forward): 5'-GGACCCACGGCCGATGGCTTAGAT-3' (mutated codon underlined, TGC→GCC)

C357A-R (reverse): 5'-ATCTAAGCCATCGGCCGTGGGTCC-3'

2.9.2 *XCL-2* constructs

Both wild type and dominant negative expression construct were made for *XCL-2*. To subclone the ORF of *XCL-2*, first-strand cDNA was synthesized in exactly the same way as used in RACE, except that the cDNA synthesis primer was simple11#rorf. Wild-type ORF was PCR amplified from the purified cDNA using primers n11#forf and n11#rorf. To construct a dominant negative mutant, in which the active site C105 was mutated to S, two fragments were PCR amplified from the same cDNA above, using primer pairs n11#forf and 11#C105Sr (300 bp), and 11#C105Sf and n11#rorf (1800 bp), respectively. Then a mutated complete ORF was generated by PCR linking the two fragments together using primer pair n11#forf and n11#rorf. Finally, the amplified wild-type ORF and mutated ORF, both of 2100 bp, were purified from agarose gel, double digested with *Cla*I and *Xba*I, and ligated to the *Cla*I and *Xba*I sites of pCS2+ to make pCS2+*XCL-2* and pCS2+*C105S*, separately. Both constructs were confirmed by sequencing.

Primers:

simple11#rorf: 5'-TCAGACCAATGTTGCGCAGAGCC-3'

n11#forf: 5'-CC**ATCGAT**GGCCCATCATGTCGAGAAGTGCTG-3'

n11#rorf: 5'-GC**TCTAGA**GCTCAGACCAATGTTGCGCAGAGCC-3'

11#C105Sf: 5'-CCTCGGGGATTCCTGGCTTCTG-3' (mutated codon underlined, TGC→TCC)

11#C105Sr: 5'-CAGAAGCCAGGAATCCCCGAGG-3'

2.9.3 *XETOR* constructs

To make an expression construct for microinjection, the open reading frame of *XETOR* was PCR amplified from cDNA reverse transcribed with primer 13#Rorf from stage 30 Poly(A)$^+$ RNA, and cloned to *Eco*RI-*Xba*I sites of pCS2+ to generate pCS2+*XETOR*. A series of constructs of truncations (cf. Fig.3.15) were also made using PCR method. Inserts were all ligated to *Eco*RI-*Xba*I sites of pCS2+. Truncation construct 1 (assigned as p13#trunc1) consists of amino acids from 1 to 496 with NHR4 deleted using primers 13#Forf and R13#496Δ; truncation construct 2 (p13#trunc2) from aa1-425 with NHR3 and 4 deleted using primers 13#Forf and R13#425Δ; construct 3 (p13#trunc3) from aa216-425 with NHR1, 3 and 4 deleted

using primers F13#Δ216 and R13#425Δ; construct 4 from (p13#trunc4) aa216-586 with NHR1 deleted using primers F13#Δ216 and 13#Rorf; and truncation construct 5 (p13#trunc5) consists of aa364-586 with NHR1 and 2 deleted using primers F13#Δ363 and 13#Rorf. All constructs were confirmed by sequencing.

Primers:

13#Forf: 5'-CCGG**GAATTC**GATAGAATGGTTGGGATTCCAGGA-3'

13#Rorf: 5'-GC**TCTAGA**GCTCACAGGCCATCAACAGCAGTGAC-3'

R13#425Δ: 5'-GC**TCTAGA**GCTCAATCTGTTACATAGCCTGCTCCTGT-3'

R13#496Δ: 5'-GC**TCTAGA**GCTCAGCTCTCAGTGGACTCTTCCTGCTC-3'

F13#Δ216: 5'-CCGG**GAATTC**GATAGAATGGAAATGAATGGCAATGGG AAA-3'

F13#Δ363: 5'-CCGG**GAATTC**GATAGAATGCGTCGCTGTCAGGAAGTG GAT-3'

2.10 DNA Ligation

The DNA Ligation Kit (Fermentas, cat.no.: K1412) was used for DNA ligation and the protocol in the kit was essentially followed.

Preparation of ligation mixture:

Double digested pCS2+ (0.25 μg/μl)	1.5 μl
Double digested insert	X μl
10× ligation buffer	2 μl
T4 DNA ligase (2 U/μl)	1 μl
H_2O	Y μl
	20 μl

The volume of DNA to be inserted was variable according to its concentration. In principle, the more foreign DNA is used, the higher is the possibility to obtain positive clones and also the higher is the ratio of positive clones. Ligation reaction was carried out at 22°C for 6-24 hrs, depending the quantity of foreign DNA in the ligation mixture. After ligation, 5 μl of the ligation mixture was used for *E.coli* transformation. Either PCR or minipreparation of plasmids from single colonies could be used to confirm positive clones. However, it is not reliable to check whether or not a ligation is successful by directly comparing the DNAs before and after ligation reaction with agarose gel electrophoresis.

2.11 Large-scale preparation of competent *E. coli* and transformation

2.11.1 Preparation of competent *E. coli*

1) Inoculate 1 ml of *E.coli* (strain XLOLR or XL1-Blue MFR'; Stratagene, cat.no.: #200304 or #200301) overnight culture into 500 ml LB broth with tetracycline;

2) Incubate in the orbital shaker at 37°C. Cells are ready for harvesting when OD_{660nm} is between 0.6 and 1;

3) Quickly cool cells on ice for 10 min;

4) Transfer cells to cooled 50 ml Falcon tube and spin cells at 4,000 rpm for 10 min at 4°C using a Megafuge 1.0R tabletop centrifuge and a 3360 rotor (Heraeus Instruments), discard supernatant;

5) Wash cells with 50 ml of 0.1 M ice-cold sterile $CaCl_2$;

6) Resuspend cells in 50 ml of 0.1 M ice-cold sterile $CaCl_2$;

7) Leave cells on ice for 40 min, then spin cells in the same way as in step 4), discard supernatant.

8) Resuspend cells with 10 ml of ice-cold sterile 0.1 M $CaCl_2$/20% glycerol;

9) Aliquot on ice as 100μl aliquots, snap-frozen in liquid nitrogen and store cells at -80°C.

2.11.2 *E. coli* Transformation

1) Ligation mix and controls or plasmids to be amplified were diluted to a volume of 10 μl, and added to pre-thawed 100 μl competent cells;

2) Incubate on ice for 30 minutes;

3) Cells were then heat shocked by placing at 42°C for 2 minutes, then quickly placed on ice for 5 minutes;

4) 400 μl (for transforming ligation products) or 800 μl (for transforming plasmids) of LB broth was added to the cells and incubated at 37°C for 42 min;

5) Plate out cells on agar containing appropriate antibiotics, such as ampicillin;

6) Single colonies would appear after incubation overnight at 37°C.

2.12 Microinjection

mRNAs used for injection were prepared as follow: NLS*LacZ*, pCS2+*XODC2*, pCS2+*dnXODC2*, pCS2+*XCL-2*, pCS2+*C105S*, pCS2+*XETOR*, *p13#trunc1*,

p13#trunc2, *p13#trunc3*, *p13#trunc4*, *p13#trunc5*, *X-Delta-1*^{STU}, *X-Notch-1ICD* (Chitnis et al., 1995), *Xngnr-1* (Ma et al., 1996), *XMyT1* (Bellefroid et al., 1996), *XNeuroD* (Lee et al., 1995), and *Xash-3* (Zimmerman et al., 1993) were linearized with *Not*I; and *Xath3* (Takebayashi et al., 1997; Perron et al., 1999) was linearized with *Acc*I. All capped mRNAs for microinjection were prepared with SP6 CapScribe kit (Roche Molecular Biochemicals, cat.no.: 1581040). 1.0, 1.5 or 2.0 ng of mRNA of either *XODC2* or *dnXODC2* was injected into two dorsal or ventral blastomeres at equatorial region at 4-cell stage. 2.0 or 2.5 ng of mRNA of *XCL-2*, or 1.5 or 2.0 ng of mRNA of *C105S* alone was also injected into two dorsal or ventral blastomeres at either animal, equatorial or vegetal region at 4-cell stage. 3.0 ng, 3.75 ng or 4.5 ng of *XCL-2* together with 2.0 ng of *C105S* was coinjected respectively in rescue experiments. The above mRNAs were injected in a total of 10 nl; 1-1.5 ng of mRNAs of *XETOR* and the 5 *XETOR* truncation mutant constructs, 500 pg of *X-Delta-1*^{STU}, *X-Notch-1ICD*, *XMyT1* or *XNeuroD*, 200 pg of *Xngnr-1*, *Xash-3* or *Xath3* was injected into one blastomere at equatorial region at 2-cell stage in a total of 5 or 10 nl together with 50 pg of *LacZ* mRNA serving as lineage tracer. *LacZ* alone was always injected as control.

For loss-of-function analysis on *XETOR*, a morpholino antisense oligo *MOXETOR* with base composition 5'-GATAGGGTCCTGGAATCCCAACCAT-3' (Gene Tools, LLC), was designed against the first 25 bases in the ORF of *XETOR*. A standard control antisense morpholino oligo, *ctrlMO* (Gene Tools, LLC), was also used for microinjection. Morpholino oligos were dissolved in RNase-free water and injected into the equatorial region of one blastomere at 2-cell stage with doses ranging 7-30 ng in a volume of 10 nl. 50 pg of *LacZ* mRNA was always included in the injections.

Microinjection was made in 0.1× MMR containing 4% Ficoll-400 (Sigma, cat.no.: F-4375). The injected embryos were kept for several hours or overnight at 14-16°C for healing. Afterwards the embryos were grown in 0.1× MMR till desired stages. Then injected embryos were subject to HEMFA fixation, β-gal staining and subsequent whole mount *in situ* hybridization or sectioning.

2.13 β-galactosidase staining

Embryos microinjected with β-galactosidase mRNA were fixed in HEMFA for

1 hr, then washed twice in PBS containing 1 mM $MgCl_2$ and twice in staining buffer (SB: 10 mM $K_3Fe(CN)_6$, 10 mM $K_4Fe(CN)_6$, 1 mM $MgCl_2$, in PBS), 5-10 min each time. Embryos were stained in SB containing 1.5 mg/ml freshly added 5-bromo-4-chloro-3-indolyl-β-D-galactopyranoside (X-gal, Sigma, cat.no.: B-4252) for 1-2 hrs at 37°C. After staining, embryos were washed twice in PBS, fixed in HEMFA for 30 min, and stored in 100% ethanol at –20°C, until processed for *in situ* hybridization.

3. RESULTS

3.1 Identification of *XODC2*, *XCL-2* and *XETOR*

Using large-scale whole mount *in situ* hybridization, expression patterns were generated for altogether 384 clones, among which the patterns of 29 clones were specific. For the others, 332 were expressed ubiquitously on the embryos, and 23 had no discernible staining on any stage of embryos. On the basis of staining patterns, 383 clones were ectoderm- or mesoderm-related; only 1 was with certainty derived from endoderm (20D8, *endodermin*).

Through comparison with GenBank DNA sequence databases, it was demonstrated that among the 29 clones, 11 are homologous to already known *X. laevis* genes with high similarities (>90%), nine are similar in the most parts of their sequences to known genes in other species as human and mouse, suggesting that these clones may be *X. laevis* homologues. While for the remaining nine clones, the search results revealed little information, suggesting that they may be completely novel genes (Table 3.1).

Table 3.1 Brief summary of BLAST comparison results

No. of clone	Best hit and its functional classification (?: function unknown)	E-value[1)] of best hit	Accession no.
18B2	*C. elegans* cosmid C14F11. ?	0.51	AI880918
18D7	Human malate dehydrogenase precursor mRNA. Metabolism	1e-47	AI880919
18D11	Human Cosmid Clone p129d11. ?	0.13	AI880920
18E3	*X. laevis* Xlim-1 mRNA. Homeobox transcription factor	0.0	
18E9	Mouse mRNA for p38-2G4. Cell cycle	4-e11	AI880921
18F3	*X. laevis* mRNA for calreticulin (clone 3). Metabolism	0.0	

18F6	*X. laevis* 71.0 kDa protein (retrotransposon 1a11 related) mRNA. DNA transposable element	0.0	
18G1	Human pre-B-cell colony-enhancing factor mRNA. Signal transduction	7e-25	AI880922
18G6	*X. laevis* cytokeratin type II mRNA. Structure	0.0	
18G11	Human Calpain, large polypeptide L2 mRNA; human Ca2-activated neural protease large subunit mRNA.	1e-04	AI880923
18H1	*X. laevis* mRNA for Xsox17-beta protein	7e-61	
18H2	Human core-binding factor, runt domain, alpha subunit 2. Putative transcription factor	1e-11	AI880924
18H7	*X. laevis* Xotx2 mRNA. Homeobox transcription factor	e-152	
20A7	Human desmoplakin (DPI, DPII) mRNA. Cell adhesion	7e-28	AI880934
20A9	*X. laevis* mRNA for alpha-tubulin. Structure	0.0	
20D8	*X. laevis* endodermin gene. ?	0.0	
20E7	Chicken retinaldehyde dehydrogenase 2 mRNA. ?	e-102	AI880925
20F1	*X. laevis* cytokeratin type II mRNA. Structure	0.0	
20G12	*X. laevis* mRNA for elongation factor 1-alpha. Metabolism	0.0	
2B10	Rat intestinal epithelium proliferating cell-associated mRNA sequence. Cell proliferation	6e-16	AI880926
2C3	Human genomic DNA sequence. ?	0.51	AI880927
2C4	*A. thaliana* chromosome II BAC F27I1 genome sequence. ?	0.13	AI880928
2G8	Human actin-related protein 3 homologue (yeast) mRNA. Structure	3e-21	AI880929
7C7	Human insulin receptor gene, last exon. ?	0.51	AI880930
7E4	Human genomic sequence. ?	0.13	AI880931
7F1	*X. laevis* mitochondrial DNA. Metabolism	0.0	
7F4	Mouse mRNA for serine/threonine protein kinase. Metabolism	8e-40	AI880932
7F12	*X. laevis* alpha-tubulin gene. Structure	0.0	
7G3	Rat L-arginine:glycine amidinotransferase mRNA. Metabolism	4e-23	AI880933

1) The E-value is a parameter that describes the number of hits one can "expect" to see just by chance when searching a Genbank database. It is used as a convenient way to create a significance threshold for reporting results, as well as to report the significance of sequence matches.

Based on localized staining patterns, three clones, 18D11, 18G11 and 18H2, were selected for further investigation.

3.1.1 cDNA and amino acid sequences of *XODC2*

A cDNA sequence of 1842 bp was obtained from clone 18D11. The 1368 bp of open reading frame (ORF) could be conceptually translated into a protein of 456 amino acids (Fig.3.1A). Comparisons using BLAST search program showed that this protein shares 66% identity in amino acid sequence with the ubiquitous ornithine decarboxylase (ODC) in human, 65% in *Xenopus laevis* and rat, and 63% in chicken (Fig.3.1B). In addition, the active sites in ubiquitous ODCs are also conserved in the protein (Almrud et al., 2000; Fig.3.1B). Therefore it most

(A)

```
                                                                gttagtctgagtaccа   16
gggacggagacacttccacatttctattaatgggcaacggccgtgtcaatgcatgttaagaaagcgataaac   88
gccagaagcggcgacttcactcacagcccggggtgttgcaaaatctccgagttcactgcggagcctccctgg  160
ttgctctgataaaagcttgttgcgtacttaaaaacaatcttggtagaagtgcttaaaatcccagatttcaaa  232
atgcaagggtatatccaggagtcagattttaacttggttgaagaaggctttttggccagagacttgatggag  304
M  Q  G  Y  I  Q  E  S  D  F  N  L  V  E  E  G  F  L  A  R  D  L  M  E    24
gaaatcattaatgaagtctcacagactgaggatcgtgatgccttttttgtggctgatctaggggatgtggta  376
E  I  I  N  E  V  S  Q  T  E  D  R  D  A  F  F  V  A  D  L  G  D  V  V    48
aggaaacatctccgttttctgaaagccttgcctcgtgtgaagcctttctatgcagtgaagtgtaacagcagc  448
R  K  H  L  R  F  L  K  A  L  P  R  V  K  P  F  Y  A  V  K  C  N  S  S    72
aaaggagtggtgaagatcttggctgagctgggagctggatttgactgcgccagcaagacagagattgagcta  520
K  G  V  V  K  I  L  A  E  L  G  A  G  F  D  C  A  S  K  T  E  I  E  L    96
gtccaggacgttggtgtggcaccagaacgtatcatctatgccaacccatgcaagcagatttcccagattaag  592
V  Q  D  V  G  V  A  P  E  R  I  I  Y  A  N  P  C  K  Q  I  S  Q  I  K   120
tatgcagctaagaatggtgtccaaatgatgacgtttgacaatgaagtagagctttccaaggtgtcaagaagc  664
Y  A  A  K  N  G  V  Q  M  M  T  F  D  N  E  V  E  L  S  K  V  S  R  S   144
catcccaatgcaagaatggttctgcgtatagcaacggatgactctaaatcctctgctcgtttaagtgtgaaa  736
H  P  N  A  R  M  V  L  R  I  A  T  D  D  S  K  S  S  A  R  L  S  V  K   168
tttggcgccccttaaaatcctgcagacgcttattggaaatggctaaaaacctcagtgtggatgtcattggt  808
F  G  A  P  L  K  S  C  R  R  L  L  E  M  A  K  N  L  S  V  D  V  I  G   192
gttagtttccacgttggtagtggatgcactgattccaaggcctatactcaggctatttctgatgcacgcttg  880
V  S  F  H  V  G  S  G  C  T  D  S  K  A  Y  T  Q  A  I  S  D  A  R  L   216
gtttttgaaatggcatctgagtttgggtacaaaatgtggctgctggatattggtggtggcttccctggaaca  952
V  F  E  M  A  S  E  F  G  Y  K  M  W  L  L  D  I  G  G  G  F  P  G  T   240
gaggattccaaaattagatttgaggagattgcaggtgtaataaatccagcactggacatgtatttccctgag 1024
E  D  S  K  I  R  F  E  E  I  A  G  V  I  N  P  A  L  D  M  Y  F  P  E   264
agctctgacgtgcaaattatcgctgaaccaggaagatattacgtagcatctgcttttttcattggctgttaac 1096
S  S  D  V  Q  I  I  A  E  P  G  R  Y  Y  V  A  S  A  F  S  L  A  V  N   288
gttattgctaagaaagaagtggaacactctgtatctgatgatgaggaaaatgagtccagcaaaagcatcatg 1168
V  I  A  K  K  E  V  E  H  S  V  S  D  D  E  E  N  E  S  S  K  S  I  M   312
tattatgttaatgatggagtgtatggatcctttaattgcttggtctttgatcatgctcatccaaaaccaatc 1240
Y  Y  V  N  D  G  V  Y  G  S  F  N  C  L  V  F  D  H  A  H  P  K  P  I   336
ctccacaagaaaccttctccagatcagccattatacaccagtagcctttggggacccacgtgcgatggctta 1312
L  H  K  K  P  S  P  D  Q  P  L  Y  T  S  S  L  W  G  P  T  C  D  G  L   360
gatcagattgcagagcgcgttcagctgcctgagcttcatgttggcgactggcttttgtttgagaatatgggt 1384
D  Q  I  A  E  R  V  Q  L  P  E  L  H  V  G  D  W  L  L  F  E  N  M  G   384
gcatacaccatagcagcatcttccaatttcaatggtttccagcagtctccagtacattacgccatgccccgt 1456
A  Y  T  I  A  A  S  S  N  F  N  G  F  Q  Q  S  P  V  H  Y  A  M  P  R   408
gctgcttggaaagctgttcagttgctgcagagaggattacagcaaaccgaggagaaagaaaatgtgtgcacc 1528
A  A  W  K  A  V  Q  L  L  Q  R  G  L  Q  Q  T  E  E  K  E  N  V  C  T   432
cctatgtcttgtggctgggagatttctgattccttgtgcttcactcgtacctttgcagccaccagcatcatt 1600
P  M  S  C  G  W  E  I  S  D  S  L  C  F  T  R  T  F  A  A  T  S  I  I   456
tgaattcctgcatcatgggagtgacatgcaaatgcttgtcttagcgtagcttgtctcttgtttttaagtatg 1672
stop
caacataaagcatttgtaccttcctggatttgtctctgtatcatctgggagcaatttatgcataagaaacgg 1744
atatttttatcattaattgcatgcagccaccgacatcaattgattttcattaaatttttttttcatttgaaaa 1816
aaaaaaaaaaaaaaaaaaaaaaaaa                                               1842
```

(B)

```
XODC2    MQGYIQES.DFNLVEEGFLARDLMEEIINEVSQTEDRDAFFVADLGDVVRKHLRFLKALP 59
XODC1    -NSFSNDDF-FSFLE---S-R-IVEQK-----LSD-K---Y---F--IVK--V-WF---- 60
hODC     -NNFGNEEF-CHFLD---T-K-ILDQK-----SSD-K---Y---L--ILK--L-WL---- 60
rODC     -GSFTKEEF-CHILD---T-K-ILDQK-----SSD-K---Y---L--VLK--L-WL---- 60
cODC     ..........FTFLD---T-K-ILDQK-----SSD-K---Y---L--IVK--M-WH---- 50

XODC2    RVKPFYAVKCNSSKGVVKILAELGAGFDCASKTEIELVQDVGVAPERIIYANPCKQISQI 119
XODC1    --T--------DGKAI-KT-SIL-A----------Q---SI--S----------V--- 120
hODC     --T--------DSKAI-KT-AAT-T----------Q---SL--P----------V--- 120
rODC     --T--------DSRAI-ST-AAI-T----------Q---GL--P----------V--- 120
cODC     --T--------DSEAV-KT-AVL-A----------Q---SI--P----------L--- 110
                *                *

XODC2    KYAAKNGVQMMTFDNEVELSKVSRSHPNARMVLRIATDDSKSSARLSVKFGAPLKSCRRL 179
XODC1    -Y--SC--EK----S-V--M-VA-N--N-KLV---A-----AVC--------T-KTS-L- 180
hODC     -Y--NN--QM----S-V--M-VA-A--K-KLV---A-----AVC--------T-RTS-L- 180
rODC     -Y--SN--QM----S-I--M-VA-A--K-KLV---A-----AVC--------T-KTS-L- 180
cODC     -H--NS--RM----S-V--M-IA-P--K-KLL---T-----AVC--------T-KTS-L- 170
                                      *          *

XODC2    LEMAKNLSVDVIGVSFHVGSGCTDSKAYTQAISDARLVFEMASEFGYKMWLLDIGGGFPG 239
XODC1    --R--E-NVDII----------PQTYV--V----C--D-GA-L-FN-H---------- 240
hODC     --R--E-NIDVV----------PETFV--I----C--D-GA-V-FS-Y---------- 240
rODC     --R--E-NIDVI----------PETFV--V----C--D-GT-V-FS-Y---------- 240
cODC     --R--E-DLAIV----------PETFV--I----C--D-GA-L-FN-Y---------- 230
                    *                                    ***

XODC2    TEDSKIRFEEIAGVINPALDMYFPESSDVQIIAEPGRYYVASAFSLAVNVIAKKEV..EH 297
XODC1    S--V-LK----TS-------K---AD-G-K----------SFT----I----VMVN-Q 300
hODC     S--V-LK----TG-------K---SD-G-R----------AFT----I----IVLK-Q 300
rODC     S--T-LK----TS-------K---SD-G-R----------AFT----I----TVWK-Q 300
cODC     S--V-LK----TS-------K---LD-E-T----------AFT----I----IVSK-Q 290
                                          *

XODC2    SVSDDE.ENESSKSIMYYVNDGVYGSFNCLVFDHAHPKPILHKKPSPDQPLYTSSLWGPT 356
XODC1    SG----EDAANDKTL--------------ILF----V-PV-T-K-K--EKF-SS-I---- 360
hODC     TG-----.DESSEQTF-------------ILY----V-PL-Q-R-K--EKY-SS-I---- 359
rODC     TG-----.DESNEQTL-------------ILY----V-AL-Q-R-K--EKY-SS-I---- 359
cODC     TG-----.DDVNDKTL-------------ILY----V-PV-Q-R-K--DGC-SC-I---- 349
                        *        *

XODC2    CDGLDQIAERVQLPELHVGDWLLFENMGAYTIAASSNFNGFQQSPVHYAMPRAAWKAVQL 416
XODC1    -----R-V--FEL--LQ----M----------V--A-T-----RPTLY-V-SRPH-QLMHD 420
hODC     -----R-V--CDL--MH----M----------V--A-T-----RPTIY-V-SGPA-ELMQQ 419
rODC     -----R-V--CSL--MH----M----------V--A-T-----RPNIY-V-SRSM-QLMKQ 419
cODC     -----R-V--CNM--LQ----I----------V--A-T-----RPTIH-V-SRPA-QLMQQ 409
         **                        *        *
XODC2    LQRG..LQQTEEKENVCTPMSCGWEISDSLCFTRTFAATSII 456
XODC1    IKEHGILPEVP..DLSALHV--AQ-SGMELAPAVCTA-SINV 460
hODC     FQNPDFPPEVEEQDASTLPV--AW-SGMKRHRAACAS-SINV 461
rODC     IQSHGFPPEVEEQDVGTLPM--AQ-SGMDRHPAACAS-SINV 461
cODC     IKEQEFLAEVEEQDVASLPL--AC-SGIE-YPATCAS-SINV 450
```

Fig.3.1 XODC2 is a paralogue to ubiquitous ODCs. (A) Conceptual translation of XODC2. The putative translation start codon is preceded by a stop codon 21 triplets upstream (underlined). (B) Multi-alignment of amino acid sequences of *Xenopus* ODC2 (XODC2) and the ubiquitous ODCs from *Xenopus laevis* (XODC1), human (hODC), rat (rODC) and chicken (cODC). Amino acids marked underneath with asterisks are active sites in ODCs. Dashes represent identical residues. Dots are introduced for optimal alignment. The same as in following alignments.

likely represents a paralogue of *Xenopus* ubiquitous ODC (Bassez et al., 1990; hereafter designated as XODC1). Here the cDNA was designated as *XODC2* (Genbank accession number: AF217544).

3.1.2 cDNA and amino acid sequences of *XCL-2*

A cDNA sequence of 2033 bp was obtained from clone 18G11. However, it was found that the coding region of this cDNA was not complete at its 5'-end. Therefore, 5'RACE (Rapid Amplification of cDNA ends; Frohman et al., 1988) was employed to extend the coding sequence to the 5'-end. Finally, a cDNA

sequence of 2639 bp with a complete ORF for a Calpain protein large subunit was obtained (Fig.3.2A). The protein was found to be mostly related to rat

(A)

```
                                        aatctgactctgcaaagtctgggacaccaaaaggcccatc    40
atgtcgagaagtgctgctgtgatagccaaggacaggacattggctgatggtggtggaacgaagaggaaccca   112
M  S  R  S  A  A  V  I  A  K  D  R  T  L  A  D  G  G  G  T  K  R  N  P     24
gaaaaatatttggatcaagaatttgagaagctgagggcacaatgcttggcatctggtgctctgtataaagat   184
E  K  Y  L  D  Q  E  F  E  K  L  R  A  Q  C  L  A  S  G  A  L  Y  K  D     48
gaagaattcccagcatgcccatctgcactgggttacaatgaactaagacccggctcatacaaaaccagtggg   256
E  E  F  P  A  C  P  S  A  L  G  Y  N  E  L  R  P  G  S  Y  K  T  S  G     72
gtcatatggaagagacctacggaaatttgtcccaacccccagttcattgtggatggagcaacacgaggagac   328
V* I  W  K  R  P  T  E  I  C  P  N  P  Q  F  I  V  D  G  A  T  R  G  D     96
atccgtcaaggggccctcggggattgctggcttctggctgccatcgcatctcttacactggagccagatctt   400
I  R  Q  G  A  L  G  D  C  W  L  L  A  A  I  A  S  L  T  L  E  P  D  L    120
gtagctcaagtggttcctgagaatcaaagtttccagaaaaactacgctggaatcttccacttccggttctgg   472
V  A  Q  V  V  P  E  N  Q  S  F  Q  K  N  Y  A  G  I  F  H  F  R  F  W    144
cagtatggagagtgggtggatgtggtggtggatgaccggctgccgacaaagaatgggaaactggtatttgtc   544
Q  Y  G  E  W  V  D  V  V  V  D  D  R  L  P  T  K  N  G  K  L  V  F  V    168
cactcagcagaaggggatgagttctggagtgctctgcttgaaaaggcctacgcaaagttgaacggctcctac   616
H  S  A  E  G  D  E  F  W  S  A  L  L  E  K  A  Y  A  K  L  N  G  S  Y    192
gaggctctgactggcggttctaccatagagggatttgaagactttaccggaggtatcgctgaggtgtatgaa   688
E  A  L  T  G  G  S  T  I  E  G  F  E  D  F  T  G  G  I  A  E  V  Y  E    216
ctgaagaaggctccacctaatttattccagatcatccagaaagcccttaaggctgaatcactgcttggctgc   760
L  K  K  A  P  P  N  L  F  Q  I  I  Q  K  A  L  K  A  E  S  L  L  G  C    240
tctattgatattacaaacgcctatgatactgaagccatcacaagcagaaagctggttaaagggcacgcctat   832
S  I  D  I  T  N  A  Y  D  T  E  A  I  T  S  R  K  L  V  K  G  H  A  Y    264
tctgtcactggtgctgaggaggtgttgtacagaggtcgccaggagaagttgatccgagtgagaaatccctgg   904
S  V  T  G  A  E  E  V  L  Y  R  G  R  Q  E  K  L  I  R  V  R  N  P  W    288
ggtgaggtagaatggactggaccttggagtgatgaggctccagaatggaattatgttgatccaaaagtaaaa   976
G  E  V  E  W  T  G  P  W  S  D  E  A  P  E  W  N  Y  V  D  P  K  V  K    312
gctgttctggataaaaaatctgaggatggagaattttggatggcgttttcagactttctcagagagtattcc  1048
A  V  L  D  K  K  S  E  D  G  E  F  W  M  A  F  S  D  F  L* R  E  Y  S    336
cgtctggagatctgtaacctgtctcctgacaccctcaccagcaaccaccaacataaatggaacataacattg  1120
R  L  E  I  C  N  L  S  P  D  T  L  T  S  N  H  Q  H  K  W  N  I  T  L    360
tacaccgggagctgggcacgggggtctactgccggaggctgccaaaattacccagcaacattttggaccaac  1192
Y  T  G  S  W  A  R  G  S  T  A  G  G  C  Q  N  Y  P  A  T  F  W  T  N    384
ccgcaatttcgcattaaactggatgagcccgatgatgatcatcaggggacgaacaatgagccgtgctgtacc  1264
P  Q  F  R  I  K  L  D  E  P  D  D  D  H  Q  G  T  N  N  E  P  C  C  T    408
gtcattgtgggactgatgcagaaaaaccgcagaagaaagaagaagatgggggaggacttgctcagcattggc  1336
V  I  V  G  L  M  Q  K  N  R  R  R  K  K  K  M  G  E  D  L  L  S  I  G    432
tactcactctttaagatccctgatcagcttcaggaccatacagatgcccacctcggcagggacttcttgcaa  1408
Y  S  L  F  K  I  P  D  Q  L  Q  D  H  T  D  A  H  L  G  R  D  F  L  Q    456
aagactccaacggccgcccgatctgacacctatatcaacgtacgggaggtgtccaaccgcttccacctaccg  1480
K  T  P  T  A  A  R  S  D  T  Y  I  N  V  R  E  V  S  N  R  F  H  L  P    480
gtcggggattatctgattgtgccatccacctttgagccctttaaaaatggcgacttctgccttcgtgtcttc  1552
V  G  D  Y  L  I  V  P  S  T  F  E  P  F  K  N  G  D  F  C  L  R  V  F    504
tcagaaaaggaggccaaatcgctagaagttggtgatgtagtgattgcgaaaccatatgaacctcagatttct  1624
S  E  K  E  A  K  S  L  E  V  G  D  V  V  I  A  K  P  Y  E  P  Q  I  S    528
aacaaggatgtccctgatgatttcaagaatatttttgacaagctggcgggagataaagaagaagttgatgca  1696
N  K  D  V* P  D  D  F  K  N  I  F  D  K  L  A  G  D  K  E  E  V  D  A    552
agagaacttcaaaccattctaaataaactcatttcaaagaggccggacttgagatccaatggatttactctt  1768
R  E  L  Q  T  I  L  N  K  L  I  S  K  R  P  D  L  R  S  N  G  F  T  L    576
aacacatgcagagagatgatcagcttacaagatatggatggaaccgcaacactgagccttctggagttccgt  1840
N  T  C  R  E  M  I  S  L  Q  D  M  D  G  T  A  T  L  S  L  L  E  F  R    600
attctgtggatgaagatacagaaatatttggcaatctatttaaaggcagactcggatcgttctggaatcatg  1912
I  L  W  M  K  I  Q  K  Y  L  A  I  Y  L  K  A  D  S  D  R  S  G  I  M    624
gactctcatgagctgagaacagctttgcaagaagcaggttttactctgaataataagatccatgaatcaatt  1984
D  S  H  E  L  R  T  A  L  Q  E  A  G  F  T  L  N  N  K  I  H  E  S  I    648
gtgcagcgctacgcatccaatgacctggctcttaactttgatggctttatcgcttgtatgatgcgcctggag  2056
V  Q  R  Y  A  S  N  D  L  A  L  N  F  D  G  F  I  A  C  M  M  R  L  E    672
accttgttcaaaatgtttcagatgttggacaagagtaagagaggggtcgttgagctgagtttacaagagtgg  2128
T  L  F  K  M  F  Q  M  L  D  K  S  K  R  G  V  V  E  L  S  L  Q  E  W    696
ctctgcgcaacattggtctgaacctttactgccgtcgctgtgcaattctgtctccgtctggaagtgcattgc  2200
L  C  A  T  L  V  stop                                                     702
acttgatgtaaaaacagatacacacacacatgtaaatgagagaatatttgtaaaatagaatattatttcttg  2272
gaaaggttgttacgcacagataatgacatgtatgtgcactcgtttgaagggatggttcacctttgggttaac  2344
ttttggtatgttatagaatgccctattcatagcaatttttcaattggtcttcattatttatttgtataggt  2416
ttttaagtatttgccccatctcctgactcttcccggctttcaaatgggtcactgaccccatttaaaacagat  2488
gctttgtaaggctacagatttagtgggttatttattaaatatcaaattgtgacatctcaaaaaattcactag  2560
aaaacttgaatttttagagggaaaaaaagtttttcaagatttattataccttgatgctgcaaaaaaaaaaa  2632
aaaaaaa                                                                    2639
```

(B)

```
XCL-2       MSRSAAVIAKDRTLADGGGTKRNPEKYLDQEFEKLRAQCLASGALYKDEEFPACPSALGY 60
nCL-2       -AAL--GVS-Q-AV-E-L-SNQNAVK--G-DFET--KQ--NS-V-FK-PE---C-S---Y 60
hCalpain    -AGI--KLA-D-EA-E-L-SHERAIK--N-DYEA--NE--EA-T-FQ-PS---I-S---F 60
cCalpain    -AGM--ALA-E-AA-A-A-RHGQAVP--G-DFGA--RE--QG-R-FH-PS---G-A---Y 60

XCL-2       NELRPGSYKTSGVIWKRPTEICPNPQFIVDGATRGDIRQGALGDCWLLAAIASLTLEPDL 120
nCL-2       KD-G-G-PD-Q-IV-K----L-PN-Q--VG----T--R--G-V-------------NEKL 120
hCalpain    KE-G-Y-SK-R-MR-K----I-AD-Q--IG----T--C--A-G-------------NEEI 120
cCalpain    RE-G-N-YK-K-VV-C----L-SC-R--AG----T--C--A-G-------------NEEI 120

XCL-2       VAQVVPENQSFQKNYAGIFHFRFWQYGEWVDVVVDDRLPTKNGKLVFVHSAEGDEFWSAL 180
nCL-2       LYR-L-RD----KD-------Q--------E--I-------N-Q-L-L--E--N------ 180
hCalpain    LAR-V-LN----EN-------Q--------E--V-------D-E-L-V--A--S------ 180
cCalpain    LAR-V-RD----DE-------Q--------D--V-------N-E-L-V--A--S------ 180

XCL-2       LEKAYAKLNGSYEALTGGSTIEGFEDFTGGIAEVYELKKAPPNLFQIIQKALKAESLLGC 240
nCL-2       -------L--S----V--S-I----------S-F-D-K-P-E--YY------RKG----- 240
hCalpain    -------I--C----S--A-T----------A-W-E-K-P-P--FK------QKG----- 240
cCalpian    -------L--S----S--T-T----------A-W-E-Q-A-P--FK------QKG----- 240

XCL-2       SIDITNAYDTEAITSRKLVKGHAYSVTGAEEVLYRGRQEKLIRVRNPWGEVEWTGPWSDE 300
nCL-2       ---VST-AEA--T-RQ------------V---NFH-RPE----L---------S-A-S-N 300
hCalpain    ---ITS-ADS--I-FQ------------A---ESN-SLQ----I---------T-R-N-N 300
cCalpain    ---ITS-AET--V-SQ------------A---NFR-SIQ----I---------T-K-N-N 300

XCL-2       APEWNYVDPKVKAVLDKKSEDGEFWMAFSDFLREYSRLEICNLSPDTLTSNHQHKWNITL 360
nCL-2       A-E-NYI--RRKEE-DKKA-------S-S---KQ---------S--S-S-EEIH--NLVL 360
hCalpain    C-S-NTI--EERER-TRRH-------S-S---RH---------T--T-T-DTYK--KLTK 360
cCalpain    C-N-SGV--EVRER-TRRH-------A-N---RH---------T--T-A-DRYK--SLLK 360

XCL-2       YTGSWARGSTAGGCQNYPATFWTNPQFRIKLDEPDDDHQGTNNEPCCTVIVGLMQKNRRR 420
nCL-2       FN-R-T--S-----L---G-Y-T---FK-H-D-V-E-QEEGTS-PC--VLL--M--N--R 420
hCalpain    MD-N-R--S-----R---N-F-M---YL-K-E-E-E-EEDG..-SG--FLV--I--H--R 418
cCalpain    LD-N-R--A-----R---N-F-T---YL-K-E-E-E-PDDP..-GG--FLI--I--H--K 418

XCL-2       KKKMGEDLLSIGYSLFKIPDQLQDHTDAHLGRDFLQKTPTAARSDTYINVREVSNRFHLP 480
nCL-2       QKRI-QGMLS--YAVYQI-KELESH-DA--GRD-FLGRQPSTC-S-YM-L---SS-VR-- 480
hCalpain    QRKM-EDMHT--FGIYEV-EELSGQ-NI--SKN-FLTNRARER-D-FI-L---LN-FK-- 478
cCalpain    QRKM-EDMHT--FAIYEV-PEFSGQ-NI--SKN-FLTNKAREK-N-FI-L---LN-FK-- 478

XCL-2       VGDYLIVPSTFEPFKNGDFCLRVFSEKEAKSLEVGDVVIAKPYEPQISNKDVPD.DFKNI 539
nCL-2       P-Q-LV-------FKD----L------K-KALEIG-TVSGHPH-PHPRDM-EEDEHVRSL 540
hCalpain    P-E-IL-------NKD----I------K-DYQAVD-EIEANLE-FDISED-IDD.GVRRL 537
cCalpain    A-E-II-------NLN----L------N-NSTVID-EIEANFE-TEIDED-IEP.SFKKL 537

XCL-2       FDKLAGDKEEVDARELQTILNKLISKRPDLRSNGFTLNTCREMISLQDMDGTATLSLLEF 599
nCL-2       -EEFV-KDS-IS-NQ-KRV-NEVLS--T-MKFD--NIN--RE-ISLL-S--TGS-GPM-- 600
hCalpain    -AQLA-EDA-IS-FE-QTI-RRVLA--Q-IKSD--SIE--KI-VDML-S--SGK-GLK-- 597
cCalpain    -GQLA-SDA-IS-FE-RSI-NKILA--Q-IKSD--SIE--KI-VDLL-N--SGK-GLK-- 597

XCL-2       RILWMKIQKYLAIYLKADSDRSGIMDSHELRTALQEAGFTLNNKIHESIVQRYASNDLAL 659
nCL-2       KT--L--RT-LE-FQEM-HNHV-TIEAH-M-T--KK---TLNNQVQQT-AM-Y-CSK-GV 660
hCalpain    YI--T--QK-QK-YREI-VDRS-TMNSY-M-K--EE---KMPCQLHQV-VA-F-DDQ-II 657
cCalpain    HT--T--QK-QK-YREI-VDRS-TMNSY-M-R--EA---KLSCQLHQI-VA-F-DED-II 657

XCL-2       NFDGFIACMMRLETLFKMFQMLDKSKRGVVELSLQEWLCATLV 702
nCL-2       D-NGFVA-MI-----F-L-RL--KDQN-IVQ-S-AE--CCVLV 703
hCalpain    D-DNFVR-LV-----F-I-KQ--PENT-TIE-D-IS--CFSVL 700
cCalpain    D-DNCVR-LI-----Y-M-RK--TEKT-TIE-N-IN--FFTVI 700
```

Fig.3.2 XCL-2 is novel member of m-type Calpain protease family. (A) Conceptual translation of XCL-2. The putative translation start codon is preceded by a stop codon 12 triplets upstream (underlined). The four domains are separated by asterisks, the tentative active sites Cys 105, His 262 and Asn 286 in proteolytic domain are in bold and the four calcium-binding EF-hand motifs in Ca^{2+} domain are underlined. (B) Multi-alignment between the amino acid sequences of XCL-2, rat stomach-specific m-type Calpain nCL-2, human ubiquitous m-type Calpain (hCalpain), and chicken ubiquitous m-type Calpain (cCalpain).

stomach-specific m-type Calpain nCL-2 (Sorimachi et al., 1993), with 64% identity in amino acids, and ubiquitous m-type Calpains in species such as human and chicken, both with 60% identity (Fig.3.2B). Moreover, the protein

has exactly the same domain structure, the calcium-binding motifs (EF-hands) and the three active sites (Cys 105, His 262 and Asn 286) in proteolytic domain, as in other typical Calpains (Arthur et al., 1995; Sorimachi et al., 1997; Fig.3.3). It was hence designated as *Xenopus* CL-2 *(*XCL-2*)* (Genbank accession number: AF212199).

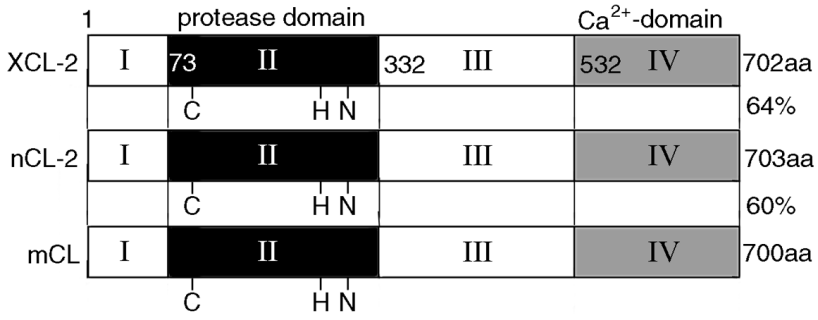

Fig.3.3 Schematic structure of XCL-2, nCL-2 and the ubiquitous m-type Calpain large subunit (mCL). The four domains are indicated with I, II, III, and IV, respectively; per-centages represent the identities between XCL-2, nCL-2 and ubiquitous Calpains in human or chicken; and C, H and N are the three active sites in Fig. 3.2A. aa, amino acid.

3.1.3 cDNA and amino acid sequences of *XETOR*

A cDNA sequence of 2377 bp was obtained from clone 18H2. Similarly, the coding region of this cDNA was not complete at its 5'-end, either, and 5'RACE was again applied to extend the coding sequence to the 5'-end. Finally, a cDNA sequence of 2936 bp with a complete ORF was obtained (Fig.3.4A). The complete open reading frame encodes a protein of 586 amino acids with an overall homology of 72% to MTG8-like protein MTGR1, 59% to ETO in human and 29% to Nervy in *Drosophila* (Fig.3.4B). *MTG8* (also known as *ETO* or *CDR*) is a proto-oncogene because it composes most of the fusion transcript that is consistently present in acute myeloid leukemias containing the t(8;21) translocation. XETOR in structure like other ETO/MTG8 related proteins has four conserved domains termed Nervy Homologous Regions (NHRs; NHR1, aa101-198; NHR2, aa336-363; NHR3, aa426-474; NHR4, aa497-534; Fig.3.4B) because they share greater than 45% homology in these regions. Analysis of NHR1 showed that it is homologous to TATA-binding protein-associated factors (Erickson et al., 1994; Feinstein et al., 1995) and NHR2 is a helical domain (Kitabayashi et al., 1998) with an oligomerization function (Zhang et al., 2001). NHR3 has also a helical structure (Hildebrand et al., 2001). While NHR4 corresponds to two zinc-finger motifs (-C-x-x-C-7x-C-x-x-C-; -C-x-x-x-C-7x-H-

x-x-x-C-; Fig.3.4B)(Feinstein et al., 1995; Kitabayashi et al., 1998). It was therefore named as *Xenopus* ETO Related protein (XETOR), and the nucleotide sequence was deposited in Genbank with accession number AF212198.

(A)

```
                                                        ggccctttaaccttctgtgtatt    23
gtagcaacatcaagattatattcattttactggggacttgtgtgacattgtggctttgcatttgctttggataga    98
atggttgggattccaggaccctatcagtttactggggacaagagggtgccagccatgcctgggtctcccatggaa   173
M  V  G  I  P  G  P  Y  Q  F  T  G  D  K  R  V  P  A  M  P  G  S  P  M  E     25
gtgaagatccactccagatcctcgccgccaatcatggcaccacttcctcctgtgaatcctggtggacttcggcct   248
V  K  I  H  S  R  S  S  P  P  I  M  A  P  L  P  P  V  N  P  G  G  L  R  P     50
gtcggctttcccccatcatcacattccaatggtatcaaccattctccccccacacttaatggagccccatcccca   323
V  G  F  P  P  S  S  H  S  N  G  I  N  H  S  P  P  T  L  N  G  A  P  S  P     75
cctcagcgttccagcaatggtccatcatcatcatcctcctcttccctggccaatcagcagcttcctgccacctgt   398
P  Q  R  S  S  N  G  P  S  S  S  S  S  S  L  A  N  Q  Q  L  P  A  T  C     100
ggggtgaggcaactcagcaaactgaaaagatttctcactacattgcagcagtttggaaacgacatctctccagag   473
G  V  R  Q  L  S  K  L  K  R  F  L  T  T  L  Q  Q  F  G  N  D  I  S  P  E     125
atagggaaaaggtccgcaccctagttttggccctggtgaactcaactgtaaccattgaggaatttcactgcaaa   548
I  G  E  K  V  R  T  L  V  L  A  L  V  N  S  T  V  T  I  E  E  F  H  C  K     150
ctgcaagaagccaccaattttcccttgcgccccttgtcattccattcctgaaggccaacttgcctcttctgcag   623
L  Q  E  A  T  N  F  P  L  R  P  F  V  I  P  F  L  K  A  N  L  P  L  L  Q     175
cgggagttactacactgtgcccgagctggcaagcagacccctcccagtacctggcacagcatgaacatattctc   698
R  E  L  L  H  C  A  R  A  G  K  Q  T  P  S  Q  Y  L  A  Q  H  E  H  I  L     200
ctgaataccagcacttcttccccagcagattcctcagaactgcttatggaaatgaatggcaatgggaaacgacat   773
L  N  T  S  T  S  S  P  A  D  S  S  E  L  L  M  E  M  N  G  N  G  K  R  H     225
agccctgacaggagagaagaagagagagaaactgcacccgcggaacctccagttaagagagtctgcactatcagt   848
S  P  D  R  R  E  E  E  R  E  T  A  P  A  E  P  P  V  K  R  V  C  T  I  S     250
ccagcccccagacacagcccggctttgtccctccctctcgtgaacagcaccagccacttccacccaacaccacca   923
P  A  P  R  H  S  P  A  L  S  L  P  L  V  N  S  T  S  H  F  H  P  T  P  P     275
ccccttcagcactactccttggaggatattcccagctctcagctttacagagaccacctaaacaagatcggcgaa   998
P  L  Q  H  Y  S  L  E  D  I  P  S  S  Q  L  Y  R  D  H  L  N  K  I  G  E     300
caccgggacgttagagatcggcatcacagttctggagtcaatggcaacttaaataatggctaccaggaagaactt  1073
H  R  D  V  R  D  R  H  H  S  S  G  V  N  G  N  L  N  N  G  Y  Q  E  E  L     325
gtagaccatcggctgacagagcgagaatgggcagaagaatggaagcatctggaccatgcattgaactgtatcatg  1148
V  D  H  R  L  T  E  R  E  W  A  E  E  W  K  H  L  D  H  A  L  N  C  I  M     350
gagatggtagagaagactcggcgctcaatggccgtgctgcgtcgctgtcaggaagtggatagagacgagctcaac  1223
E  M  V  E  K  T  R  R  S  M  A  V  L  R  R  C  Q  E  V  D  R  D  E  L  N     375
tactggaaacggagattcaacgagtcaaatgagatccggaagggaagtgagcatcccagcaggcaacatagccct  1298
Y  W  K  R  R  F  N  E  S  N  E  I  R  K  G  S  E  H  P  S  R  Q  H  S  P     400
tccagcaccgattcaggagccagcgattccgttcgtgactttgggagcagaacaggagcaggctatgtaacagat  1373
S  S  T  D  S  G  A  S  D  S  V  R  D  F  G  S  R  T  G  A  G  Y  V  T  D     425
gagatctggagaaaagcagaggaggcagtgaatgaagtcaaacggcaggcaatgtctgaagtacaaaaggctgtc  1448
E  I  W  R  K  A  E  E  A  V  N  E  V  K  R  Q  A  M  S  E  V  Q  K  A  V     450
tcggaagcagagcagaaagcatttgagatgatagcatcagagagagcaaggatggaacagaccattgtggacgca  1523
S  E  A  E  Q  K  A  F  E  M  I  A  S  E  R  A  R  M  E  Q  T  I  V  D  A     475
aagaggagggctgcagaagacgccgtcttggttgtgaatgagcaggaagagtccactgagagctgctggaattgt  1598
K  R  R  A  A  E  D  A  V  L  V  V  N  E  Q  E  E  S  T  E  S  C  W  N  C     500
ggtcggaaagcgagcgagacatgcagtggctgtaacatcgctcgctactgtggctccttctgtcagcacaaggac  1673
G  R  K  A  S  E  T  C  S  G  C  N  I  A  R  Y  C  G  S  F  C  Q  H  K  D     525
tgggagaaacatcaccgcatctgtggccaaagcatgcatacacaggcaaaaccactcaccccatctcgttccctg  1748
W  E  K  H  H  R  I  C  G  Q  S  M  H  T  Q  A  K  P  L  T  P  S  R  S  L     550
atccccaaagcctctgaccccgtccttctgagccccactctggagaggtcttccagcgccacctcacgctcctct  1823
I  P  K  A  S  D  P  V  L  L  S  P  T  L  E  R  S  S  S  A  T  S  R  S  S     575
acacctgcttctgtcactgctgttgatggcctgtgaagagagaatgagaatgagtctttttcccccctatggattt  1898
T  P  A  S  V  T  A  V  D  G  L  stop                                          586
atttacccccttttgcgctcagagtaacataataagtccacgagacagcagcaattcggcctttctctgaagag  1973
aaaatttcatccatcttgatgtatttaaataattgctggtgcagcaaaatacaagaagagacagttaataaagaa  2048
gatgggaaaaaaactgaaatcgcccggagacctattggcccatctctttaaaaaggcaattgcccaaatgggatc  2123
taaattgtgtgtgtatatatatatatatatatttgaaatggacattcatttggctgatttctagtggaccagatt  2198
gctagggacttctatctgggcctcaaagtgttatcccagttatagactgcattctggactaaccaagcaatcggt  2273
atgttcgtgtttggccctttgcatcccgtattttcttgcccagaagaaaaagcagatatgtaatatatctccctca  2348
gcctaacccatgttgtctatcaggaagagtcagcatgagtcgtttggttgttaaatgggcaaatatcagggccat  2423
acaataaagactatttgtgaaactgagattttataagagatcatgtacccccctattgttaagtatgaatatatta  2498
catcacttagcatatggatatgcatatggactgtgctattgtctaggagcagttgtgcctatggctttgcagcac  2573
aagggatttgcaaaatggcagactggccaaaccaaatgtaaacttcagatggattatttttcacttccaaagatg  2648
tcaccaaatatgagattaaattgtcagtctttccgtgtagataatgtaacataataaggattattctcactccgt  2723
attttcgtgtctgttgaaagtgataaacgtttcctcccatcgtcagagctgcgttggttcattgttggaaattgc  2798
tcattttataaagtgctgtttcatgaataagctacatatattatgtgagtcctgtacagattacagatatactaa  2873
tcatttattatggagtttattcaataaagttcattttaccagtaaaaaaaaaaaaaaaaaaaa              2936
```

(B)

```
XETOR    ..........................................................
MTGR1    ..........................................................
ETO      ..........................................................
Nervy    MMALDGKAIIKEEITDKDAYDAAAAAAAAVAAGRALAVASAAAVQVPPASSSSAGSASSA 60

XETOR    .................MVGIPGPYQFTG........DKRVPAMPGSPMEVKIHSRS... 32
MTGR1    ......MAKESGISLKEIQVLARQWKVGP........EKRVPAMPG-PVEVKIQS-S... 43
ETO      ......MISVKRNTWRALSLVIGDCRKKGNFEYCQDRTEKHSTMPD-PVDVKTQS-L... 51
Nervy    AAAATNNTTSAAATAAAISRRLKASSSGGDKSSTSSSSSKDSSHTS-SRSERDRE-ERER 120

XETOR    .............SPP....IMAPLPPVNPGGLRPVGFPPSSHSNGINHSPPTLNGAPSP 75
MTGR1    .............S--....TMP-LP-INPGGPRPVSFTPTALSNGINH-PPTLN-AP-P 86
ETO      .............T--....TMP-.P-TTQGAPRTSSFTPTTLTNGTSH-PTALN-AP-P 93
Nervy    ERERDRLCRTPPDS--DSSRSLA-RS-HSPLQLHQRPQRNASVSPVVNG-SSGGG-VG-S 180

XETOR    PQRSSNGPSSSSSSSLANQQLPATCG....VRQLSKLKRFLTTLQQFGNDIS.PEIGEKV 130
MTGR1    PQRFSNG-A-STSSA-TNQQLPATCG....A-QL--LKR--TT-Q--GNDIS.--IG-K- 141
ETO      PNGFSNG-S-SSSSS-ANQQLPPACG....A-QL--LKR--TT-Q--GNDIS.--IG-R- 148
Nervy    GTSPTPT-G-QHAAS-AAAAAAAAAAHVEQA-LV--MRK--GA-V--SQELGQ--VS-R- 240

XETOR    RTLVLALVNSTVTIEEFHCKLQEATNFPLRPFVIPFLKANLPLLQRELLHCARAGKQTPS 190
MTGR1    -T---A-VNSTVTI---HCK----T-F----F-I-F--ANLP-L---L-HC--AAK-TPS 201
ETO      -T---G-VNSTLTI---HSK----T-F----F-I-F--ANLP-L---L-HC--LAK-NPA 208
Nervy    -A---S-CSGSISV---RLA----I-L----Y-V-L--NSIA-V---I-AL--ATN-SAL 300
                                  I
XETOR    QYLAQHEHILLNTSTS..SPADSSELLMEMNG...NGKRHSPDRREE...ERETAPAEPP 242
MTGR1    --LAQH-HLLLNTSIA..SPADSSELLMEVHG...--KRPSPE-REENSFDRDTIAPEPP 256
ETO      --LAQH-QLLLDASTT..SPVDSSELLLDVNE...--KRRTPD-TKENGFDREPLHSEHP 263
Nervy    --VTNN-QAVMEFAPHGVASAEFGDIFIQLEAPTS--SSAVFK-RSSDSMMEHGGHNGLQ 360

XETOR    VKRVCTISPAPRHSPALSLPLVNSTSHFHPTPPPLQHYSLEDIPSSQLYRDHLNKIGEHR 302
MTGR1    AKRVCTI-PAPRHS-ALTVPLMNPGGQFHPTPPPLQHYTLEDIATSHLYRE.PNKMLEHR 315
ETO      SKRPCTI-PGQRYS-NNGLSYQ.PNGLPHPTPPPPQHYRLDDMAIAHHYRD.SYRHPSHR 321
Nervy    EWSEYMA-GGAGYP-PPSKRLTLHPAHSVVAYGEYGVSSAEGLPSAAAFMQRDERDLRMS 420

XETOR    DVRDRHHSSGVNGNLNNGYQEELVDHRLTEREWAEEWKHLDHALNCIMEMVEKTRRSMAV 362
MTGR1    EVRD-HHSLGLNG....GYQDELVDHRLTEREWAD---HLDHA----ME--E--R-SMAV 371
ETO      DLRD-NRPMGLHG....TRQEEMIDHRLTDREWAE---HLDHL----MD--E--R-SLTV 377
Nervy    EAQA-HAAPPQRAG-NPQPNPNAAAPGAPGAGGEE---NIHTM----SA--D--K-AITI 479
                                                          II
XETOR    LRRCQEVDRDELNYWKRRFNESNEIRK.GSEHP..SRQHSPSSTDSGASDSVRDFGSRTG 419
MTGR1    -RRCQESDREELNYWKRRYNENTELRKTGTELV..SRQHS-GSADSLSNDSQREFNSRPG 429
ETO      -RRCQEADREELNYWIRRYSDAEDLKKGGGSSSSHSRQQS-VNPDPVALDAHREFLHRPA 437
Nervy    -QQRG.............................IEPQH-NSGQEVTPAAMAELRR..Q 507

XETOR    AGYVTDEIWRKAEEAVNEVKRQAMSEVQKAVSEAEQKAFEMIASERARMEQTIVDAKRRA 479
MTGR1    TGYVPV-FWKKT-E--NK--I--MS-V-K--AE--QK-FEVIAT--AR--QTIADVK-QA 489
ETO      SGYVPE-IWKKA-E--NE--R--MT-L-K--SE--RK-HDMITT--AK--RTVAEAK-QA 497
Nervy    TEEKVA-FKRNA-D--TQ--R--VI-I-R--VA--TR-AEIMTQ--LR--KFFMEMS-HS 567
                                  III
XETOR    AED........AVLVVNEQEESTE**SCWNCGRKASETCSGCN**IAR**YCGSFCQHKDWEKHHR** 531
MTGR1    AED........AFLVINEQEESTE**N--------S-------**I----**GSF--HK--ER--R** 541
ETO      AED........ALAVINQQEDSSE**S--------S-------**T----**GSF--HK--EK--H** 549
Nervy    SGERDLDNKSPSMASAQNGSNLQQ**Q--------T-------**M----**SAS--YR--DS--Q** 627
                                  *  *       *  *  IV *   *       *
XETOR    **ICG**.........QSMHT.........QAKPLTPS.RSLIPKASDPVLLSPTLERSSSATS 572
MTGR1    **L--**.........QNLHGQS....PHGQGRPLL-VGRGSSARSADCSVPSPALDKTSATTS 588
ETO      **I--**.........QTLQA.........QQQGDT-AVSSSVTPNSGAGSP...MDTPPAATP 588
Nervy    **V--**NTRASELSAKHLHSASNLSLRNAMATRSP-TPNSAAHLQAAAAAAAAAAGAREAVSA 687
          *
XETOR    RSSTPASVTAVD..GL..................................... 586
MTGR1    RSST-ASVTAIDTNGL..................................... 604
ETO      RSTT-GTPSTIETTPR..................................... 604
Nervy    PVGG-GAGIAVGTGAGSGGQSGGGGGGGGGGGGGAAAAAVAAATPGALVANGLGSK 743
```

Fig. 3.4 XETOR is a novel member of ETO oncoprotein family. (A) Conceptual translation of XETOR. The translation start codon is preceded by a stop codon 11 triplets upstream (underlined). (B) Amino acid sequence comparison between XETOR and human MTG8-related protein (MTGR1), human ETO and *Drosophila* Nervy proteins. The four conserved Nervy Homologous Regions are underlined and marked with I, II, III, and IV underneath. The two zinc finger motifs (-C-x-x-C-7x-C-x-x-C-; -C-x-x-x-C-7x-H-x-x-x-C-) are in bold and the cysteine and histidine residues in the motifs are marked with asterisks.

3.2 Spatial and temporal expression of *XODC2*, *XCL-2* and *XETOR*

3.2.1 Expression pattern of *XODC2*

The expression of *XODC2* was first detected by whole mount *in situ* hybridization at stage 9 at the animal pole (Fig.3.5D), and increases during gastrulation (Fig.3.5E). At neurula stages the expression shifts to neural folds but more pronounced in the two extreme cranial and caudal regions along the anterior-posterior axis (Fig.3.5F). However, starting from tailbud stage, its expression is gradually restricted to certain tissues: forebrain, inner layer of epidermis of the head area, stomodeal-hypophyseal anlage, frontal gland, ear vesicle, branchial arches, the most anterior neural tube, the inner- and outer fin of the tail and proctodeum (Fig.3.5G, H). This prominent localized expression was also confirmed by histological sections through the head and tail areas (Fig.3.5I, J, K). After stage 34 the expression was no longer detectable by *in situ* hybridization. RT-PCR was also used to study the temporal expression of the gene. It could be shown that this gene is already expressed in the unfertilized egg, but at a very low level. Starting from stage 9 its expression increases gradually and reaches the highest level at the end of neurula and the beginning of the tailbud stage, and then decreases gradually (Fig.3.6).

Since the gene encodes a protein that is highly homologous to *XODC1*, which has been found ubiquitously in almost every cell type studied, it is of certain interest to compare the expression of the two genes. No discernible signals of *XODC2* could be seen in embryos before stage 9, while significant staining is already observed in the animal pole of unfertilized eggs, cleavage and gastrula embryos (Fig.3.5L and data not shown). Starting from neurula stage, expression of *XODC2* is gradually localized as described above, while in contrast, during neurula and tailbud stages, as expected the expression of *XODC1* is ubiquitously observed throughout the whole embryos except cement glands in tailbud embryos (Fig.3.5M, N). Additional studies with RT-PCR demonstrated that *XODC2* is different from *XODC1* in its temporal expression. In the case of *XODC1*, the expression is nearly uniform through all stages examined, but the expression level of *XODC2* varies to a certain degree during embryonic development. It is quite low in embryos before stage 9 followed by a dramatic increase up till stage 29, and then decreases gradually (Fig.3.6). In

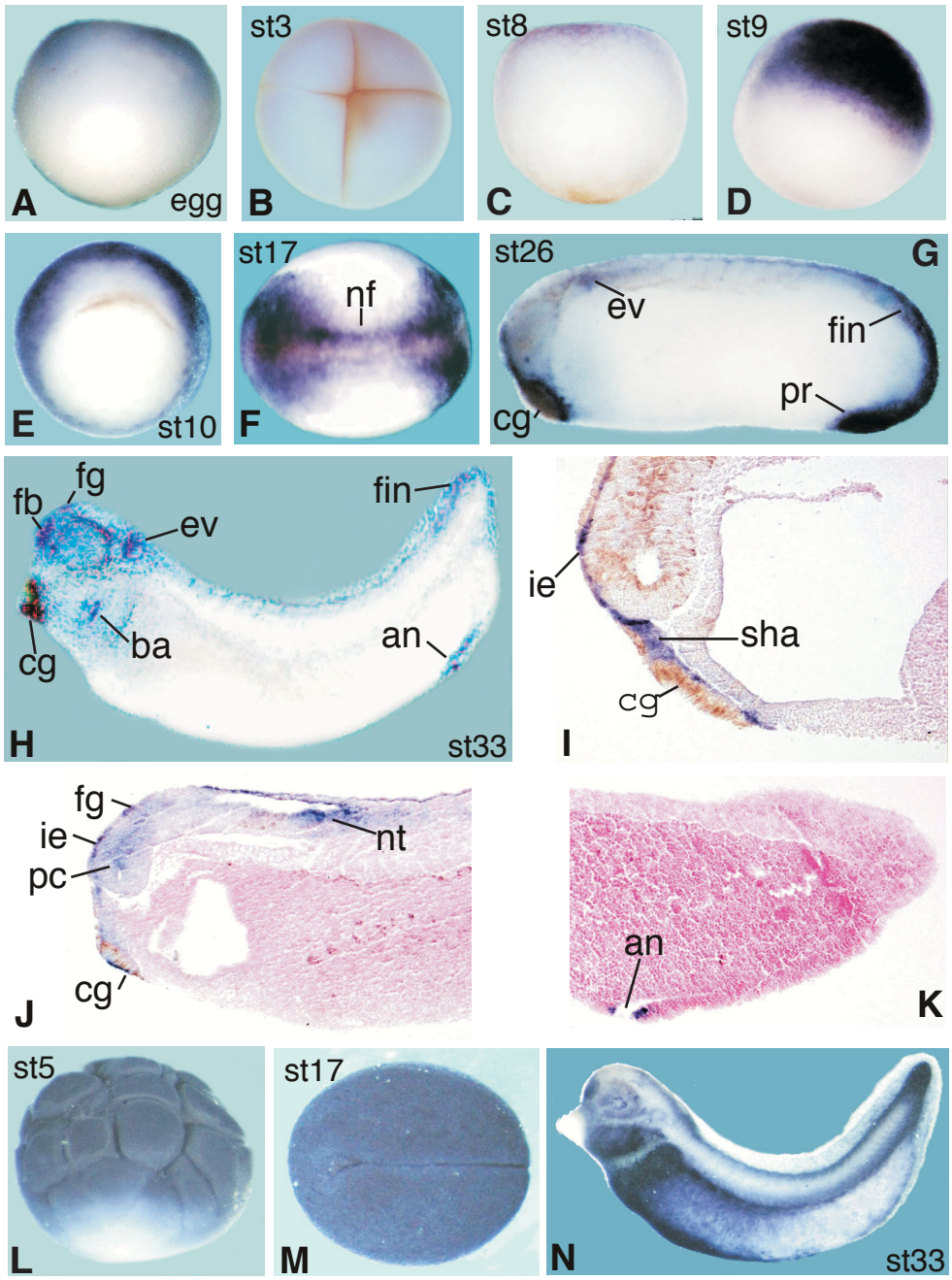

Fig. 3.5 Expression patterns of *XODC2* (A-K) and *XODC1* (L-N) by whole mount *in situ* hybridization. (A-C) Unfertilized egg and early embryos before stage 8 showing no significant signal for *XODC2*. (D, E) Late blastula and gastrula embryos showing strong signal. (F, G) During neurula and early tailbud stages the expression extends to both ends of body axis and becomes gradually localized. (H) stage 33 embryo showing tissue-specific expression in anus, branchial arches, the surface of the lower part of cement gland, ear vesicle, forebrain, frontal gland, and inner- and outer-fin at tail tip. (I) A mid-sagittal section through the head of a stage 26 embryo, showing the expression of *XODC2* in stomodeal-hypophyseal anlage, and the inner layer of epidermis of the forehead area and underneath the cement gland. (J) A mid-sagittal section through the head of a late tailbud (stage 30) embryo, confirming the expression in frontal gland, prosencephalon and lower surface of cement gland, as revealed in (H); moreover, it also confirms its expression in most anterior neural tube. (K) A sagittal section through the tail of a stage 33 embryo confirming the expression of *XODC2* in anus. (L-N) Ubiquitous expression of *XODC1* in early embryogenesis. In all the figures the animal pole or dorsal is up and the anterior is left. an, anus; ba, branchial arch; cg, cement gland; ev, ear vesicle; fb, forebrain; fin, fin; fg, frontal gland; ie, inner layer of epidermis; nt, neural tube; pc, prosencephalon; pr, proctodeum; sha: stomodeal-hypophyseal anlage.

conclusion, by whole mount *in situ* hybridization the author could show the tissue-specific expression pattern of a novel cDNA paralogous to ubiquitous *ODC* in *Xenopus laevis*.

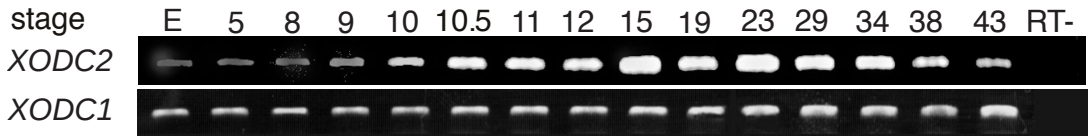

Fig.3.6 Tem-poral expres-sion of *XODC2* and *XODC1* revealed by RT-PCR. The expressions of both genes were detected since unfertilized egg. However, there is little variation in the expression level of *XODC1*, while the expression level of *XODC2* in different stages changes significantly, with quite low level before stage 9 and dramatic increase thenceforth until stage 34. Numbers indicate embryonic stages. E, unfertilized egg; RT-, control reverse transcription without transcriptase.

3.2.2 Expression pattern of *XCL-2*

Spatial expression of *XCL-2* was examined by whole mount *in situ* hybridization. Signals were first detected in the area close to the ventral blastopore lip at stage 12.5 (Fig. 3.7A). As neurulation proceeds, its expression is mainly localized to the most anterior and posterior areas; that is, the most anterior part of the neural plate (Fig. 3.7B) and a very restricted area ventral to the closed slit-like blastopore (Fig. 3.7C). Sagittal histological sections through a stage 15 embryo revealed that in the anterior *XCL-2* was expressed in the mesoderm-free zone at the most anterior tip of neural plate, where the stomodeum and cement gland form. In the posterior area, it was expressed in the ventral part of circumblastoporal collar (Fig. 3.7G). From the late neurula stage, it was expressed significantly in the cement gland and proctodeum (Fig. 3.7D). The staining pattern was also confirmed by sagittal sections through the head or tail area of stage 23 embryos, respectively (Fig. 3.7H, I). After stage 34, expression was only found in the cement gland (Fig. 3.7F). Temporal expression pattern was also examined using RT-PCR. The signal is already detectable at stage 10. The expression level increases gradually during neurulation and

reaches the highest level at stage 30. In the late tailbud and swimming tadpole stages, only low levels were detected (Fig. 3.8A).

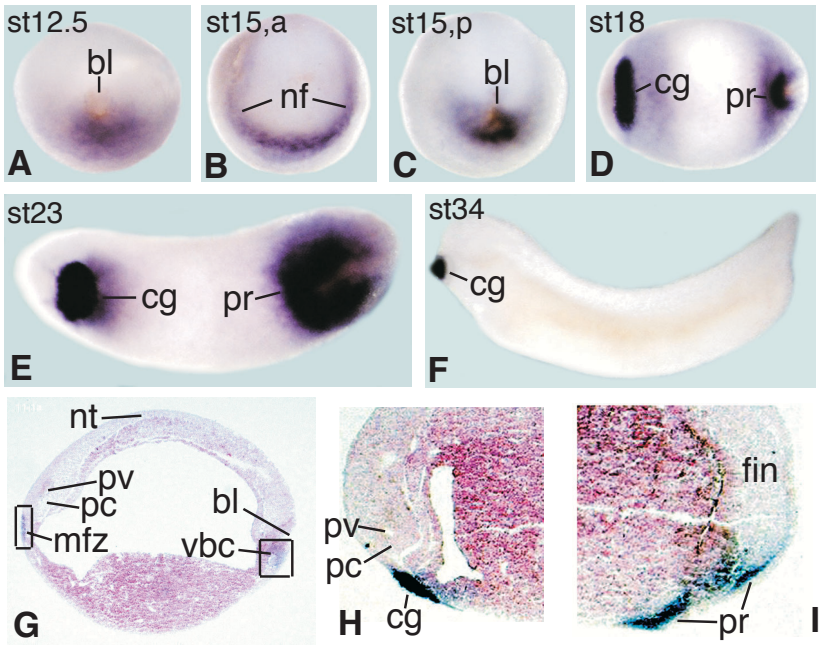

Fig.3.7 Spatial expression of *XCL-2*. (A) Posterior view of stage 12.5 embryos. Dorsal is up. Signal appears at a restricted area ventral to blastopore. (B, C) Anterior and posterior views, respectively, of a same stage 15 embryo. Dorsal is up. In (B), expression is detected at the most anterior of neural plate; in (C) it shows the same expression zone as in (A). (D) Ventral view of a late neurula. Anterior is left. It shows the localized expression in cement gland and proctodeum. (E) Ventral view of an early tailbud. Anterior is left. The expression in cement gland and proctodeum becomes even stronger. (F) In late tailbud stages, expression is only detected in the cement gland. (G) A sagittal section through a stage 15 embryo, confirming that the expression in (B) and (C) is only localized to the mesoderm-free zone and the ventral circumblastoporal collar. The expression zone is highlighted with boxes. (H, I) Sagittal sections through the head and tail of a stage 23 embryo, respectively, confirming that the expression in (E) is only localized to cement gland and proctodeum. a, anterior view; bl, blastopore; cg, cement gland; mfz, mesoderm-free zone; nf, neural fold; nt, neural tube; p, posterior view; pc, prosencephalon; pr, proctoduem; pv, procencephalic ventricle; vbc, ventral circumblastoporal collar.

Expression pattern of *XCL-2* in adult tissues was further examined. RNA was extracted from brain, eye, heart, intestine, kidney, liver, lung, muscle, nerve, ovary, skin, spleen, stomach and testis. Relatively high levels of expression of *XCL-2* were detected in kidney, lung and stomach, and low levels were detected in brain, eye, heart, intestine and testis. Expression was not detected in liver, muscle, nerve, ovary, skin and spleen (Fig. 3.8B). The stomach expression of *XCL-2* confirms that it is closely related to *nCL-2*, which is predominantly expressed in rat stomach (Sorimachi et al., 1993).

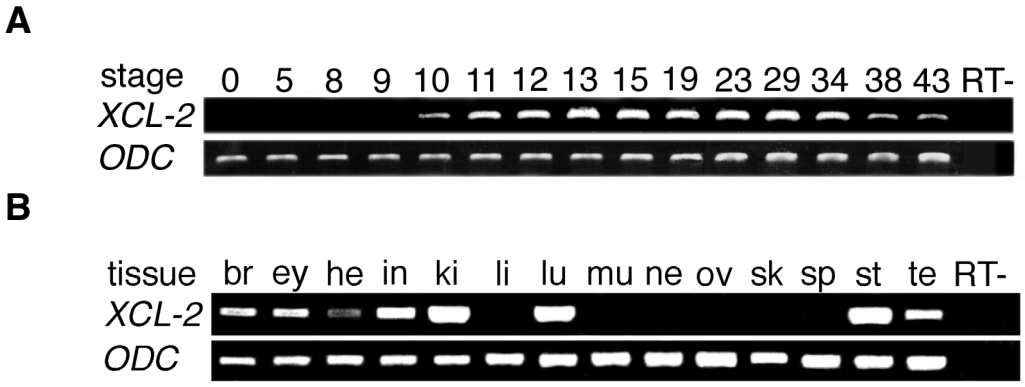

Fig. 3.8 Expression patterns of *XCL-2* detected with RT-PCR. (A) Temporal expression during embryogenesis. Numbers indicate developmental stages. Expression was detected from the onset of gastrulation (stage 10). The expression level continuously increases until the middle of tailbud stage. After approximately stage 30, the expression level decreases gradually. (B) Expression in adult tissues. Various levels of expression of *XCL-2* were detected in adult tissues such as brain, eye, heart, intestine, kidney, lung, stomach and testis, but not in liver, muscle, nerve, ovary, skin and spleen. *ODC* was used as loading control in both cases. br, brain; ey, eye; he, heart; in, intestine; ki, kidney; li, liver; lu, lung; mu, muscle; ne, nerve; ov, ovary; sk, skin; sp., spleen; st, stomach; te, testis; RT-, reverse transcription without reverse transcriptase.

3.2.3 Expression pattern of *XETOR*

XETOR transcripts in the nervous system were first detected within the dorsal ectoderm at stage 12.5 in a pattern of radially symmetrical stripes on either side of the dorsal midline of the posterior neural plate (Fig.3.9A). This pattern grows more prominent with the completion of gastrulation and ongoing of neurulation, after the neural plate has narrowed by convergent extension movements (Fig. 3.9B, D, E). The pattern of three longitudinal domains anticipates the expression of *N-tubulin*, which was previously shown to mark primary neurons. These primary neurons are formed in lateral, intermediate and medial stripes that will differentiate into motorneurons, interneurons and sensory neurons (Rohon-Beard cells), respectively (Oschwald et al., 1991; Chitnis et al., 1995), on either side of dorsal midline. In the anterior neural plate, expression of *XETOR* was also detected in a lateral group of cells associated with trigeminal ganglia, an extreme anterior group of cells associated with olfactory placode, a central stripe corresponding to the sites of future brain and in the prospective anterior neural crest cells (Fig.3.9B, C, D). It is noteworthy that during early stages of neurulation, there is also an expression domain of *XETOR* in the ventral side (Fig.3.9C). This domain is reminiscent of the expression of *Xaml* in

ventral blood island (Tracey et al., 1998). The ventral expression of *XETOR* seems to persist only in a very short time window between stages 12-14. Before and after this time, no expression was observed in this domain at all. Double *in situ* hybridization showed that the expression domain of *XETOR* is overlapping with that of *N-tubulin*. However, the medial stripe of *XETOR* expression is broader than the corresponding stripe of *N-tubulin*, thus some cells located more laterally with respect to dorsal midline expressing *XETOR* do not express *N-tubulin* (Fig.3.9H, I). This may suggest the role of *XETOR* in refining the localization of primary neuron formation. In summary, such an expression pattern shows that *XETOR* is expressed at the location where primary neurogenesis occurs, and hence a marker for early embryonic neurogenesis.

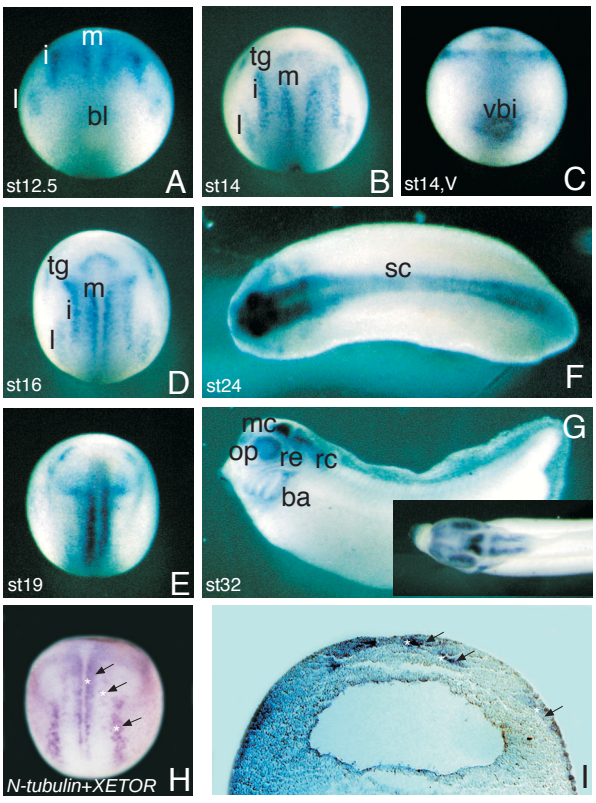

Fig. 3.9 Spatial expression of *XETOR* during embryogenesis revealed with whole mount *in situ* hybridization. (A) From stage 12.5 the signal appears in three stripes marked with l, i and m on each side of the embryo. (B) Expression in stripes grows more prominent as neurogenesis proceeds, and the expression is also observed in the trigeminal ganglia. (C) In addition to expression in neural system, *XETOR* is also expressed in the presumptive ventral blood island. (D) and (E) The expression moves towards the midline as the neural plate narrows due to convergent extension movements. (F) During early tailbud stage, *XETOR* expression is localized to brain and spinal cord. (G) At late tailbud stage, the expression domain in spinal cord disappears but becomes more prominent in midbrain, hindbrain and sensory organs in head area. (H) Double *in situ* hybridization reveals that the expression domain of *XETOR* (purple, and indicated with arrow heads) is overlapping with but broader than that of *N-tubulin* (magenta, and indicated with asterisks), in particular the medial stripe. (I) Transversal section through an embryo in (H) confirms the coexpression of the two genes. (A), (B), (D), (E) and (H) are dorsal view of neurulae, anterior is up; (C) is ventral view of a neurula as in (B), anterior is up; (F) is doral view of a tailbud, anterior is left; (G) lateral and dorsal view (inset) of a same tailbud, anterior is left. ba, branchial arch; bl, blastopore; i, intermediate stripe; l, lateral stripe; m, medial stripe; mc, mescencephalon; op, olfactory placode; rc, rhombencephalon; re, retina; vbi, ventral blood island.

From stage 24 on, *XETOR* was detected to express exclusively in the neural system, incuding the spinal cord, forebrain, midbrain, hindbrain, eyes, and olfactory placodes (Fig.3.9F). At around stage 32, the expression in spinal cord fades out and principally restricts to midbrain, hindbrain and the sensory organs in the head area (Fig.3.9G).

Expression of *XETOR* during secondary neurogenesis was also compared to that of other genes involved in neural development. It can be observed that the expression of *Xngnr-1*, *XDelta-1*, *Xath3*, and *XNeuroD* locates in the inner, mitotically active ventricular zone (Fig. 3.10A, B, C, F). In contrast, *N-tubulin* is expressed exclusively in the outer lateral layer of differentiated cells (Fig. 3.10D). The expression of *XETOR* is different from those above in that the transcripts seem to be distributed evenly in the dorsal part of neural tube (Fig. 3.10E).

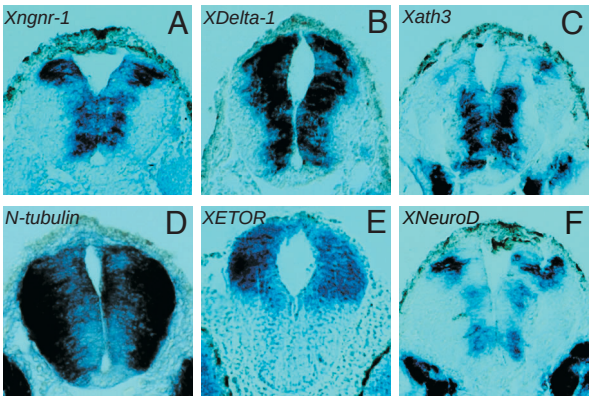

Fig. 3.10 Comparison between expression of *XETOR* (E) and the expression of *Xngnr-1* (A), *X-Delta-1* (B), *Xath3* (C), *N-tubulin* (D), and *XNeuroD* (F) in the neural tube during secondary neuro-genesis. Embryos at stage 32 were hybridized with probes indicated in the figures. Transversal sections were made approximately through hindbrain.

3.3 Functional analyses on *XODC2*, *XCL-2* and *XETOR*

3.3.1 Functional analysis on *XODC2*

mRNA of *XODC2* or *dnXODC2* was injected into either two dorsal or two ventral blastomeres of 4-cell stage embryos. However, no significant disruptions of embryogenesis in response to *XODC2* or *dnXODC2* overexpression were observed (data not shown). This observation suggests that *XODC2* might not play pivotal roles for embryonic development. Therefore, further functional investigation was not made for *XODC2*.

3.3.2 Functional analysis on *XCL-2*

3.3.2.1 Overexpression of *XCL-2* causes severe developmental defects in *Xenopus* embryos

In order to examine the effects of the *XCL-2* gene on the embryonic development of *X. laevis*, various doses of mRNA were injected into embryos at early stages. Injection of mRNA at doses of 2 ng or 2.5 ng into two dorsal blastomeres close to the vegetal pole of the 4-cell stage embryo did not result in significant changes in embryonic morphology (data not shown). However, injections at the equatorial or animal region of two dorsal blastomeres caused significant developmental defects. The percentage of affected embryos rose with the increase in injected dose: 2 ng of *XCL-2* mRNA resulted in 67% of embryos with defects, while 97% of embryos showed defects with a dose of 2.5 ng (Table 3.2). In control embryos injected with 2 ng of β-galactosidase mRNA, only 10% of the injected embryos showed developmental defects (Table 3.2). Affected embryos with *XCL-2* injection first showed a delay in the gastrulation process, which resulted in a distinct phenotype at later stages. At the onset of gastrulation, the dorsal blastoporal lip formed, similar to control embryos. However, as gastrulation proceeded, the injected embryos showed a much larger blastopore and yolk plug (Fig. 3.11B) than untreated controls (Fig. 3.11A). The neural folds of these embryos did not close at the end of neurulation and the blastopore remained open. Therefore, the endoderm involuted only partially. Tailbud stage embryos and swimming tadpoles showed a reduction of the anterior-posterior axis, microcephaly and a bifurcate tail (Fig. 3.11D). The number of affected embryos and the degree of the phenotypic disorder increased with higher doses of injected mRNA (Table 3.2). In some cases, head structures were no longer formed.

Histological sections of the embryos were also prepared to analyze the phenotypic aberrations in more details. Head formation was disturbed to varying degrees in most injected embryos. It was difficult to discriminate between prosencephalon and mesencephalon in most embryos, either. The prosencephalic and mesencephalic ventricles were much smaller than those in normal embryos. However, the rhombencephalon developed quite normally. The embryos generally formed smaller eyes and otic vesicles. In some cases they were totally missing. Another target of defects was the notochord. Most embryos injected with *XCL-2* had notochords with an enlarged anterior part. The elongated part

was oriented in a dorsal-ventral direction. The notochords bifurcated behind the otic vesicles (Fig. 3.11E, F).

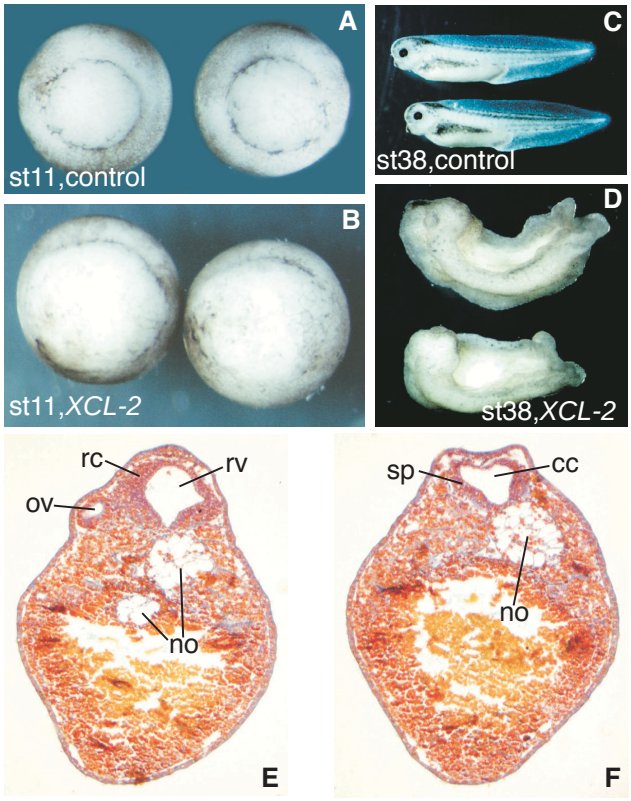

Fig. 3.11 Overexpression of *XCL-2* disrupts gastrulation movements and causes a significant phenotype. mRNA was injected into two dorsal blastomeres at the 4-cell stage. (A) Control embryos at stage 11 with normal blastopores. (B) Injected embryos showing blastopores of a much larger size than in the controls. (C) Control normal swimming tadpoles at stage 38. (D) Injected embryos at the same stage as in (C). The embryos show significant microcephaly (top) and even no discernible head structure (bottom), and shortening of the anterior-posterior axis. The foreheads shift dorsalwards. The endoderm of the embryos can be clearly seen externally and bifurcate tails are formed. (E, F) Transversal sections through the otic vesicle (E) and the trunk region behind the otic vesicle (F) of an injected embryo at stage 30, showing bifurcation and further shifting of notochord towards one side of the body. cc, central canal; no, notochord; ov, otic vesicle; rc, rhombencephalon; rv, rombencephalic ventricle; sp, spinal cord.

3.3.2.2 Ectopic expression of *XCL-2* affects the location of mesodermal or neural markers and disrupts convergent extension

To determine whether ectopic expression of *XCL-2* causes changes in pattern formation, whole mount *in situ* hybridization with different mesodermal and neural markers was carried out. In normal embryos at stage 11, the *Xbra* signal formed a ring around the yolk plug (Fig. 3.12A). However, in embryos injected with *XCL-2*, *Xbra* was still expressed around blastopore but was absent in the dorsal lip (Fig. 3.12D). The expression of *Xvent-1* in the lateral mesoderm was much weaker or even absent in *XCL-2*-injected embryos (Fig. 3.12E), hence expression was more restricted to the ventral-most mesoderm than in the control (Fig. 3.12B). In midgastrulae, *Chordin* and *Xotx2* are normally expressed only in

dorsal blastopore lip (Fig. 3.12C, G), and in late gastrulae or early neurulae *Chordin* is also expressed in the midline (Fig. 3.12M). In contrast, their expression was extended laterally and posteriorly rather than anteriorly in embryos overexpressing *XCL-2* (Fig. 3.12F, J, P). Further analysis with the paraxial mesodermal marker *XMyoD* (Fig. 3.12H, K, N, Q) and the neural marker *Xsox3* (Fig. 3.12I, L, O, R) in midgastrula and midneurula embryos indicated that expression of these genes was not correctly localized compared with control embryos.

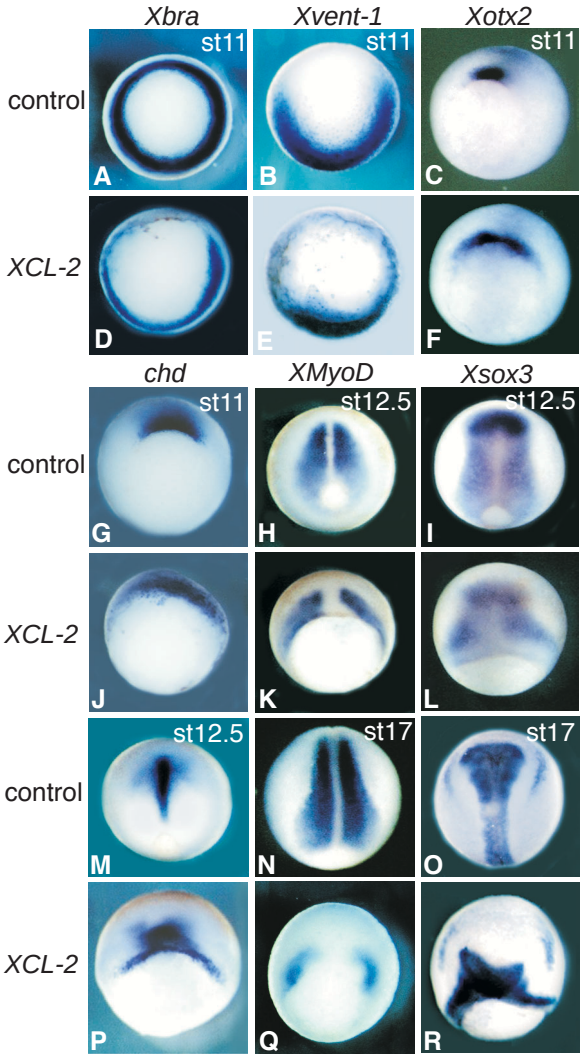

Fig. 3.12 Overexpression of *XCL-2* affects the localization of mesodermal or neural markers and disrupts convergent extension movements. mRNA was injected into two dorsal blastomeres at the 4-cell stage. (A) Expression of *Xbra* is localized to a ring surrounding the blastopore of control midgastrulae. In injected embryos the expression is absent at dorsal blastopore lip (D). (B) In control embryos of mid-gastrulae, *Xvent-1* is expressed in ventral and lateral mesoderm, while overexpression of *XCL-2* renders the expression shift more ventralwards (E). (C) *Xotx2* in control midgastrulae is expressed in the dorsal blastopre lip, but in injected embryos its expression extends laterally (F). (G) *Chordin* (*chd*) is expressed at the dorsal blastopore lip of control midgastrulae and (M) at the midline in late gastrulae, but in injected embryos its expression extends posteriorly and laterally (J, P), showing disruption of convergent extension movement. (H) *XMyoD* is expressed in the paraxial mesoderm in late gastrulae and (N) mid-neurulae, but in injected embryos at equivalent stages (K, Q) it is expressed in a distance away from the midline, showing that paraxial mesoderm does not converge to the midline. (I, O) The neural plate is shown by the neural marker *Xsox3* in normal late gastrulae and mid-neurulae, respectively, and also undergoes convergent extension. However, overexpression of *XCL-2* causes the posterior expression area of *Xsox3* to shift away from the midline, a further indication for the failure of convergence of the posterior neural plate towards the midline (L, R).

These results reveal that XCL-2 affects the localization of mesodermal or neural markers, but does not alter cell fate significantly. In addition, they also show that XCL-2 disrupts convergent extension movements. During gastrulation and neurulation, dorsal tissues, including the prospective notochord, somitic mesoderm and posterior neural plate, converge to the midline of the embryos and extend along the future anterior-posterior axis. This process of convergent extension is a prerequisite for the transformation of the spherical early embryo into an elongated, bilaterally symmetrical organism (Keller et al., 1991; Keller et al., 1992). In normal embryos, *Chordin* was expressed in the midline of late gastrulae or early neurulae formed by convergent extension of the notochord precursor cells (Fig. 3.12M), whereas the expression domain of *Chordin* in *XCL-2* injected embryos was not at the midline but extended laterally and posteriorly (Fig. 3.12P). *XMyoD* is expressed in the dorsal-lateral mesoderm that also undergoes convergent extension to a paraxial position and forms future somites in control embryos (Fig. 3.12H, N). In injected embryos, however, it was expressed some distance away from the midline and towards the posterior (Fig. 3.12K, Q). In addition, the results with the neural marker *Xsox3* reveal that the posterior neural plate of injected embryos also does not converge to the midline (Fig. 3.12L, R) compared with that in the control (Fig. 3.12I, O). This is a further indication of disruption of convergent extension of the posterior neural plate.

3.3.2.3 Overexpression of a dominant-negative type mutant of *XCL-2*

It was subsequently tested in a loss-of-function analysis whether a dominant-negative *XCL-2* mutant interferes with the *in vivo* function of XCL-2. It has been reported that a point mutation of active site Cys 105 functions in a dominant-negative manner *in vivo* (Arthur et al., 1995; Huang and Forsberg 1998; Masumoto et al., 1998). A similar mutant was therefore generated in which Cys105 was changed to serine (hereafter referred to as *C105S*). Different doses of *C105S* mRNA were injected close to the animal pole, equatorial region or vegetal pole of two ventral blastomeres of 4-cell stage embryos. Injection close to the vegetal pole did not result in significant development defects (9%, $n = 53$). When injection was made in the equatorial region, the number of

affected embryos increased (26%, $n = 57$). When injection was done at the animal pole, the number of affected embryos increased more significantly. The affected embryos showed a distinct phenotype (see later). When 1.5 ng of *C105S* was injected, 64% of embryos were affected. A higher dose of 2 ng caused defects in 100% of cases (Table 3.2). Interestingly, overexpression of *C105S* and wild-type *XCL-2* yielded similar phenotypes at the macroscopic level. During midgastrulae, enlarged yolk plugs were observed (Fig. 3.13B), which were not reduced in size in subsequent stages. The endoderm remained externally visible and bifurcate tails were formed (Fig. 3.13D). However, histological sections showed that the notochord malformations and bifurcation of the tail were quite different after *XCL-2* and *C105S* overexpression. In contrast to embryos with *XCL-2* overexpression (Fig. 3.11D, E, F), *C105S*-injected embryos showed a distinct bifurcation of the tail and a branched notochord (Fig. 3.13D, F, G).

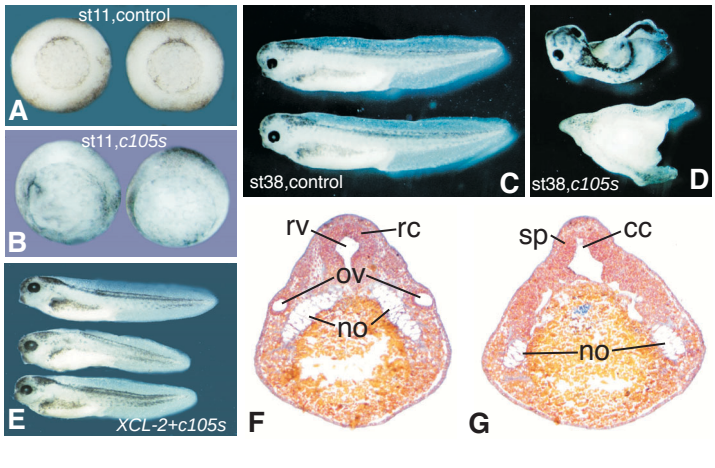

Fig. 3.13 Dominant-negative mutant C105S also disrupts gastrulation movement and results in a significant phenotype, which can be rescued by coinjection with wild-type mRNA. mRNA of *C105S* or *XCL-2* was injected into two ventral blastomeres at the 4-cell stage. (A) Control embryos at stage 11. (B) Injected embryos at an equivalent stage showing larger-sized blasto-pores. (C) Control embryos at stage 38. (D) Injected embryos at an equivalent stage showing nearly normal head structure, externally visible endoderm and bifurcate tail (top) or even no head in an extreme case (bottom). (F, G) Transversal sections through the otic vesicle (F) and the trunk region behind the otic vesicle (G) of an embryo injected with *C105S* at stage 30, showing ventralward movement of otic vesicles, flattening, ventralward bending, bifurcation and further shifting of notochord toward each side of the body (compare Fig. 3.11E, F). (E) Embryos rescued by co-injecting *C105S* and *XCL-2* mRNA. cc, central canal; no, notochord; ov, otic vesicle; rc, rhombencephalon; rv, rombencephalic ventricle; sp, spinal cord.

3.3.2.4 Rescue of the *C105S* phenotype by wild-type *XCL-2*

To test whether the C105S phenotype can be rescued by increasing levels of wild-type XCL-2, *XCL-2* and *C105S* were coinjected in different amounts. It

was found that a ratio of *XCL-2*:*C105S* of 1:2 ng or 2:2 ng did not result in a significant rescue effect (data not shown). When the dose of *XCL-2* was increased to 3 ng, the number of normal embryos increased significantly (44%); 3.75 ng *XCL-2* rescued 83% of the injected embryos. The rescued embryos showed a normal or nearly normal phenotype (Fig. 3.13E). At a higher dose, say, 4.5 ng, the rescue rate decreased again (37%; Table 3.2). These results demonstrate that the mutant functions in a dominant-negative manner and the resultant phenotype can be rescued by the wild-type protein at the right concentration ratio.

Table 3.2 Effect of mRNA overexpression on embryonic development

	Number of embryos/percent		
mRNA injected (ng)	normal	defected	total
XCL-2 (2)	18/33	37/67	55/100
XCL-2 (2.5)	3/3	93/97	96/100
C105S (1.5)	26/36	46/64	72/100
C105S (2)	0/0	69/100	69/100
XCL-2:*C105S* (3:2)	27/44	35/56	62/100
XCL-2:*C105S* (3.75:2)	93/83	19/17	112/100
XCL-2:*C105S* (4.5:2)	31/37	52/63	83/100
LacZ (2)	27/90	3/10	30/100

3.3.3 Functional analysis on XETOR

3.3.3.1 *XETOR* overexpression inhibits formation of primary neurons but does not disrupt the neural plates

XETOR mRNA was injected together with *LacZ* serving as lineage tracer in the equatorial region of one blastomere at 2-cell stage, while the other served as internal control. When the embryos were grown to neural plate stage (stage 14-16), they were fixed and subject to whole mount *in situ* hybridization using primary neuron markers. First, it was observed that expression of *N-tubulin*, a marker gene for differentiated neurons (Oschwald et al., 1991), was dramatically downregulated and even totally eradicated in embryos overexpressing *XETOR* (45/48 embryos; Fig.3.14A). While in control embryos overexpressing only *LacZ*, there was no appreciable change in *N-tubulin* expression (41/43 embryos;

Fig.3.14B). Second, it was also observed that overexpression of *XETOR* inhibited the expression of *Xaml* (29/29 embryos; Fig.3.14C), a sensory neuron marker gene (Tracey et al., 1998; Perron et al., 1999; Koyano-Nakagawa et al., 2000). The evidence did show that XETOR inhibits the formation of primary neurons. Then the following question was asked if the inhibition of primary neurons was the consequence of disruption of neural plate. It was found not to be the case because the expression of a neural plate marker gene *Xsox3* (Penzel et al., 1997) was not affected in response to *XETOR* overexpression (Fig.3.14D). This primary data indicate the specific inhibition of expression of primary neuron marker genes by *XETOR* overexpression, and therefore suggest that XETOR should have functions regulating neuronal differentiation but not neural plate patterning.

3.3.3.2 Truncation mutants of XETOR behave similarly to the wild type protein

All the members of ETO oncoprotein family have four conservative domains (Fig.3.4). Then it is interesting to investigate the functions of these domains for XETOR activity. A series of truncated mutants were made and tested how these mutants behave in primary neurogenesis. p13#trunc1 is composed of aa 1-496, with NHR4 truncated; p13#trunc2 is composed of aa 1-425, with NHR3 and 4 truncated; p13#trunc3 is composed of aa 216-425, with NHR1, 3 and 4 truncated; p13#trunc4 is composed of aa 216-586, with NHR1 truncated; while p13#trunc5 is composed of aa 364-586, with NHR1 and 2 truncated (Fig.3.15). mRNAs of these mutants were injected separately into again one blastomere of 2-cell stage embryos and *N-tubulin* expression was examined. Interestingly, overexpression of either of these mutants caused inhibition of *N-tubulin* expression, resulting in a phenotype similar to that by *XETOR* overexpression (data not shown). In all 25 embryos overexpressing *p13#trunc1*, expression of *N-tubulin* was inhibited; in 25 out of 29 embryos overexpressing *p13#trunc2, N-tubulin* expression was repressed; for *p13#trunc4* and *p13#trunc5* overexpression, *N-tubulin* expression was repressed in 26/26 and 30/36 embryos, respectively. The data demonstrate that the four mutants have effect on *N-tubulin* expression indistinguishable from the wild type protein.

However, although overexpression of *p13#trunc3* inhibits *N-tubulin* expression, too, it behaves not as efficiently as the other mutants and the wild type protein. In 29 embryos, only 14 showed the phenotype of inhibited *N-tubulin* expression (Fig.3.14E). Moreover, the inhibition effect in these affected embryos is also not as robust as in embryos overexpressing the wild type *XETOR* or other mutants, in which the *N-tubulin* expression was completely eradicated in most cases. The data suggest that either NHR1 and 2 together or NHR3 and 4 together are sufficient for functions in the regulation of primary neurogenesis.

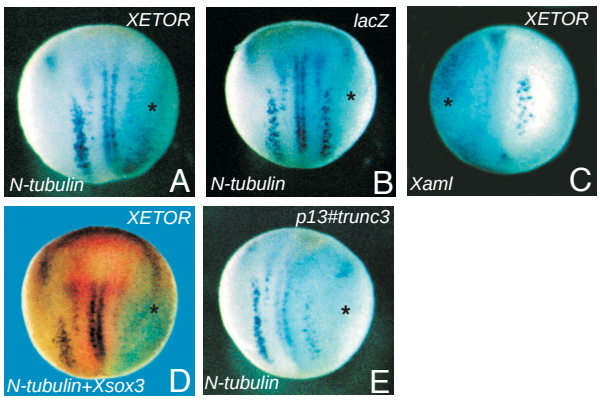

Fig. 3.14 Overexpression of *XETOR* or the truncation mutants inhibit the expression of *N-tubulin*, *Xaml* but not the expression of *Xsox3*. In embryos injected with *XETOR* (A, C and D) or the mutants (E), expression of *N-tubulin* or *Xaml* is dramatically inhibited. However, the expression of *Xsox3* (red signal) is not inhibited in the injected side (D). (B) is a control in which only *LacZ* was injected, the expresion of *N-tubulin* is intact. In all the figures, mRNAs injected are shown in upper right and genes for which expression were detected are shown in lower left. The anterior of the embryos is up. The injected side is marked with X-gal staining, which reveals light blue, and also indicated with an asterisk. The same as in the following figures.

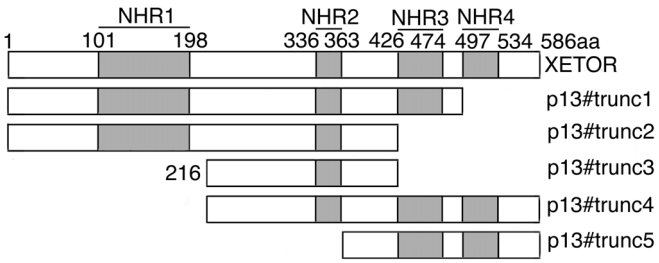

Fig. 3.15 Schematic structures of XETOR and truncation mutants. The four Nervy Homologous Regions are shown in shadowed areas. aa, amino acid.

3.3.3.3 *XETOR* is required for primary neurogenesis

As it was observed that overexpression of *XETOR* and a series of truncated mutants exclusively inhibits the expression of the primary neuron markers *N-*

tubulin and *Xaml*, it is logic to ask the question what would happen if the function of endogenous XETOR is inhibited. Therefore, the antisense morpholino oligo, a gradually popular approach to loss-of-function analysis (Heasman et al., 2000; Deardorf et al., 2001; Dibner et al., 2001; Tan et al., 2001; Zhao et al., 2001), was employed to antagonize the function of XETOR *in vivo*. 7-30 ng of antisense morpholino oligo against *XETOR* (*MOXETOR*) was injected together with *LacZ* into one blastomere at 2-cell stage and the embryos were analyzed with *N-tubulin* expression. It was observed that the lateral stripe

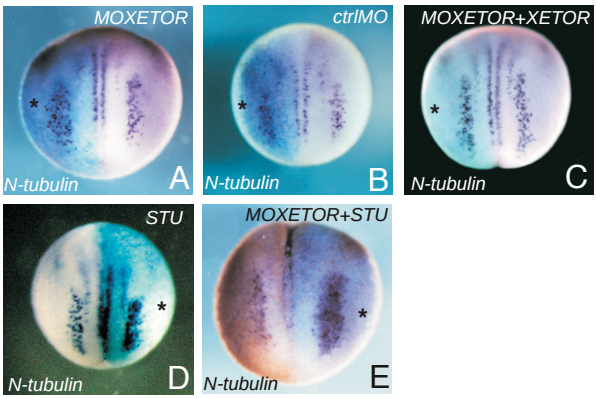

Fig.3.16 XETOR is prerequisite for primary neurogenesis. (A) Injection of the antisense morpholino oligo against *XETOR* (*MOXETOR*) results in an expansion of lateral stripe of *N-tubulin* expression. (B) Injection of a control oligo (*ctrlMO*) does not cause any significant change in *N-tubulin* expression. (C) Co-injection of *MOXETOR* and *XETOR* rescues the pheno-types caused by injection of *XETOR* or *MOXETOR*, suggesting *MOXETOR* speci-fically blocks the function of XETOR. (D) Blocking lateral inhibition by injecting *X-Delta-1*^{STU} results in an increased density of neurons without change in the size of proneural domain. (E) When XETOR and lateral inhibition are both blocked by coinjection of *MOXETOR* and *X-Delta-1*^{STU}, an increased density of primary neurons in a lateral stripe of significantly enlarged size is observed, showing a phenotype distinct from those in (A) and (D).

of *N-tubulin* expression domain expanded but the density of primary neurons looked similar to those in the control side (43/50 embryos, Fig.3.16A). A control morpholino oligo (*ctrlMO*) was also injected, however, no discernible influence was observed on *N-tubulin* expression in response to *ctrlMO* injection (22/26 embryos, Fig.3.16B). This indicates that injection of *MOXETOR* generated a neurogenic phenotype as the neurogenic domain expands. Further injections were made to see if the phenotype by *XETOR* overexpression could be rescued by *MOXETOR*, or vice versa. It proved to be the case because when *XETOR* was coinjected with *MOXETOR*, the expression of *N-tubulin* was neither inhibited

nor increased appreciably (49/55 embryos, Fig.3.16C). These data indicate that the effect of the antisense morpholino oligo is able to abolish specifically the function of *XETOR*. Albeit inhibition of XETOR function results in an increase of neurogenic domain, the salt-and-pepper pattern of primary neuron in the domain seems to be resulted from the action of lateral inhibition. It was further examined, therefore, what would happen when XETOR is eradicated in the absence of lateral inhibition. As previously reported, when lateral inhibition alone was blocked by overexpressing *X-Delta-1*^{STU}, a dominant-negative form of *X-Delta-1*, an increased density of neurons in the lateral stripe was observed as shown by increased *N-tubulin* expression, but the size of the stripe was largely unchanged (Chitnis et al., 1995; Chitnis and Kintner, 1996; Fig.3.16D). However, when *MOXETOR* and *X-Delta-1*^{STU} were coinjected, an increased density of neurons was observed in an enlarged lateral stripe (55/59 embryos; Fig. 3.16E). This phenotype is in striking contrast not only with that generated by *MOXETOR* injection alone (Fig.3.16A) but also with that generated by *X-Delta-1*^{STU} injection alone (Fig.3.16D). These data confirm that XETOR is required for primary neurogenesis.

3.3.3.4 *XETOR* and lateral inhibition are negatively crossregulated

It has been demonstrated that *XETOR* overexpression generated a phenotype similar to that caused by activating lateral inhibition, the primary signaling pathway known so far for repressing neurogenesis. It is therefore important to ask whether the function of XETOR is orchestrated by lateral inhibition or whether there is a crosstalk between XETOR and lateral inhibition. First, it was observed that overexpression of *XETOR* repressed the expression of ligand gene *X-Delta-1* (25/27 embryos; Fig.3.17A). When lateral inhibition was activated by overexpression of *X-Notch-1ICD*, which encodes the constitutively active form of X-Notch-1, expression of *XETOR* was inhibited (24/24 embryos; Fig.3.17B). *XETOR* expression was also tested in embryos in which the lateral inhibition signaling was blocked by overexpressing *X-Delta-1*^{STU}. Similar to the neurogenic phenotype of increased density of neuron formation in the absence of lateral inhibition (Chitnis et al., 1995; Chitnis and Kintner, 1996; Fig.3.16D), it was noted that expression of *XETOR* increased significantly (35/35 embryos),

too, when lateral inhibition signaling was blocked (Fig.3.17C). The data demonstrate that *XETOR* and lateral inhibition signaling are mutually inhibited. Second, as blocking of lateral inhibition signaling can increase the expression of both *XETOR* and *N-tubulin*, it was therefore examined whether *XETOR* still inhibits primary neuron formation in absence of lateral inhibition. It was proved to be the case because *N-tubulin* expression was repressed when *XETOR* was coinjected together with *X-Delta-1*^{STU}, showing that *X-Delta-1*^{STU} does not have any rescuing effect on the inhibition by XETOR (14/15 embryos; Fig.3.17D). These data suggest that XETOR is not a component of lateral inhibition signaling pathway but functions in independence of lateral inhibition.

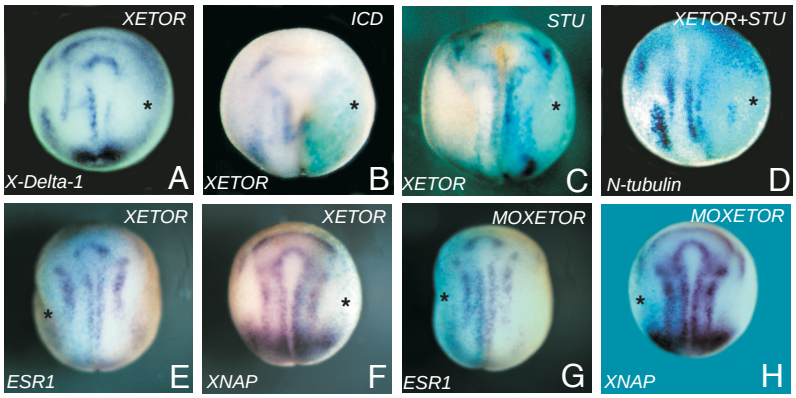

Fig.3.17 *XETOR* and lateral inhibition are mutually repressed and *XETOR* functions independent of lateral inhibition. (A) Overexpression of *XETOR* inhibits the expression of *X-Delta-1*. (B) *XETOR* expression is in turn inhibited by activated lateral inhibition via overexpression of dominant active form of *X-Notch-1*. (C) When lateral inhibition is blocked by overexpressing a dominant negative form of *X-Delta-1*, *XETOR* expression is also augmented. (D) When *XETOR* is co-overexpressed with *X-Delta-1*^{STU}, it still represses the expression of *N-tubulin*, showing that blocking lateral inhibition does not rescue the inhibitory effect of XETOR. (E, F) Overexpressed XETOR does not affect the expression of *ESR1* and *XNAP*. (G, H) XETOR knockout by morpholino oligo does not affect the expression of *ESR1* and *XNAP*, either.

To gain further support for this idea, expression of two Notch downstream targets, *ESR1* (Wettstein et al., 1997) and *XNAP* (Lahaye et al., 2002), were examined in response to *XETOR* overexpression. Both these genes are expressed during primary neurogenesis similarly to other genes involved in Notch signaling, such as *X-Delta-1*. Expression of these genes is positively regulated by Notch pathway. It was observed that, however, no changes occurred in the expression of *ESR1* (40/42 embryos) and *XNAP* (29/29 embryos) in response to

XETOR overexpression (Fig.3.17E, F). Moreover, intact expression of *ESR1* (28/31 embryos) and *XNAP* (30/31 embryos) were likewise observed when endogenous XETOR activity was extirpated via *MOXETOR* injection (Fig.3.17G, H). All the evidence shows that XETOR is not a constituent of the Notch pathway, it works independently for the negative regulation of primary neurogenesis but not via the mediation of lateral inhibition signaling.

3.3.3.5 Crossregulation between the expression of *XETOR* and proneural genes

In order to know more details about the concrete function of *XETOR* during *Xenopus* primary neurogenesis, crossregulation between the expressions of XETOR and proneural genes were examined. Again mRNAs for *XETOR* or other proneural genes along with *LacZ* were injected into one blastomere at 2-cell stage and the other left as internal control, and their expressions were

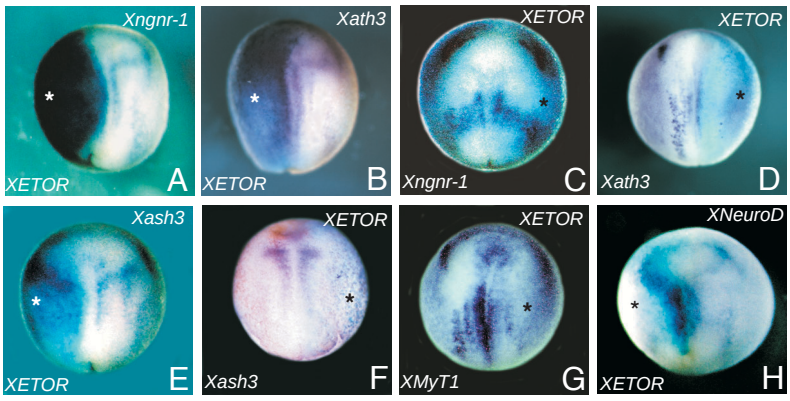

Fig. 3.18 Crossregulation between the expression of *XETOR* and proneural genes. Overexpression of *Xngnr-1* (A) or *Xath3* (B) induces significant ectopic *XETOR* expression. In turn, overexpression of *XETOR* does not affect *Xngnr-1* expression (C), but inhibits *Xath3* expression (D). *XETOR* expression is also activated or enhanced by overexpressed *Xash-3* (E), or *XNeuroD* (H). Conversely, Overexpression of *XETOR* inhibits the expression of *XMyT1* (G), but not *Xash3* (F).

analyzed using whole mount *in situ* hybridization. It was observed that overexpression of both *Xngnr-1* (32/32 embryos; Fig.3.18A) and *Xath3* (25/25 embryos; Fig.3.18B) activated strong ectopic expression of *XETOR*. Conversely, overexpressed *XETOR* had no appreciable effects on the expression of *Xngnr-1* (43/43 embryos; Fig.3.18C), but downregulated the expression of *Xath-3* (20/22 embryos; Fig.3.18D). Overexpression of *Xash-3*, a neural determination gene, caused an enhancement of *XETOR* expression within its normal expression

domains (36/40 embryos; Fig.3.18E), but no discernible change in *Xash-3* expression was observed in response to *XETOR* overexpression (55/59 embryos, Fig.3.18F). It was further observed that expression of the zinc-finger protein gene *XMyT1* was inhibited by *XETOR* overexpression (17/19 embryos; Fig.3.18G), while overexpressed *XMyT1* did not affect *XETOR* expression (data not shown). *XNeuroD*, a gene expressed for terminal differentiation of neurons in later stage, was found to enhance *XETOR* expression, too (37/39 embryos; Fig.3.18H).

3.3.3.6 XETOR overexpression inhibits the function of proneural genes except *Xngnr-1*

The crossregulation at transcriptional level between *XETOR* proneural genes gave rise to another question whether XETOR also regulates these genes post-transcriptionally. mRNA of *XETOR* was coinjected together with mRNA of either of the proneural genes *XMyT1*, *Xash-3*, *Xath3* and *XNeuroD*, and *N-tubulin* expression was analyzed in injected embryos using whole mount *in situ* hybridization. *XMyT1* is a gene with weak neuron inducing activity, overexpression of *XMyT1* results in an increased density of neurons within *N-tubulin* expression domain (Fig.3.19A). It serves to confer insensitivity to lateral inhibition, and when overexpressed together with *Xash-3*, strong ectopic neuron formation is resulted (Bellefroid et al., 1996). While when *XMyT1* was coinjected with *XETOR*, its neuron inducing activity was abolished (Fig.3.19B), showing a decreased expression of *N-tubulin* as compared to the control side (29/29 embryos). Further, it is revealed that overexpressed either *Xath3* or *XNeuroD* causes strong ectopic neuron formation (Fig.3.19C, E), as reported formerly (Lee et al., 1995; Chitnis and Kintner, 1996; Perron et al., 1999). However, ectopic and even endogenous expression of *N-tubulin* was dramatically reduced or totally eradicated in embryos coinjected of *XETOR* with either *Xath3* (23/23 embryos; Fig.3.19D) or *XNeuroD* (10/10 embryos; Fig.3.19F), forming a striking contrast to the control embryos. In the case of *Xash-3*, it enhances neuron formation when overexpressed in low doses while suppresses neuron formation when overexpressed in high doses due to activation of lateral inhibition. Nevertheless, it consistently induces neuron formation

within proneural domains when lateral inhibition is blocked, as shown previously (Chitnis and Kintner, 1996; Fig.3.19J). Here it is shown that, in the absence of lateral inhibition, neuron-inducing activity of Xash-3 was blocked in embryos coinjected with *Xash-3* and *XETOR* (7/8 embryos; Fig.3.19K). These data clearly show that XETOR inhibits not only the expression of these genes, but also their functions *in vivo*.

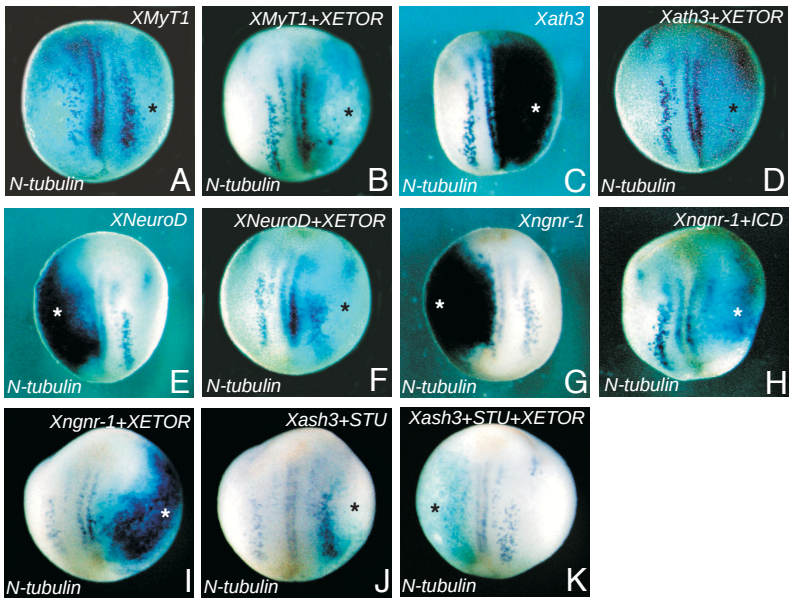

Fig. 3.19 Overexpression of *XETOR* inhibits the function of proneural genes, except *Xngnr-1*. (A) *XMyT1* has a weak neuron-inducing activity, such an activity is inhibited in response to *XETOR* over-expression (B). When over-expressed alone, *Xath3* (C) or *XNeuroD* (E) induces strong ectopic expression of *N-tubulin*; while in contrast, when *XETOR* is coinjected with them (D, F), not only the ectopic but also the endogenous expression of *N-tubulin* is inhibited. (G) Overexpressed *Xngnr-1* induces strong ectopic expression of *N-tubulin*, and (H) such a proneural activity of *Xngnr-1* is inhibited by activated *X-Notch-1*, in contrast overexpression of *XETOR* does not affect the proneural activity of Xngnr-1 (I). (J) When lateral inhibition is blocked, *Xash-3* consistently induces ectopic neuron formation, while this induction is abrogated when coinjected with *XETOR* (K).

It was previously reported that proneural genes have different sensitivity to lateral inhibition (Chitnis and Kintner, 1996). Lateral inhibition tends to repress the functions of genes that are expressed in earlier stages, for instance the neural determination genes *Xngnr-1* and *Xash-3*. But it does not repress the functions of genes that are expressed in later stages, for instance the neural differentiation genes *XNeuroD* and *Xebf3* (Pozzoli et al., 2001). As a result, co-overexpression of *Xngnr-1* and *X-Notch-1ICD* will lead to the inhibition of ectopic neuron

formation by Xngnr-1 (Ma et al., 1996; Fig.3.19H), while co-overexpression of *XNeuroD* and *X-Notch-1ICD* results in a phenotype similar to that by overexpressing *XNeuroD* alone (Chitnis and Kintner, 1996). These data set a groundwork for the idea of different sensitivity of proneural genes to lateral inhibition. Now that it has been shown that XETOR inhibits the function of XNeuroD and XMyT1, which escapes or helps to escape lateral inhibition, then it would be interesting to ask whether XETOR affects the function of earlier proneural genes, albeit it was known at least that overexpression of *XETOR* does not affect the expression of *Xngnr-1*. The findings will address the question whether proneural genes also have different sensitivity to the inhibitory effect of XETOR. As previously shown, overexpression of *Xngnr-1* leads to strong ectopic expression of *N-tubulin* (Ma et al., 1996; Fig.3.19G). When *Xngnr-1* was coinjected with *XETOR*, the ectopic formation of neurons by Xngnr-1 was not significantly affected (15/15 embryos; Fig.3.19I), showing that Xngnr-1 is not sensitive to the inhibition by XETOR at both transcriptional and post-transcriptional levels. Considering together that *Xash-3* is not inhibited transcriptionally, either, these data suggest that proneural genes also have different sensitivity to XETOR inhibition, i.e., earlier genes are refractory while later ones are sensitive to the inhibitory function of XETOR.

4. DISCUSSION

The research done here proved that large-scale whole mount *in situ* hybridization is an efficient way to screen genes involved in embryogenesis from cDNA libraries. The advantage of the approach is that it allows direct identification of single clones and hence single genes according to expression patterns. 29 of 384 single clones were sorted out because of specific expressions. Subsequently, 3 of 29 genes, namely, *XODC2*, *XCL-2*, and *XETOR* were selected for further study based on comparison with Genbank databases and their expression patterns. Actually, XODC2 is a piece of evidence that there exists a second type of ornithine decarboxylase in specific cells besides the ubiquitous form, although no solid indication was acquired in the present study that it plays a significant role in embryonic development. While the other two genes, *XCL-2* and *XETOR*, were shown to play pivotal functions respectively in two developmental procedures: morphogenetic movements and primary neurogenesis.

4.1 XCL-2 and its role during embryogenesis

4.1.1XCL-2 is a novel m-type Calpain and disrupts morphogenetic movements during embryogenesis in *Xenopus laevis*

It has been shown that *XCL-2* encodes a large subunit of m-type Calpain, a novel family member of the calcium-dependent proteases. Typical Calpains, either ubiquitous or tissue-specific, are around 700 amino acids in length and consist of four domains. The first domain is responsible for autolysis, which reduces calcium requirement for proteolytic activity; the second domain has three active sites, Cys 105, His 262 and Asn 286, for proteolytic activity; the third domain has an unknown function; and the fourth domain, comprising EF-hand motifs, is for Ca^{2+} binding. This domain structure and the active sites are

conserved in all typical Calpains identified so far, including XCL-2 in the present study. Therefore, it is reasonable to assume that XCL-2 also possesses the calcium-dependent proteolytic activity. As a prerequisite for functional analyses, whole mount *in situ* hybridization and RT-PCR were performed to examine the expression patterns of *XCL-2* during *X. laevis* development. Using whole mount *in situ* hybridization, embryos showed no detectable signals earlier than the late gastrula stage. Expression was first detected in the area close beneath ventral blastopore lip at around stage 12.5. During neurulation, signals were found in the mesoderm-free zone at the most anterior and ventral parts of the circumblastoporal collar at the most posterior zone. At the tailbud stages, expression was restricted to the cement gland and proctodeum, and to the cement gland only at the late tailbud stages. Using RT-PCR, weak expression could already be observed at stage 10. It also demonstrated the tissue-specific expression of *XCL-2* in adult tissues, such as brain, eye, heart, intestine, kidney, lung, stomach and testis. The relatively high level of expression in stomach suggests that XCL-2 and nCL-2 are evolutionarily conserved homologues. The latter is predominantly expressed in rat stomach.

The restricted expression of *XCL-2* in late gastrulae or early neurulae in the ventral circumblastoporal collar could be suggestive for its function. The circumblastoporal collar, including the dorsal and ventral parts, represents a massive accumulation of mesodermal cells. From this region, dorsal axial mesoderm is continuously generated by radial intercalation and convergent extension. This was the initial impetus to investigate whether XCL-2 could be involved in cell movements during *X. laevis* early embryogenesis.

Overexpression of *XCL-2* and a dominant-negative mutant, *C105S*, were therefore carried out to investigate its functions during early embryogenesis. Injections were made into either two dorsal blastomeres or two ventral blastomeres at the 4-cell stage. It was found that overexpression at the vegetal pole did not affect embryonic development significantly, in contrast to overexpression at the animal pole or even the equatorial region. This is probably due to the fact that the injected RNA at the vegetal pole will mainly be distributed in the endoderm and therefore it cannot exert its activity in the circumblastoporal collar. Therefore the effect of overexpression of the mRNAs at the animal pole was studied.

Overexpression of *XCL-2* results in a delay of the involution of mesoderm. At the beginning of gastrulation, the blastopore in injected embryos formed normally, as in uninjected control embryos. However, during gastrulation the blastopore of injected embryos failed to close and a large yolk plug was observed in subsequent developmental stages. This disturbance of involution generates a significant phenotype. The results suggest that overexpression of *XCL-2* causes the disruption of the blastopore and disturbance of the gastrulation movements. It was examined whether there are obvious cell fate changes in these affected embryos using mesodermal or neural markers, including *Xbra*, *Chordin*, *Xvent-1*, *XMyoD*, *Xotx2* and *Xsox3*. In fact, all of these markers are expressed at similar levels to the controls but are not correctly localized, which suggests that no obvious cell fate alteration takes place, but rather distinct changes in cell migration. Furthermore, it was shown with *Chordin, XMyoD* and *Xsox3* in injected embryos that during gastrulation and neurulation the mesoderm and the posterior neural plate do not converge towards the midline, as in normal embryos. These data suggest that XCL-2 participates in the convergent extension movements starting from the midgastrula stage.

It was further revealed, by overexpressing a dominant-negative-type mutant *C105S*, that XCL-2 activity is required for morphogenetic movements. Overexpression of *C105S* and wild-type *XCL-2* resulted in similar phenotypes (open blastopore and bifurcate tail). These on the first glimpse confusing results could be explained by the observation that both overexpression of wild-type *XCL-2* or inhibition (partial or total loss of function) by a dominant-negative mutant, *C105S*, will cause the disturbance of morphogenetic movements. These data are in agreement with results using other genes, where overexpression of both wild-type and truncated forms of *Wnt11* (Tada and Smith, 2000) or *Frizzled-7* (Djiane et al., 2000) also blocks convergent extension movements and generates similar phenotypes. However, our histological sections show that the embryos injected with *C105S* form distinct bifurcate notochord malformations, in contrast to wild-type *XCL-2* overexpression. This phenotype can be rescued by coinjection of *XCL-2* and *C105S* mRNA at the proper ratio. These results suggest that the mutant acts specifically *in vivo* by competition with wild-type protein for proteolytic substrates. However, because Calpains have been identified as a large gene family in other vertebrates, such as human

and rat, it can be suggested that such a family also exists in *X. laevis*. Therefore, the possibility cannot be ruled out that the dominant-negative mutant *C105S* also suppresses other related members. In summary, present data suggest that XCL-2 is a prerequisite for morphogenetic movements during early embryogenesis in *X. laevis*. It is highly probable that Calpain regulates cell movements by changing cell adhesive activity via proteolytic cleavage of proteins that are essential for morphogenesis, but this remains to be elucidated.

4.2 XETOR and its role during primary neurogenesis

Here in this study it is presented for the first time the expression and function of an *ETO* related gene, *XETOR*, during primary neurogenesis in *Xenopus laevis*. Like other members of *ETO* oncogene family, *XETOR* is also expressed primarily in the nervous system. Both gain- and loss-of-function studies showed that *XETOR* plays key roles in primary neurogenesis. It inhibits primary neuron formation by establishing a negative feedback loop with proneural genes. This inhibition is not mediated by lateral inhibition signaling but a result of an independent action. Lateral inhibition and XETOR antagonize each other but both are required for primary neurogenesis. They consist of a dual inhibitory mechanism to refine the exact localization and number of primary neurons.

4.2.1 XETOR is an inhibitory factor for primary neurogenesis in independence of lateral inhibition

XETOR encodes a putative protein that shares all characteristics of other members of oncoprotein family ETO/MTG8: the four conserved Nervy Homologous Regions and the two unusual zinc-finger motifs. Besides the common structure, another feature shared among these genes examined, including *Nervy* in *Drosophila*, is that they all have expression in the nervous system (Feinstein et al., 1995; Wolford and Prochazka, 1998). This suggests a conserved function of ETO proteins in nervous system. In *Xenopus laevis*, expression of *XETOR* during primary neurogenesis begins at stage 12.5 in a pattern of longitudinal stripes at either side of dorsal midline, similar to the patterns of primary neuron marker genes. Double *in situ* hybridization showed that expression domain of *XETOR* is overlapping with, however broader than

that of *N-tubulin*, confirming that *XETOR* is another marker gene for primary neurogenesis. The broader expression domain of XETOR may suggest that it plays to refine the localization of primary neurons, and this has been confirmed by the study. Temporally, expression of *XETOR* starts at stage 12.5, following that of *Xngnr-1*, *Xash-3*, *XMyT1*, *X-Delta-1, Xath3* and preceding that of *XNeuroD*, but at the same time when the differentiated neuron marker gene *N-tubulin* is turned on. This temporal sequence should suggest that *XETOR* is turned on when neuronal differentiation begins and hence a role in regulating neuronal differentiation.

Further lines of evidence support this idea more directly. It was proved that, on the contrary to promoting neuronal differentiation as bHLH proneural proteins do, it acts to repress the procedure. First, gain-of-function data show that XETOR inhibits expression of neuron marker genes *N-tubulin* and *Xaml*. This loss of primary neuron formation is not a result of disruption of neural plate, as indicated by intact expression of *Xsox3* in response to *XETOR* ovexpression. Second, overexpressed *XETOR* extirpates the neuron-inducing activity of proneural genes, *Xash-3*, *Xath3* and *XNeuroD*, as well as the zinc-finger gene *XMyT1*, as revealed by coinjections of *XETOR* together with any one of these genes. Therefore, XETOR should be able to inhibit primary neuron formation via repressing the function of proneural genes. Third, inhibition of XETOR function *in vivo* leading to a neurogenic phenotype of expanded neurogenic domain also suggests that XETOR is a key negative regulatory factor for primary neurogenesis.

It seems that a negative feedback loop is established between *XETOR* and proneural genes. The reason is that expression of *XETOR* is exclusively activated or promoted by the genes examined in the study except the zinc-finger gene *XMyT1*, and in turn, XETOR inhibits the function of these genes, with the exception of *Xngnr-1*. Although all proneural genes can activate *XETOR* expression, it is proposed here that *XETOR* is more likely to be activated directly by *Xath3* than by *Xngnr-1*. The first reason is that Xngnr-1 activates *Xath3* in a unidirectional way and *Xath3* is a direct downstream target of Xngnr-1. The second reason is that, in temporal sequence, *XETOR* begins to express at stage 12.5 almost immediately after *Xath3*, which starts to express at stage 12 (Perron et al., 1999). Therefore, the temporal expression of XETOR suggests that it

functions in the late stage of primary neurogenesis. This is also confirmed by the fact that XETOR does not affect the expression or/and function of neuronal determination genes *Xngnr-1* and *Xash-3*, but instead inhibits the function of neuronal differentiation genes.

In the data and discussion above, it can be noticed that XETOR and lateral inhibition signaling have certain characteristics in common: both are activated by proneural genes, and conversely, both inhibit the function of proneural genes and hence primary neuron formation. Considering the similarity between the expression of *XETOR*, *X-Delta-1* and other components in lateral inhibition, it was asked whether XETOR is also a component of this signaling pathway such that XETOR function is orchestrated by lateral inhibition. A few lines of evidence negate the idea but support that XETOR and lateral inhibition are two different working mechanisms. The first point is that expression of *X-Delta-1* is repressed in response to overexpressed *XETOR*, and vice versa, *XETOR* expression is inhibited by activated lateral inhibition signaling pathway. In addition, when lateral inhibition is blocked, *XETOR* expression is promoted. This phenomenon is just contrary to that for Notch targets, which are promoted by activated lateral inhibition pathway while repressed by the blocked pathway. Therefore, lateral inhibition and XETOR is a pair of antagonists. The second is that XETOR still efficiently inhibits *N-tubulin* expression in the absence of lateral inhibition, as shown by coinjection of *XETOR* and *X-Delta-1*^{STU}. The third is that the expression of Notch targets, *ESR1* and *XNAP*, is not affected either with XETOR or without XETOR. Finally, that Xngnr-1 is refractory while XNeuroD is sensitive to XETOR activity suggests again that XETOR should not be a component of lateral inhibition pathway, because it was previously shown that early proneural genes as *Xngnr-1* and *Xash-3* are sensitive to lateral inhibition while late genes as *XNeuroD* and *Xebf3* are refractory.

4.2.2 The molecular mechanism for transcriptional repression activity of XETOR

The initial idea for constructing truncation mutants of XETOR was to test whether any one of them could function antimorphically to the wild type protein, such that loss-of-function assays could be performed. Unexpectedly, all these truncation mutants exclusively exhibit a repression effect, showing that

XETOR is a robust transcription repressor. The data on these mutants revealed important information on the function of different Nervy Homologous Regions (NHRs). One principal mechanism for transcriptional repression is the modification of chromatin conformation by histone deacetylases (HDACs; for reviews, see Grunstein, 1997; Struhl, 1998; Torchia et al., 1998). ETO has been identified as a potent repressor of transcription by recruitment of HDAC1 and 2 via corepressors N-CoR (nuclear receptor corepressor), mSin3 or SMRT (silencing mediator for retinoid and thyroid-hormone receptors) (Gelmetti et al., 1998; Lutterbach et al., 1998; Wang et al., 1998). Moreover, ETO itself acts also as a corepressor recruited by promyelocytic leukemia zinc finger protein (PLZF), which mediates transcriptional repression via the action of HDACs (Melnick et al., 2000). Multiple regions in ETO have been shown to cooperate in transcriptional repression. In the four conserved NHRs, both NHR3 and NHR4 but not NHR4 alone were shown to be essential for the interaction between ETO and N-CoR (Hildebrand et al., 2001). However, the binding of N-CoR with NHR3 and 4 *per se* is not sufficient for the mediation of transcriptional repression. While the core repressor domain (CRD), consisting of NHR2 and its N- and C-terminal flanking sequences, is the smallest region that shows significant repression activity on its own. Furthermore, this domain interacts strongly with mSin3A (Hildebrand et al., 2001). It is somewhat mystic for the function of NHR1, as ETO short of this region still induces maximal repression. While it is interesting for the sequence between NHR2 and NHR3, because it was clarified as the binding site for PLZF, and ETO short of this part significantly decreases repression activity (Melnick et al., 2000; Hildebrand et al., 2001).

The information on ETO domain functions may help explain the results of overexpression of XETOR truncation mutants. It was observed that the inhibitory effects of overexpression of truncation mutants *p13#trunc1*, *2*, *4*, and *5* on primary neuron formation are indistinguishable from that of the wild type *XETOR*. Therefore, these data suggest that single truncations of either NHR1 or NHR4, or double truncations of either NHR1 and 2 or NHR3 and 4 have no dramatic influences on their repression activity. The data are reasonable because the CRD homologous sequence is intact in p13#trunc1, 2 and 4. Especially, p13#trunc4 should retain the maximal repression activity because NHR1 is not

essential for ETO activity. Although p13#trunc3, containing only the CRD homologous sequence, showed also repression activity, it functions not as efficiently as other mutants. These data suggest that CDR need the cooperation with either NHR1 (as in p13#trunc2) or NHR3 and 4 (as in p13#trunc4) to exert a similar level of transcriptional repression activity to that of the wild type protein. However, based on the information available so far, it is not readily able to explain the result of *p13#trunc5* overexpression, because this mutant showed similar inhibitory effect to those of other mutants. In the case of ETO as mentioned above, NHR3 and 4 can bind N-CoR, but this binding by itself is not sufficient for the mediation of transcriptional repression. The present data suggest that XETOR may mediate transcriptional repression not only through machineries that are well known, but also those that are not well known. Up to today, XETOR has been the only protein of ETO oncoprotein family identified in *Xenopus*. Therefore, it is difficult to conclude whether it is an orthologue or paralogue of ETO. According to amino acid identity data, XETOR is more closely related to MTGR1 (72%) than to ETO (59%), hence it is more likely to be a paralogue. There is evidence that MTGR1 tends to form heterodimers with ETO via the oligomerization domain NHR2. It remains to be elucidated that if this also holds true in *Xenopus*.

4.2.3 XETOR and lateral inhibition comprise a dual inhibitory mechanism to refine the number and localization of primary neurons

The data have shown that *XETOR* can be exclusively activated by proneural genes. Conversely, XETOR tends to inhibit the neuron-inducing functions of proneural genes, with the exception of Xngnr-1. Thus a negative feedback loop is formed between XETOR and proneural genes. Such a responding mechanism is reminiscent of that between proneural genes and lateral inhibition signaling. Are these two the same machinery? There is evidence that they are different because they inhibit each other and work independently, as discussed above. Why do they coexist during certain period of primary neurogenesis?

Loss-of-function assay discloses important clues for such a question. When XETOR alone is knocked out, a neurogenic phenotype of significantly enlarged neurogenic domain is resulted. It is in congruence with the fact that the

expression domain of *XETOR* is broader than, though overlapping with, that of *N-tubulin*. However, the density of neurons does not vary appreciably. These data suggest a role of XETOR in refining the localization of primary neuron formation. The nearly normal salt-and-pepper pattern of *N-tubulin* expression should be generated by an increased level of lateral inhibition signaling, because XETOR can antagonize lateral inhibition by disabling the ligand gene *X-Delta-1*, and consequently an enhancement of lateral inhibition could be expected when XETOR activity is repressed. It was confirmed by double depletion of XETOR and lateral inhibition, which caused a phenotype of increased density of neurons in enlarged proneural domain. Such a phenotype is apparently distinct from that generated either by depletion of XETOR alone (enlarged proneural domain with an unaltered density of neurons) or by depletion of lateral inhibition alone (increased density of neurons with an unaltered proneural domain). These data suggest that XETOR and lateral inhibition are both required for primary neurogenesis: lack of either one will lead to overproduction of primary neurons either in an extra large sized neurogenic domain or in an excessive density. Hence, lateral inhibition and XETOR must cooperate to define the exact number and localization of primary neurons.

The unidirectional genetic cascade Xngnr-1-Xath3-XNeuroD underlies the major pathway promoting neurogenesis, which is in turn regulated by lateral inhibition. At the beginning of primary neurogenesis, expression of *Xngnr-1* defines the proneural domains where primary neurogenesis will occur. As a result of lateral inhibition, Xngnr-1 makes neuroectodermal cells competent to a neuronal state. While this state is unstable, genes like *XMyT1*, *Xath3* and *XCoe2* are subsequently activated by Xngnr-1 to stabilize the competent state (Bellefroid et al., 1996; Takabayashi et al., 1997; Dubois et al., 1998; Perron et al., 1999). By this way early proneural genes and lateral inhibition establish a mechanism for defining the number of primary neurons. However, this is possibly only part of the landscape for primary neurogenesis. It is known that proneural gene *Xngnr-1* defines a proneural domain much broader than the area where primary neurons form. Similarly, the expression domains of early expressed genes are much broader than that of late expressed proneural genes. Such a correlation of temporal and spatial expression is also reported between *XMyT1* and *N-tubulin* (Bellefroid et al., 1996). Therefore a regulatory system

should be there for the refinement of the neurogenic domains in the later period of primary neurogenesis. Proneural genes should be not the candidates because the consistently promote neuron formation. Neither is lateral inhibition because it is primarily responsible for cell fate selection, and knockout of lateral inhibition does not alter the proneural domain size but only the density of primary neurons. It is proposed here that XETOR is such a factor because of a few lines of evidence. First, the most direct evidence is that eradication of XETOR function *in vivo* results in an enlargement of proneural domain, as discussed above. Second, XETOR begins to express at a time later than *X-Delta-1* and does not inhibit neuron determination genes, especially *Xngnr-1*. This feature of XETOR function will ensure the initiation of early neuronal determination, which is regulated by lateral inhibition. Third, evidence has shown that each proneural gene activates three things: *X-Delta-1*, *XETOR* and the downstream proneural genes. Considering additionally that *X-Delta-1* is activated earlier than *XETOR* and that *X-Delta-1* and *XETOR* antagonize each other, it would be reasonable to assume that some cells expressing *X-Delta-1* will not express *XETOR*, and vice versa. Due to the inhibitory effect of XETOR on the expression and function of proneural genes, the neurogenic domain defined by the downstream proneural gene will be more restricted than the domain defined by the upstream gene.

Although late expressed neuronal differentiation genes, as *XNeuroD* and *Xebf3*, are resistant to lateral inhibition, they still activate lateral inhibition. This activation might be reasonable because it can serve to regulate the expression of *XETOR* during this stage of primary neurogenesis.

Based on the data and discussion above, a fresh model for primary neurogenesis is summarized as follow: expression of proneural gene *Xngnr-1* marks the initiation of primary neurogenesis and defines the proneural domain. At the same time, *Xngnr-1* also activates downstream proneural genes and lateral inhibition. Some cells are committed to a neuronal fate and others remain ectodermal via a negative feedback loop. In this way lateral inhibition determines the density of primary neurons. However, the size of neurogenic domain where primary neurons will form is not determined. At the time approximately when neuronal differentiation begins, *XETOR* is activated also by proneural genes. Because *XETOR* expression is antagonized by lateral

inhibition, and XETOR represses the expression and function of late expressed proneural genes, thus it is possible to restrict the neurogenic domain to a correct localization.

The functions of proneural and neurogenic genes are all proved to be conserved throughout the spectrum of organisms from *Drosophila* to *Xenopus*. It has been shown that there also exist XETOR homologues in other organisms, including Nervy in *Drosophila*. Moreover, the expression of these homologues is restricted to the nervous system, too. It is logic to deduce that certain XETOR homologue in other organisms play the same or at least similar role. Hence the dual inhibitory mechanism identified in this study may also conserve in other organisms.

It should be mentioned in passing that XETOR could also be involved in hematopoiesis. The *XETOR* homologue *ETO/MTG8* in human is often translocated to *AML1* to make a fusion transcript in acute myeloid leukemias. It has been shown that Xaml, the AML1 homologue in *Xenopus laevis*, functions in the specification of hematopoietic stem cells in vertebrate embryos (Tracey et al., 1998). Considering their expression in both primary neurons and the presumptive ventral blood island, therefore it is proposed here that XETOR may also play a role in primitive hematopoiesis.

In summary, based on the present data, it is proposed here that during primary neurogenesis, lateral inhibition and XETOR comprise a dual inhibitory mechanism to refine the exact number and localization of primary neurons, via repression of the expression and function of proneural genes.

5. SUMMARY

Using a strategy of large-scale whole mount *in situ* hybridization, three genes were identified from a cDNA library constructed from endoderm-like tissue induced from activin treated animal caps. One gene, *XODC2*, encodes a paralogue to ubiquitous ODC (Genbank accession number: AF217544); another, *XCL-2*, encodes a tissue-specific m-type Calpain (Genbank accession number: AF212199); while the third one, *XETOR*, encodes a novel member of the ETO/MTG8 oncoprotein family (Genbank accession number: AF212198).

Spatial and temporal expressions of these genes were examined by ways of whole mount *in situ* hybridization and RT-PCR. Functional analyses were focused on *XCL-2* and *XETOR*.

Overexpression of wild-type *XCL-2* suggests that this gene is involved in gastrulation movement and convergent extension during gastrulation and neurulation. Overexpression of a dominant-negative mutant caused a phenotype morphologically similar to, but histologically different from, that caused by overexpression of wild-type *XCL-2*. The mutant phenotype can be rescued by injection of wild-type *XCL-2*. These data suggest that XCL-2 plays an important role in convergent extension movements during embryogenesis in *Xenopus laevis*.

XETOR is expressed during neurula stage in three bilaterally symmetrical stripes at each side of dorsal midline, a pattern similar to that of the genes involved in primary neurogenesis. Indeed, overexpression of *XETOR* or a series of truncated mutants led to the inhibition of primary neuron formation without disruption of neural plates. Such an inhibitory effect is not mediated by lateral inhibition, but an independent action. Moreover, it was shown that *XETOR* and lateral inhibition antagonizes each other. Further evidence showed that

expression of *XETOR* is activated or promoted by overexpressed proneural genes such as *Xngnr-1*, *Xash-3*, *Xath3*, and *XNeuroD*, and conversely, overexpressed *XETOR* inhibits the expression and function of *Xath3* and *XNeuroD*. The neuron inducing activity but not expression of *Xash-3* is inhibited in response to *XETOR* overexpression, while neither the expression nor the function of *Xngnr-1* is inhibited. Thus a negative feedback loop is established between XETOR and proneural genes. Blocking of XETOR function *in vivo* resulted in a neurogenic phenotype of an enlarged neurogenic domain without alteration in neuron density. Nevertheless, double depletion of XETOR and lateral inhibition led to primary neuron formation with an increased density in enlarged domains. Based on these data, it is concluded that during primary neurogenesis, lateral inhibition and XETOR comprise a dual inhibitory mechanism to refine the number and localization of primary neurons via repression of the expression and function of proneural genes.

6. ZUSAMMENFASSUNG

Mittels in großem Maßstab (large-scale) durchgeführte Whole Mount *in situ* Hybridisierung konnten 3 Gene aus einer cDNA Bibliothek isoliert werden, die in entoderm-ähnlichem Gewebe (Activin behandelte animalen Kappen) exprimiert wurden. Ein Gen, *XODC2*, kodiert für ein Paralog zum ubiquitären ODC; ein weiteres *XCL-2* kodiert für gewebespezifisches m-type Calpain; und schließlich *XETOR* dessen Produkt ein weiteres Mitglied der ETO/MTG8 Oncoprotein-Familie representiert.

Die räumliche und zeitliche Expression dieser Gene wurde untersucht mittels whole mount *in situ* Hybridisierung und RT-PCR. Funktionelle Analysen konzentrierten sich auf *XCL-2* und *XETOR*.

Überexpresssionsexperimente des Wildtypes *XLC-2* deuten darauf hin, dass dieses Gen beteiligt ist an Gastrulationsbewegungen und der sog. konvergenten Extension während der Gastrulation und Neurulation. Überexpression einer dominant negativen Mutante resultierte in einem Phänotyp, der morphologisch ähnlich, aber histologisch unterschiedlich zu dem Typ der Überexpression des Wildtypes *XCL-2* ist. Der annormale Phänotyp der Mutante kann gerettet werden (rescued) durch gleichzeitige Injektion des Wildtyps *XCL-2*. Diese Ergebnisse deuten darauf hin, dass XCL-2 eine wichtige Rolle in der konvergenten Extensionsbewegung während der Embryogenese bei *Xenopus laevis* spielt.

XETOR wird während der Neurulation in Form von 3 bilateral symmetrischen Streifen auf jeder Seite der dorsalen Mittellinie exprimiert, ein Muster ähnlich zu dem der Gene, die beteiligt sind in der primären Neurogenese. Tatsächlich führt die Überexpression von *XETOR* oder einer Reihe von Rumpfmutanten (truncated) zu einer Inhibition der primären Neuronbildung

ohne Veränderung der Neuralplatte. Ein solcher Inhibitionseffekt wird nicht durch laterale Inhibition bewirkt, sondern durch eine unabhängige, eigenständige Aktion. Darüber hinaus konnte gezeigt werden, dass *XETOR* und laterale Inhibition antagonistisch wirken. Weiterhin ergaben sich Hinweise, daß die Expression von *XETOR* aktiviert oder gefördert wird durch die Überexpression proneuraler Gene wie *Xngnr-1*, *Xash-3* und *XNeuroD*, und daß umgekehrt die Überexpression von *XETOR* die Expression und die Funktion von *Xath3* und *XNeuroD* inhibiert. Die Neuroninduktionsaktivität, aber nicht die Expression, von *Xash-3* wird inhibiert in Abhängigkeit zur *XETOR* Überexpression, während weder die Expression, noch die Funktion von *Xngnr-1* igehemmt wird. Das zeigt, dass eine negative Rückkoppelung (negative feedback loop) etabliert ist zwischen XETOR und proneuralen Genen. Die Blockade der XETOR-Funktion *in vivo* ergibt einen neurogenen Phänotyp mit vergrößerter neurogener Domäne, ohne Veränderungen der Neurondichte. Trotz gleichzeitiger Ausschaltung von XETOR und der lateralen Inhibition kommt es zur primären Neuronformation mit einer erhöhten Dichte in vergrößerten Domänen. Auf der Basis dieser Daten kann angenommen werden, dass XETOR während der primären Neurogenese eine wesentliche Rolle bei der primären Neurogenese via Repression der Expression und Funktion proneuraler Gene spielt.

7. SYNOPSIS

7.1 Eine kurze Darstellung der frühen Embryogenese und das Ziel dieser Untersuchungen

Effektive entwicklungsbiologische Untersuchungen sind eng korreliert mit einem geeigneten Modellsystem. Wegen der hohen Zahl der abgelegten Eier (ca. 1500 pro Weibchen) mit einer Eigröße (1-2 mm im Durchmesser) und einer schnellen embryonalen Entwicklung ist der afrikanische Krallenfrosch *Xenous laevis* besonders geeignet für das Studium der Wirbeltierentwicklung. Dies war auch der Grund, warum gerade mit diesem Modellsystem große zellbiologische und molekulargenetische Fortschritte erzielt wurden.

Verschiedene zentrale Ereignisse während der Embryonalentwicklung sind durch elegante Studien belegt. Vor der Befruchtung weist das *Xenopus*-Ei eine animale-vegetative Polarität auf. Durch die Befruchtung ergibt sich eine neue dorsal ventrale Polarität, die sich durch die corticale Rotation und Akkumulation von β-catenin auch auf der Dorsalseite ergibt (Moon und Kimelman, 1998; De Robertis et al., 2000). Eine dieser Konsequenzen ist die Formation des sog. Nieuwkoop-Centers, das gebildet wird auf der dorsalen Seite der vegetativen Zone (Nieuwkoop, 1952; Nieuwkoop, 1973). β-catenin ist die erste Komponente des Signalweges, die erforderlich ist, für die Formation der dorsalen Achsenformation und die Dorsalisierung der drei Keimschichten. Ein Zwei-Stufen-Modell wurde für die Induktion des Entoderms vorgeschlagen (Yasuo und Lemaire, 1999; Yasuo und Lemaire, 2001), in dem der maternale Transkriptionsfaktor VegT eine wichtige Rolle spielt. Mesoderm wird durch 3 Signale determiniert (Dale and Jones, 1999; Chan und Etkin, 2001) bzw. auch verschiedentlich als Zwei-Signal-Weg definiert (De Robertis et al., 2000). Das erste Signal geht aus vom ventralen Entoderm und induziert ventrales

Mesoderm, während das Nieuwkoop-Center ein zweites Signal abgibt, um das dorsale Mesoderm zu induzieren. Ergebnis ist die Spemann-Mangold Organisator Region. Der Organisator selbst vermittelt dann ein drittes Signal, verantwortlich für das initiale Mesoderm. Veg1 und VegT sind beide als primäre Kandidaten für die mesoderme Induktion angesehen (Dale et al., 1993; Thomsen und Melton 1993; Kessler und Melton, 1995; Joseph und Melton, 1998; Zhang et al., 1998; Kofron et al., 1999). Ektoderm leitet sich ab von den Zellen der animalen Region. Dorsales Ektoderm in der Nähe des Organizers entwickelt sich in die Neuralfalten, woraus sich das Zentrale Nervensystem entwickelt, während aus dem ventralen Ektoderm Epidermis hervorgeht. Der BMP- und Wnt-Signalweg spielt eine zentrale Rolle für die Organisation des Ektoderm. Im dorsalen Ektoderm wird der BMP4 und Wnt Signalweg durch die Antagonisten des Organisator inhibiert, so dass es sich in neuraler Richtung entwickelt, während das ventrale Ektoderm mit aktiven (nicht blockiertem) BMP- und Wnt-Signalweg Epidermis bildet (Chan und Etkin, 2001).

Die Entdeckung des Spemannschen Organisator ist ein Meilenstein in der Entwicklungsbiologie. Die molekulare Natur des Organisators ist mittlerweile genauer beschrieben worden. Prinzipielle Funktionen des Organisators sind Körperachsenmusterbildung, neurale Induktion und Morphogenese (Harland und Gerhart, 1997; Bouwmeester, 2001). Als erstes organisiert der „Rumpforganisator“ die dorsale-ventrale Körperachse auf Grund der Sezernierung von Chordin, Noggin und Follistatin, die als dorsalisierende Faktoren und Antagonisten zu BMP-4 das ventrale Mesoderm organisieren. Zweitens, der „Kopforganisator“ organisiert die anteriore-posteriore Achse, in dem es Cerberus, dkk-1 und Frzb-1 als Antagonisten zu den Wnt Glycoproteine sezerniert. Drittens, zusätzlich zur Funktion als dorsalisierende Faktoren wirken Chordin, Noggin und Follistatin auch als neurale Induktoren. Weiterhin kontrolliert der Organisator komplexe morphogenetische Bewegungen (Harland und Gerhard, 1997; Bouwmeester, 2001).

Obwohl einige Schlüsselmoleküle während der *Xenopus*-Entwicklung charakterisiert worden sind und auch weitere Zusammenhänge während der Embryonalentwicklung genauer beschrieben wurden, sind trotzdem eine große Zahl von Genen in Struktur und Funktion unbekannt. Es wird angenommen,

dass 50 000 Gene bei der Embryonalentwicklung von *Xenopus laevis* beteiligt sind (Wolpert et al., 1998). Eine wichtige Methode ist es, Gene zu identifizieren, die homolog zu Genen sind, die schon bei anderen Organismen beschrieben wurden, so bei Drosophila und Maus. Ein weiterer Weg besteht darin, Gene aus cDNA-Bibliotheken zu identifizieren, die aus spezifischen Stadien oder Geweben erstellt wurden. Untersuchungen mit diesen Gen-Bibliotheken haben zur Identifizierung von vielen Genen geführt, die eine genaue Kenntnis über die frühe Embryonalentwicklung erlauben. Viele interessante Gene des Spemannschen Organisatorbereiches wurden durch Erstellung einer dorsalen Urmundlippen-Bibliothek erzielt (Bouwmeester et al., 1996) oder eine Bibliothek aus Embryonen, die mit Lithium-Chlorid im Stadium 13 behandelt wurden (Glinka et al., 1998). Andere Strategien beschäftigten sich mit der Isolierung von Genen für sezernierte Proteinen (Klein et al. 1996; Jacobs et al., 1997; Pera and De Robertis, 2000; Matsui et al., 2000; Tsuda et al., 2002) oder DNA-binding Proteine (Mead et al., 1998).

Als weiterer viel versprechender Weg war die Konstruktion cDNA-Bibliotheken, die aus Activin behandelten Ektoderm erstellt wurden. Dabei wurde ein *in vitro*-System auf der Basis früherer Untersuchungen benutzt (Grunz, 1969; Minuth und Grunz, 1980; Grunz, 1983; Grunz und Tacke, 1989). Dabei wurden disaggregierte Ektodermzellen der animalen Kappe des Stadium 8-9 mit hohen Konzentrationen von Activin behandelt, die sich darauf hin in homogener Weise in Entoderm ähnlichen Strukturen überwiegend in Chorda-Gewebe differenzierten. Die aus Entoderm-ähnlichen Gewebe konstruierte cDNA-Bibliothek wurde nach neuen Genen durchsucht. Das Expressionsmusters war bei 3 Genen besonders interessant: *XODC2*, *XCL-2* und *XETOR*. Deshalb erfolgte eine weitere Analyse ihrer Funktion während der Embrogenese (eine detaillierte Darstellung der angewandten Techniken findet sich unter Material und Methode der Dissertation.

7.2 Identifizierung von *XODC2*, *XCL-2* und *XETOR*

Eine im großen Maßstab (large-scale) durchgeführte whole mount *in situ* Hybridisierung ergab insgesamt 384 Klone, von denen 29 ein sehr interessantes whole mount in situ Expressionsmuster aufwiesen. Im Vergleich mit Sequenzen

in Gen-Banken konnte gezeigt werden, dass unter den 29 Klonen 11 homolog waren zu schon bekannten Genen von *Xenopus laevis*, mit über 90% Identität; 9 wiesen Homologien zu anderen Spezies auf, z.B. Mensch. Die übrigen 9 Klone wiesen geringe Sequenzidentität auf (siehe Tabelle 3.1). Aufgrund des interessanten whole mount in situ Expressionsmusters wurden 3 Klone ausgewählt, 18D11, 18G11 und 18H2 für weitere Untersuchungen.

Eine cDNA-Sequenz von 1842 bp wurde erhalten für den Klon 18D11. Die 1368 bp des offenen Leserahmens (ORF) ergaben 456 Aminosäuren (Abb. 3.1A). Vergleichende Untersuchungen im BLAST-Programm zeigten, dass das Protein 66% Identität in der Aminosäure-Sequenz mit der ubiquitären Ornithine Decarboxyglase (ODC) im Menschen, 65% in *Xenopus laevis* und Ratte und 63% im Huhn aufwies (Abb. 3.1B). Die Schlussfolgerung war, dass es sich um ein Paralogue des *Xenopus* ubiquitären ODC handelte (XODC1; Bassez et al., 1990.). Deshalb wurde diese cDNA bezeichnet als *XODC2* (Accession Nr. AF217544).

Anwendung von 5'RACE (Rapid Amplification der cDNA Enden; Frohmann et al., 1988), beim Klonen 18G11 wurde eine cDNA Sequenz von 2639 bp mit einem kompletten ORF, eine große Calpain Proteine Untereinheit erhalten (Abb. 3.2A). Das Protein war am nächsten verwandt mit dem Rattenmagen-spezifischen m-type Calpain nCL-2 (Sorimachi et al., 1993), mit 64% Identität auf dem Aminosäure-Niveau und ubiquitären m-typ Calpains in Spezies wie Mensch, Huhn, beide mit 60% Identität (Abb. 3.2B). Weiterhin hat das Protein exakt die gleiche Domänstruktur, Kalzium-Bindungsmotiv (EF-hands) und die drei aktiven Positionen (Cys 105, His 262 und Asn 286) in der proteolytischen Domäne wie in anderen typischen Calpains (Abb. 3.3). Deshalb wurde es bezeichnet als Xenopus CL-2 (XCL-2) (Accession Nr. AF212199).

Mittels 5'RACE wurde bei Klon 18H2 eine cDNA-Sequenz von 2936 bp mit einem kompletten ORF erhalten (Abb. 3.4A). Die abgeleitete Protein-Sequenz besteht aus 586 Aminosäuren mit einer Gesamthomologie von 72% zu MTG8 ähnlichem Protein MTGR1, 59 % zu ETO beim Menschen und 29 % zu Nervy in *Drosophila* (Abb. 3.4B). *MTG8* (auch bekannt als *ETO* oder *CDR*) ist ein Proto-Oncogen, weil es Fusionstranskripte repräsentiert, die bei akuter myeloiden Leukämie mit der t(8;21) Translocation repräsentieren. XETOR in

der Struktur ähnliche zu anderen ETO/MTG8 verwandten Proteinen hat vier konservierte Nervy homologe Regionen und zwei Zink-Finger Motive (Abb. 3.4B). Es wurde deshalb bezeichnet als *Xenopus* ETO verwandtes Protein (XETOR) und die Nukleinsäure-Sequenz wurde in der Gen-Bank mit der Accession Nr. AF212198 angemeldet.

7.3 Zeitliche und räumliche Expression von *XODC2*, *XCL-2* und *XETOR*

Die räumliche Expression von *XODC2* wurde im Bereich des animalen Pols von Stadium 9 an mittels whole mount in situ Hybridisierung nachgewiesen (Abb. 3.5D, E). Während der Neurula-Stadien finden sich Signale wohl in der extremen anterioren als auch in der posterioren Region der dorsalen Körperachse (Abb. 3.5F). Im Schwanzknospenstadium ist die Expression weiter verschoben zur Kopf- und Schwanzregion (Abb. 3.5G, H, I, J, K). Vergleichende Untersuchungen zeigen, dass *XODC1* im Gegensatz zu *XODC2* ubiquitär im ganzen Embryo während der Embryonalentwicklung verteilt ist (Abb. 3.5L, M, N). RT-PCR konnte zeigen, dass Transkripte von beiden *XODC1* und *XODC2* bereits im unbefruchteten Ei vorhanden sind und das Expressions-Niveau von *XODC1* auf dem gleichen Niveau in allen Stadien bleibt, während sich die Expression von *XODC2* ab Stadium 9 bis zum Schwanzknospenstadium kontinuierlich erhöht (Abb. 3.6).

Die räumliche Expression von *XCL-2* wurde zuerst nachgewiesen in der Zone der ventralen Urmundlippe im Stadium 12,5 (Abb. 3.7A). In der späten Gastrula und Neurula ist das Gen ausschließlich ventrale um den Urmund und der mesodermen freien Zone des anterioren Bereiches der Neuralfalte exprimiert (Abb. 3.7B, C, G). In späteren Stadien ist die Expression sichtbar in der Haftdrüse (cement gland) und dem Proctodeum (Abb. 3.7D, E, F, H, I). Die zygotische Transkription von *XCL-2* wird erstmals nachgewiesen im Stadium 10 mittels RT-PCR (Abb. 3.8A). Weiterhin ist eine gewebespezifische Expression zu beobachten. Im erwachsenen Gewebe werden unterschiedliche Expressionen im Gehirn, Auge, Herz, Darm, Niere, Lunge, Magen und Hoden, aber nicht in Leber, Muskel, Nerven, Ovar, Haut und Milz beobachtet (Abb. 3.8B).

XETOR Transkripte im Zentralennervensystem werden mittels whole mount

in situ Hybridisierung innerhalb des dorsalen Ektoderm ab Stadium 12,5 in einem Muster von radial symmetrischen Streifen seitlich der dorsalen Mittellinie gefunden (Abb. 3.9A, B, D, E). In der anterioren Neuralplatte wird die Expression in einer lateralen Gruppe von Zellen gefunden, die assoziiert sind mit trigeminalen Ganglien, einer extreme anterioren Gruppe von Zellen assoziiert mit der Riechplacode, einem zentralen Streifen, der die zukünftige Gehirnregion und Region der anterioren neuralen Ganglienleisten-Zellen bezeichnet (Abb. 3.9B, C, D). Doppelte *in situ*-Hybridisierung ergab, dass die Expressionsdomäne von *XETOR* die Region von *N-tubulin* überlappt, aber trotzdem breiter ist (Abb. 3.9H, I). Dieses Muster deutet darauf hin, dass *XETOR* ein Marker-Gen ist oder eine besondere Rolle bei der primären Neurogenese spielt.

7.4 XCL-2 unterbricht die morphogenetischen Bewegungen während der Embryogenese in *Xenopus laevis*

Der Wildtyp *XCL-2* und eine dominant-negative Mutante, *C105S*, wurden bei Überexpressionsexperimenten eingesetzt, um die Funktion von XCL-2 während der Embryogene zu studieren. Die Überexpression von *XCL-2* ergibt eine Verzögerung der Involution des Mesoderms. Die injizierte Embryonen konnten den Urmund während der Gastrulation nicht schließen und ein großer Dotterpfropf wurde in den nachfolgenden Entwicklungsstadien beobachtet (Abb. 3.11B). Dies ergab einen ganz charakteristischen Phänotyp (Abb. 3.11D). Dieses Ergebnis lässt vermuten, dass Überexpression von *XCL-2* den Verschluss des Urmundes verhindert und die weiteren Gastrulationsbewegungen behindert. Weiterhin wurde das Zell-Schicksal der betroffenen Embryonen mittels mesodermaler oder neuraler Marker wie *Xbra*, *Chordin*, *Xvent-1*, *XMyoD*, *Xotx2* und *Xsox3* untersucht. Trotz ähnlich starker Expression ergaben sich Unterschiede in der Versuchsserie und den Kontrollen in der Lokalisation der einzelnen Marker. Dies deutet auf unterschiedliche Zellmigrationen hin (Abb. 3.12). Weiterhin konnte gezeigt werden, dass während der Gastrulation und Neurulation das Mesoderm und die posteriore Neuralplatte nicht zur Mittellinie hin bewegt wurden, wie dies aus der Translokation von *Chordin*, *XMyoD* und *Xsox3* ersichtlich wurde (Abb. 3.12). Diese Ergebnisse deuten darauf hin, dass

XCL-2 beteiligt ist an der sog. convergent extension während der Midgastrula-Stadien.

In weiteren Überexpressionen-Studien mittels einer dominant-negativen Mutante *C105S*, konnte gezeigt werden, dass XCL-2 benötigt wird für morphogenetische Zellbewegungen. Die Überexpression von *C105S* und Wildtype *XCL-2* ergab ähnliche Phänotypen (offener Urmund und Doppelschwanz) (Abb. 3.13B, D). Diese auf den ersten Blick sich widersprechende Ergebnisse konnten gedeutet werden, durch die Beobachtung, daß sowohl eine Überexpression des Wildtypes *XCL-2* bzw. die Inhibition (partielle oder totaler Verlust von Funktionen (loss-of-function)) durch die dominant-negative Mutante *C105S* ähnliche Störungen der morphogenetischen Bewegungen bewirkt. Diese Ergebnisse sind in Übereinstimmung mit den Ergebnissen anderer Gene, wo die Überexpression sowohl des Wildtyps und der Rumpfform (truncated) von Wnt11 (Tada und Smith, 2000) oder Frizzled-7 (Djiane et al., 2000), ebenso die konvergente Extension inhibieren und ähnliche Phäntoypen hervorrufen. Andererseits zeigen die histologischen Schnitte von Embryonen, in die C105S injiziert wurden, im Gegensatz zur Wildtyp *XCL-2* Überexpressionen (Abb. 3.11E, F) eine zweigeteilte Chordamißbildung aufwiesen (Abb. 31.3F, G). Eine Restauration dieses Phänotypes (rescue-Experiment) kann durch Koinjektion durch *XCL-2* und *C105S* mRNA erreicht werden (Abb. 3.13E; Tabelle 3.2). Diese Ergebnisse deuten daraufhin, dass die Mutante spezifisch unter in vivo-Bedingungen durch Kompetition mit Wildtyp-Proteinen für proteolytische Substrate wirkt. Zusammenfassend kann man sagen, dass die Daten vermuten lassen, dass XCL-2 eine Voraussetzung für geordnete morphogenetische Bewegungen während der frühen Embryogenese in *Xenopus laevis* darstellt. Es ist höchstwahrscheinlich, daß Calpain die Zellbewegungen, durch Veränderungen der Zelladhesitionsaktivität via proteolytischen Spaltung von Proteinen reguliert, die essential für die Morphogenese sind.

7.5 XETOR ist ein Schlüssel Inhibitionsfaktor während der primären Neurogenese

Die Funktion von *XETOR* in vivo während der primären Neurogenese wurde erkennbar durch Expression von Markergenen für primären Neuronen wie *N-*

tubulin und *Xaml*, die als Antwort auf die Überexpression von *XETOR* oder Rumpfmutanten inhibiert wurden (Abb. 3.14A, C, E). Diese Inhibition ist keineswegs das Ergebnis einer Störung der Neuralplattenformation wie es durch die normale Expression von *Xsox3* gezeigt werden konnte (Abb. 3.14D). Andererseits, wenn die XETOR-Aktivität durch die Injektion von antisense Morpholino Oligo *MOXETOR* inhibiert wurde, ergab sich ein neurogener Phänotyp mit vergrößerter neurogenen Domäne. Die Dichte der primären Neurone war jedoch nicht signifikant erhöht (Abb. 3.16A). Da die laterale Inhibition einen prinzipiellen Mechanismus darstellt, um die Zahl der primären Neurone zu kontrollieren (Chitnis et al., 1995), wäre es von Interesse zu sehen, was passiert, wenn sowohl XETOR und die laterale Inhibition ausgeschaltet werden. In der Tat wurde ein Phänotyp einer vergrößerten neurogenen Domäne mit vergrößerter Dichte der primären Neurone beobachtet (Abb. 3.16E). Diese Beobachtungsteht im Gegensatz zu dem Phänotyp, der hervorgerufen wird durch den Verlust von XETOR (vergrößert neurogene Domäne mit unveränderter Dichte mit Neuronen, Abb. 3.16A) oder durch die Ausschaltung der lateralen Inhibition (vergrößerte Dichte der Neuronen bei unveränderter neurogener Domäne, Abb. 316D). Diese Daten sind ein solider Beweis dafür, dass XETOR benötigt wird für die korrekte Musterbildung der primären Neurogenese.

Im nächsten Schritt wurde die Korrelation zwischen *XETOR* und laterale Inhibition weiter untersucht, um nachzuweisen, ob die Funktion des ersteren Gens durch das letztere beeinflusst wird. Einige Tatsachen deuten darauf hin, dass dies nicht der Fall ist. Erstens, die Expression des Liganden-Gens *X-Delta-1* wurde herabgesetzt in Abhängigkeit der Überexpression von *XETOR* (Abb. 3.17A), und umgekehrt die Expression von XETOR wurde verringert durch den aktivierten Notch-Signalweg (Abb. 3.17B). Außerdem, wenn die laterale Inhibition blockiert ist, wird die *XETOR* Expression gesteigert (Abb. 3.17C). Deshalb stellt die laterale Inhibition und XETOR ein Antagonistenpaar dar. Weiterhin inhibiert XETOR effektiv *N-tubulin* in der Abwesenheit der lateralen Inhibition (Abb. 3.17D). Der dritte Hinweis ist, dass die Expression, der Notch-Zielgene *ESR1* und *XNAP*, nicht beeinflusst wird, sowohl in Anwesenheit (Abb. 3.17E, F) wie in Abwesenheit von XETOR (Abb. 3.17G, H). Diese Ergebnisse deuten darauf hin, dass XETOR und die laterale Inhibition Antagonisten sind,

aber unabhängig voneinander agieren.

Im nächsten Schritt wurde die gegenseitige Regulation zwischen *XETOR* und proneuralen Genen untersucht. Die Überexpression von proneuralen Genen, *Xngnr-1* (Abb. 3.18A), *Xath3* (Abb. 3.18B), *Xash-3* (Abb. 3.18E) oder *XNeuroD* (Abb. 3.18H) aktiviert die ektopische Expression von *XETOR*. Umgekehrt inhibiert überexprimiertes *XETOR* die Expression von *Xath3* (Abb. 3.18D) und *XMyT1* (Abb. 3.18G), aber nicht die Expression von *Xngnr-1* (Abb. 3.18C) und *Xash-3* (Abb. 3.18F). Außerdem wurde beobachtet, dass die Neuronen-Induktionsaktivität von XMyT1 (Abb. 3.19B), Xath3 (Abb. 3.19D), XNeuroD (Abb. 3.19F) oder Xash-3 (Abb. 3.19K) ausgeschaltet wurde, als Antwort auf eine *XETOR* Überexpression. Doch bleibt die Funktion von Xngnr-1 in Anwesenheit von überexprimierten *XETOR* intakt (Abb. 3.19I). Die Ergebnisse weisen darauf hin, dass XETOR aktiviert wird durch proneurale Gene und in Folge die Funktion der spät exprimierten proneuralen Gene unterdrückt wird wie *XNeuroD*, aber nicht die frühexprimierten wie *Xngnr-1*. Das bedeutet, dass eine negative Rückkoppelung etabliert wird zwischen *XETOR* und proneuralen Genen. Die negative Rückkoppelung ist trotzdem unterschiedlich von derjenigen proneuralen Gene und lateralen Inhibition, in der Form, dass die laterale Inhibition die Funktion der frühexprimierten Gene wie *Xngnr-1* unterdrückt, während sie ineffektiv ist für die spätexprimierten Gene wie *XNeuroD*. Dies bedeutet, daß die laterale Inhibition (Stadium 11,5) früher aktiviert wird als *XETOR* (Stadium 12,5), mit der Schlussfolgerung das die laterale Inhibition und XETOR nacheinander während der primären Neurogenese wirksam werden.

Auf der Basis der oben dargestellten Ergebnisse, postulieren wir ein neues Modell für die primäre Neurogenese. Die in einer Richtung ablaufenden Cascade Xngnr-1-Xath3-XNeuroD stellt den Hauptweg der Neurogenese dar. Die Expression von *Xngnr-1* repräsentiert die proneuralen Domäne, wo die primäre Neurogenese stattfinden wird. Gleichzeitig aktiviert es die laterale Inhibition ebenso wie *XMyT1* und *Xath3* oder andere proneurale Gene für die endgültige neuronale Zelldetermination (Bellefroid et al., 1996; Takabayashi et al., 1997; Dubois et al., 1998; Perron et al., 1999). Dieser Mechanismus determiniert die korrekte Zahl der primären Neurone. Deshalb wird *XETOR* aktiviert durch proneurale Gene und zeigt die volle Funktion zu der Zeit, wenn

die Neuronendifferenzierung beginnt. Durch Repression der Expression und Funktion der spät exprimierten proneuralen Gene, begrenzt *XETOR* deshalb die Domäne der primären Neurogenese in einem sehr limitierten Bereich. Zusammenfassend kann gesagt werden, dass die laterale Inhibition und XETOR einen dualen Inhibitionsmechanismus darstellen, um die genaue Zahl und Lokalisation der Neuronen während der primären Neurogenese zu gewährleisten.

8. REFERENCES

Almrud, J.J., Oliveira, M.A., Kern, A.D., Grishin, N.V., Phillips, M.A., Hackert, M.L. (2000). Crystal structure of human ornithine decarboxylase at 2.1Å resolution: structural insights to antizyme binding. *J. Mol. Biol.* **295**, 7-16.

Artavanis-Tsakonas, S., Matsuno, K., Fortini, M.E. (1995). Notch signaling. *Science* **268**, 225-232.

Arthur, J.S., Gauthier, S., Elce, J.S. (1995). Active site residues in m-Calpain: identification by site-directed mutagenesis. *FEBS Lett.* **368**, 397-400.

Bassez, T., Paris, J., Omilli, F., Dorel, C., Osborne, H.B. (1990). Post-transcriptional regulation of ornithine decarboxylase in *Xenopus laevis* oocytes. *Development* **110**, 955-962.

Beatus, P., Lendahl, U. (1998). Notch and neurogenesis. *J. Neurosci. Res.* **54**, 125-136.

Bellefroid, E.J., Bourguignon, C., Hollemann, T., Ma, Q., Anderson, D.J., Kintner, C., Pieler, T. (1996). X-MyT1, a *Xenopus* C2HC-type zinc finger protein with a regulatory function in neuronal differentiation. *Cell* **87**, 1191-1202.

Bouwmeester, T. (2001). The Spemann-Mangold organizer: the control of fate specification and morphogenetic rearrangements during gastrulation in *Xenopus*. *Int. J. Dev. Biol.* **45**, 251-258.

Bouwmeester, T., Kim, S., Sasai, Y., Lu, B., De Robertis, E.M. (1996). Cerberus is a head-inducing secreted factor expressed in the anterior endoderm of Spemann's organizer. *Nature* **382**, 595-601.

Cao, Y., Zhao, H., Hollemann, T., Chen, Y., Grunz, H. (2001). Tissue-specific expression of an ornithine decarboxylase paralogue, XODC2, in *Xenopus laevis*. *Mech. Dev.* **102**, 243-246.

Chalmers, A.D., Slack, J.M. (2000). The *Xenopus* tadpole gut: fate maps and

morphogenetic movements. *Development* **127**, 381-392.

Chan, A.P., Etkin, L.D. (2001). Patterning and lineage specification in the amphibian embryo. *Curr. Top. Dev. Biol.* **51**, 1-67.

Chen, Y., Hollemann, T., Grunz, H., Pieler, T. (1999). Characterization of the Ets-type protein ER81 in *Xenopus* embryos. *Mech. Dev.* **80**, 67-76.

Chitnis, A., Henrique, D., Lewis, J., Ish-Horowicz, D., Kintner, C. (1995). Primary neurogenesis in *Xenopus* embryos regulated by a homologue of the Drosophila neurogenic gene Delta. *Nature* **375**, 761-766.

Chitnis, A., Kintner, C. (1996). Sensitivity of proneural genes to lateral inhibition affects the pattern of primary neurons in *Xenopus* embryos. *Development* **122**, 2295-2301.

Chitnis, A.B. (1999). Control of neurogenesis--lessons from frogs, fish and flies. *Curr. Opin. Neurobiol.* **9**, 18-25.

Clements, D., Friday, R.V., Woodland, H.R. (1999). Mode of action of VegT in mesoderm and endoderm formation. *Development* **126**, 4903-4911.

Clements, D., Woodland, H.R. (2000). Changes in embryonic cell fate produced by expression of an endodermal transcription factor, Xsox17. *Mech. Dev.* **99**, 65-70.

Dale, L., Jones, C.M. (1999). BMP signalling in early *Xenopus* development. *Bioessays* **21**, 751-760.

Dale, L., Matthews, G., Colman, A. (1993). Secretion and mesoderm-inducing activity of the TGF-beta-related domain of *Xenopus* Vg1. *EMBO J.* **12**, 4471-4480.

De Robertis, E.M., Larrain, J., Oelgeschlager, M., Wessely, O. (2000). The establishment of Spemann's organizer and patterning of the vertebrate embryo. *Nat. Rev. Genet.* **1**,171-181.

De Robertis, E.M., Wessely, O., Oelgeschlager, M., Brizuela, B., Pera, E., Larrain, J., Abreu, J., Bachiller, D. (2001). Molecular mechanisms of cell-cell signaling by the Spemann-Mangold organizer. *Int. J. Dev. Biol.* **45**, 189-197.

Deardorff, M.A., Tan, C., Conrad, L.J., Klein, P.S. (1998). Frizzled-8 is expressed in the Spemann organizer and plays a role in early morphogenesis. *Development* **125**, 2687-2700.

Deardorff, M.A., Tan, C., Saint-Jeannet, J.P., Peter S. Klein, P.S. (2001). A role for frizzled 3 in neural crest development. *Development* **128**, 3655-3663.

DeMarais, A.A., Moon, R.T. (1992). The armadillo homologs beta-catenin and plakoglobin are differentially expressed during early development of *Xenopus laevis*. *Dev. Biol.* **153**, 337-346.

Dibner, C., Elias, S., Frank, D. (2001). XMeis3 protein activity is required for proper hindbrain patterning in *Xenopus laevis* embryos. *Development* **128**, 3415-3426.

Djiane, A., Riou, J., Umbhauer, M., Boucaut, J., Shi, D. (2000). Role of frizzled 7 in the regulation of convergent extension movements during gastrulation in *Xenopus laevis*. *Development* **127**, 3091-3100.

Dubois, L., Bally-Cuif, L., Crozatier, M., Moreau, J., Paquereau, L., Vincent, A. (1998). XCoe2, a transcription factor of the Col/Olf-1/EBF family involved in the specification of primary neurons in *Xenopus*. *Curr. Biol.* **8**, 199-209.

Engleka, M.J., Craig, E.J., Kessler, D.S. (2001). VegT activation of Sox17 at the midblastula transition alters the response to nodal signals in the vegetal endoderm domain. *Dev. Biol.* **237**, 159-172.

Erickson, P.F., Robinson, M., Owens, G., Drabkin, H.A. (1994). The ETO portion of acute myeloid leukemia t(8;21) fusion transcript encodes a highly evolutionarily conserved, putative transcription factor. *Cancer Res.* **54**, 1782-1786.

Fagotto, F., Gumbiner, B.M. (1994). Beta-catenin localization during *Xenopus* embryogenesis: accumulation at tissue and somite boundaries. *Development* **120**, 3667-3679.

Fainsod, A., Deissler, K., Yelin, R., Marom, K., Epstein, M., Pillemer, G., Steinbeisser, H., Blum, M. (1997). The dorsalizing and neural inducing gene follistatin is an antagonist of BMP-4. *Mech. Dev.* **63**, 39-50.

Feinstein, P.G., Kornfeld, K., Hogness, D.S., Mann, R.S. (1995). Identification of homeotic target genes in *Drosophila melanogaster* including nervy, a proto-oncogene homologue. *Genetics* **140**, 573-586.

Ferreiro, B., Kintner, C., Zimmerman, K., Anderson, D., Harris, W.A. (1994). XASH genes promote neurogenesis in *Xenopus* embryos. *Development* **120**, 3649-3655.

Frohman, M.A., Dush, M.K., Martin, G.R. (1988). Rapid production of full-length cDNAs from rare transcripts: amplification using a single gene-specific oligonucleotide primer. *Proc. Natl. Acad .Sci. USA* **85**, 8998-9002.

Gelmetti, V., Zhang, J., Fanelli, M., Minucci, S., Pelicci, P.G., Lazar, M.A. (1998). Aberrant recruitment of the nuclear receptor corepressor-histone deacetylase complex by the acute myeloid leukemia fusion partner ETO. *Mol. Cell Biol.* **18**, 7185-7191.

Glinka, A., Wu, W., Delius, H., Monaghan, A.P., Blumenstock, C., Niehrs, C. (1998). Dickkopf-1 is a member of a new family of secreted proteins and functions in head induction. *Nature* **391**, 357-362.

Glinka, A., Wu, W., Onichtchouk, D., Blumenstock, C., Niehrs, C. (1997). Head induction by simultaneous repression of Bmp and Wnt signalling in *Xenopus*. *Nature* **389**, 517-519.

Grunstein, M. (1997). Histone acetylation in chromatin structure and transcription. *Nature* **389**, 349-352.

Grunz, H. (1969). Hemmung der Reaggregation dissoziierter Amphibienzellen durch Inhibitoren der RNS- und Proteinsynthese. *Roux' Arch. Dev.Biol.* **163**, 184-196.

Grunz, H. (1973). The ultrastructure of amphibian ectoderm treated with an inductor or actinomycin D. *Wilhelm Roux' Arch.* **173**, 283-293.

Grunz, H. (1983). Change in the differentiation pattern of *Xenopus laevis* ectoderm by variation of the incubation time and concentration of vegetalizing factor. *Wilhelm Roux' Arch.* **192**, 130-137.

Grunz, H., Tacke, L. (1989). Neural differentiation of *Xenopus laevis* ectoderm takes place after disaggregation and delayed reaggregation without inducer. *Cell Differ. Dev.* **28**, 211-217.

Grunz, H., Tacke, L. (1990). Extracellular matrix components prevent neural differentiation of disaggregated *Xenopus* ectoderm cells. *Cell Differ. Dev.* **32**, 117-123.

Guger, K.A., Gumbiner, B.M. (1995). beta-Catenin has Wnt-like activity and mimics the Nieuwkoop signaling center in *Xenopus* dorsal-ventral patterning. *Dev. Biol.* **172**, 115-125.

Hansen, C.S., Marion, C.D., Steele, K., George, S., Smith, W.C. (1997). Direct neural induction and selective inhibition of mesoderm and epidermis inducers by Xnr3. *Development* **124**, 483-492.

Harland, R., Gerhart. J. (1997). Formation and function of Spemann's organizer. *Annu. Rev. Cell Dev. Biol.* **13**, 611-667.

Harland, R.M. (1991). *In situ* hybridization: an improved whole-mount method

for *Xenopus* embryos. *Methods Cell Biol.* **36**, 685-695.

Heasman, J., Crawford, A., Goldstone, K., Garner-Hamrick, P., Gumbiner, B., McCrea, P., Kintner, C., Noro, C.Y., Wylie, C. (1994). Overexpression of cadherins and underexpression of beta-catenin inhibit dorsal mesoderm induction in early *Xenopus* embryos. *Cell* **79**, 791-803.

Heasman, J., Kofron, M., Wylie, C. (2000). β-Catenin signaling activity dissected in the early *Xenopus* embryo: a novel antisense approach. *Dev. Biol.* **222**, 124-134.

Hemmati-Brivanlou, A., Melton, D. (1997). Vertebrate embryonic cells will become nerve cells unless told otherwise. *Cell* **88**, 13-17.

Henry, G.L., Melton, D.A. (1998). Mixer, a homeobox gene required for endoderm development. *Science* **281**, 91-96.

Hildebrand, D., Tiefenbach, J., Heinzel, T., Grez, M., Maurer, A.B. (2001). Multiple regions of ETO cooperate in transcriptional repression. *J. Biol. Chem.* **276**, 9889-9895.

Hollemann, T., Chen, Y., Grunz, H., Pieler, T. (1998). Regionalized metabolic activity establishes boundaries of retinoic acid signalling. *EMBO J.* **17**, 7361-7372.

Hongo, I., Kengaku, M., Okamoto, H. (1999). FGF signaling and the anterior neural induction in *Xenopus*. *Dev. Biol.* **216**, 561-581.

Horb, M.E., Thomsen, G.H. (1997). A vegetally localized T-box transcription factor in *Xenopus* eggs specifies mesoderm and endoderm and is essential for embryonic mesoderm formation. *Development* **124**, 1689-1698.

Huang, J., Forsberg, N.E. (1998). Role of Calpain in skeletal-muscle protein degradation. *Proc. Natl. Acad. Sci. USA* **95**, 12100-12105.

Hudson, C., Clements, D., Friday, R.V., Stott, D., Woodland, H.R. (1997). Xsox17alpha and -beta mediate endoderm formation in *Xenopus*. *Cell* **91**, 397-405.

Huston, R.B., Krebs, E.G. (1968). Activation of skeletal muscle phosphorylase kinase by Ca^{2+}. *Biochemistry* **7**, 2116-2122.

Iemura, S., Yamamoto, T.S., Takagi, C., Uchiyama, H., Natsume, T., Shimasaki, S., Sugino, H., Ueno, N. (1998). Direct binding of follistatin to a complex of bone-morphogenetic protein and its receptor inhibits ventral and epidermal cell fates in early *Xenopus* embryo. *Proc. Natl. Acad. Sci. USA* **95**, 9337-9342.

Jacobs, K.A., Collins-Racie, L.A., Colbert, M., Duckett, M., Golden-Fleet, M., Kelleher, K., Kriz, R., LaVallie, E.R., Merberg, D., Spaulding, V., Stover, J., Williamson, M.J., McCoy, J.M. (1997). A genetic selection for isolating cDNAs encoding secreted proteins. *Gene* **198**, 289-296.

Jowett, T. (2001). Double *in situ* hybridization techniques in zebrafish. *Methods* **23**, 345-358.

Joseph, E.M., Melton, D.A. (1998). Mutant Vg1 ligands disrupt endoderm and mesoderm formation in *Xenopus* embryos. *Development* **125**, 2677-2685.

Keller, R., Shih, J., Domingo, C. (1992). The patterning and functioning of protrusive activity during convergence and extension of the *Xenopus* organiser. *Dev. Suppl.* 81-91.

Keller, R., Shih, J., Wilson, P.A., Sater, A.K. (1991). Patterns of cell mobility, cell interactions, and mechanism during convergent extension in *Xenopus*. In *Cell-Cell Interactions in Early Development. Society for Developmental Biology, 49th Symposium* (Ed. G. C. Gerhard), pp31-62. Wiley-Liss, New York.

Keller, R., Tibbetts, P. (1989). Mediolateral cell intercalation in the dorsal, axial mesoderm of *Xenopus laevis*. *Dev. Biol.* **131**, 539-549.

Keller, R.E. (1986). The cellular basis of amphibian gastrulation. In *Developmental Biology, The Cellular Basis of Morphogenesis*, Vol.2 (Ed. C.W. Browder), pp 241-327. Plenum Press, New York.

Kelly, G.M., Erezyilmaz, D.F., Moon, R.T. (1995). Induction of a secondary embryonic axis in zebrafish occurs following the overexpression of beta-catenin. *Mech. Dev.* **53**, 261-273.

Kessler, D.S., Melton, D.A. (1995). Induction of dorsal mesoderm by soluble, mature Vg1 protein. *Development* **121**, 2155-2164.

Kimelman, D., Christian, J.L., Moon, R.T. (1992). Synergistic principles of development: overlapping patterning systems in *Xenopus* mesoderm induction. *Development* **116**, 1-9.

Kimelman, D., Griffin, K.J. (1998). Mesoderm induction: a postmodern view. *Cell* **94**, 419-421.

Kitabayashi, I., Ida, K., Morohoshi, F., Yokoyama, A., Mitsuhashi, N., Shimizu, K., Nomura, N., Hayashi, Y., Ohki, M. (1998). The AML1-MTG8 leukemic fusion protein forms a complex with a novel member of the MTG8 (ETO/CDR) family, MTGR1. *Mol. Cell Biol.* **18**, 846-858.

Klein, R.D., Gu, Q., Goddard, A., Rosenthal, A. (1996). Selection for genes encoding secreted proteins and receptors. *Proc. Natl. Acad. Sci. USA* **93**, 7108-7113.

Kofron, M., Demel, T., Xanthos, J., Lohr, J., Sun, B., Sive, H., Osada, S., Wright, C., Wylie, C., Heasman, J. (1999). Mesoderm induction in *Xenopus* is a zygotic event regulated by maternal VegT via TGFbeta growth factors. *Development* **126**, 5759-5770.

Kopan, R., Turner, D.L. (1996). The Notch pathway: democracy and aristocracy in the selection of cell fate. *Curr. Opin. Neurobiol.* **6**, 594-601.

Koyano-Nakagawa, N., Kim, J., Anderson, D., Kintner, C. (2000). Hes6 acts in a positive feedback loop with the neurogenins to promote neuronal differentiation. *Development* **127**, 4203-4216.

Kroll, K.L., Salic, A.N., Evans, L.M., Kirschner, M.W. (1998). Geminin, a neuralizing molecule that demarcates the future neural plate at the onset of gastrulation. *Development* **125**, 3247-3258.

Kunisch, M., Haenlin, M., Campos-Ortega, J.A. (1994). Lateral inhibition mediated by the *Drosophila* neurogenic gene delta is enhanced by proneural proteins. *Proc. Natl. Acad. Sci. USA* **91**, 10139-10143.

Lahaye, K., Kricha, S., Bellefroid, E.J. (2002). XNAP, a conserved ankyrin repeat-containing protein with a role in the Notch pathway during *Xenopus* primary neurogenesis. *Mech. Dev.* **110**, 113-124.

Larabell, C.A., Torres, M., Rowning, B.A., Yost, C., Miller, J.R., Wu, M., Kimelman, D., Moon, R.T. (1997). Establishment of the dorso-ventral axis in *Xenopus* embryos is presaged by early asymmetries in beta-catenin that are modulated by the Wnt signaling pathway. *J. Cell Biol.* **136**, 1123-1136.

Lee, C.H., Gumbiner, B.M. (1995). Disruption of gastrulation movements in *Xenopus* by a dominant-negative mutant for C-cadherin. *Dev. Biol.* **171**, 363-373.

Lee, J.E. (1997). Basic helix-loop-helix genes in neural development. *Curr. Opin. Neurobiol.* **7**, 13-20.

Lee, J.E., Hollenberg, S.M., Snider, L., Turner, D.L., Lipnick, N., Weintraub, H. (1995). Conversion of *Xenopus* ectoderm into neurons by NeuroD, a basic helix-loop-helix protein. *Science* **268**, 836-844.

Lemaire, P., Darras, S., Caillol, D., Kodjabachian, L. (1998). A role for the vegetally expressed *Xenopus* gene Mix.1 in endoderm formation and in the

restriction of mesoderm to the marginal zone. *Development* **125**, 2371-2380.

Lewis, J. (1996). Neurogenic genes and vertebrate neurogenesis. *Curr. Opin. Neurobiol.* **6**, 3-10.

Lustig, K.D., Kroll, K.L., Sun, E.E., Kirschner, M.W. (1996). Expression cloning of a *Xenopus* T-related gene (Xombi) involved in mesodermal patterning and blastopore lip formation. *Development* **122**, 4001-4012.

Lutterbach, B., Westendorf, J.J., Linggi, B., Patten, A., Moniwa, M., Davie, J.R., Huynh, K.D., Bardwell, V.J., Lavinsky, R.M., Rosenfeld, M.G., Glass, C., Seto, E., Hiebert, S.W. (1998). ETO, a target of t(8;21) in acute leukemia, interacts with the N-CoR and mSin3 corepressors. *Mol. Cell Biol.* **18**, 7176-7184.

Ma, Q., Kintner, C., Anderson, D.J. (1996). Identification of neurogenin, a vertebrate neuronal determination gene. *Cell* **87**, 43-52.

Masumoto, H., Yoshizawa, T., Sorimachi, H., Nishino, T., Ishiura, S., Suzuki, K. (1998). Overexpression, purification, and characterization of human m-Calpain and its active site mutant, m-C105S-Calpain, using a baculovirus expression system. *J. Biochem.* (Tokyo) **124**, 957-961.

Matsui, M., Mizuseki, K., Nakatani, J., Nakanishi, S., Sasai, Y. (2000). *Xenopus* kielin: A dorsalizing factor containing multiple chordin-type repeats secreted from the embryonic midline. *Proc. Natl. Acad. Sci. USA* **97**, 5291-5296.

Mead, P.E., Zhou, Y., Lustig, K.D., Huber, T.L., Kirschner, M.W., Zon, L.I. (1998). Cloning of Mix-related homeodomain proteins using fast retrieval of gel shift activities, (FROGS), a technique for the isolation of DNA-binding proteins. *Proc. Natl. Acad. Sci. USA* **95**, 11251-11256.

Melnick, A.M., Westendorf, J.J., Polinger, A., Carlile, G.W., Arai, S., Ball, H.J., Lutterbach, B., Hiebert, S.W., Licht, J.D. (2000). The ETO protein disrupted in t(8;21)-associated acute myeloid leukemia is a corepressor for the promyelocytic leukemia zinc finger protein. *Mol. Cell Biol.* **20**, 2075-2086.

Meno, C., Saijoh, Y., Fujii, H., Ikeda, M., Yokoyama, T., Yokoyama, M., Toyoda, Y., Hamada, H. (1996). Left-right asymmetric expression of the TGF beta-family member lefty in mouse embryos. *Nature* **381**, 151-155.

Minuth, M., Grunz, H. (1980). The formation of mesodermal derivates after induction with vegetalizing factor depends on secondary cell interactions. *Cell Differentiation* **9**, 229-238.

Mizuseki, K., Kishi, M., Matsui, M., Nakanishi, S., Sasai, Y. (1998a). *Xenopus* Zic-related-1 and Sox-2, two factors induced by chordin, have distinct activities in the initiation of neural induction. *Development* **125**, 579-587.

Mizuseki, K., Kishi, M., Shiota, K., Nakanish, S., Sasai, Y. (1998b). SoxD: an essential mediator of induction of anterior neural tissues in *Xenopus* embryos. *Neuron* **21**, 77-85.

Moon, R.T., Campbell, R.M., Christian, J.L., McGrew, L.L., Shih, J., Fraser, S. (1993). Xwnt-5A: a maternal Wnt that affects morphogenetic movements after overexpression in embryos of *Xenopus laevis*. *Development* **119**, 97-111.

Moon, R.T., Kimelman, D. (1998). From cortical rotation to organizer gene expression: toward a molecular explanation of axis specification in *Xenopus*. *Bioessays* **20**, 536-545.

Nakata, K., Nagai, T., Aruga, J., Mikoshiba, K. (1997). *Xenopus* Zic3, a primary regulator both in neural and neural crest development. *Proc. Natl. Acad. Sci. USA* **94**, 11980-11985.

Nieto, M.A. (1999). Reorganizing the organizer 75 years on. *Cell* **98**, 417-425.

Nieuwkoop, P.D. (1952). Activation and organization of the central nervous system in amphibians. III. Synthesis of a new working hypothesis. *J. Exp. Zool.* **120**: 83-108

Nieuwkoop, P.D., Faber, J. (1967). *Normal Table of Xenopus laevis (Daudin*). North Holland Publishing, Amsterdam.

Nieuwkoop, P.D. (1973). The organization center of the amphibian embryos: its origin, spatial organization, and morphogenetic action. *Adv. Morphog.* **10**, 1-39.

Oschwald, R., Richter, K., Grunz, H. (1991). Localization of a nervous system-specific class II beta-tubulin gene in *Xenopus laevis* embryos by whole mount *in situ* hybridization. *Int. J. Dev. Biol.* **35**, 399-405.

Penzel, R., Oschwald, R., Chen, Y., Tacke, L., Grunz, H. (1997). Characterization and early embryonic expression of a neural specific transcription factor *xSOX3* in *Xenopus laevis*. *Int. J. Dev. Biol.* **41**, 667-677.

Pera, E.M., De Robertis, E.M. (2000). A direct screen for secreted proteins in *Xenopus* embryos identifies distinct activities for the Wnt antagonists Crescent and Frzb-1. *Mech. Dev.* **96**, 183-195.

Perron, M., Opdecamp, K., Butler, K., Harris, W.A., Bellefroid, E.J. (1999). X-ngnr-1 and Xath3 promote ectopic expression of sensory neuron markers in the neurula ectoderm and have distinct inducing properties in the retina. *Proc. Natl. Acad. Sci. USA*. **96**, 14996-15001.

Piccolo, S., Agius, E., Leyns, L., Bhattacharyya, S., Grunz, H., Bouwmeester, T., De Robertis, E.M. (1999). The head inducer Cerberus is a multifunctional antagonist of Nodal, BMP and Wnt signals. *Nature* **397**, 707-710.

Piccolo, S., Sasai, Y., Lu, B., De Robertis, E.M. (1996). Dorsoventral patterning in *Xenopus*: inhibition of ventral signals by direct binding of chordin to BMP-4. *Cell* **86**, 589-598.

Pozzoli, O., Bosetti, A., Croci, L., Consalez, G.G., Vetter, M.L. (2001). Xebf3 is a regulator of neuronal differentiation during primary neurogenesis in *Xenopus*. *Dev. Biol.* **233**, 495-512.

Rosa, F.M. (1989). Mix.1, a homeobox mRNA inducible by mesoderm inducers, is expressed mostly in the presumptive endodermal cells of *Xenopus* embryos. *Cell* **57**, 965-974.

Sambrook, J., Fritsch, E.F., Maniatis, T. (1989). Molecular Cloning: a laboratory mannual (2nd ed.). Cold Spring Harbor Laboratory Press, NewYork.

Sasai, Y., Lu, B., Piccolo, S., De Robertis, E.M. (1996). Endoderm induction by the organizer-secreted factors chordin and noggin in *Xenopus* animal caps. *EMBO J.* **15**, 4547-4555.

Saxen, L. (1989). Neural induction. *Int. J. Dev. Biol.* **33**, 21-48.

Schneider, S., Steinbeisser, H., Warga, R.M., Hausen, P. (1996). Beta-catenin translocation into nuclei demarcates the dorsalizing centers in frog and fish embryos. *Mech. Dev.* **57**, 191-198.

Sorimachi, H., Ishiura, S., Suzuki, K. (1993). A novel tissue-specific Calpain species expressed predominantly in the stomach comprises two alternative splicing products with and without Ca(2+)-binding domain. *J. Biol. Chem.* **268**, 19476-19482.

Sorimachi, H., Ishiura, S., Suzuki, K. (1997). Structure and physiological function of Calpains. *Biochem. J.* **328**, 721-732.

Sorimachi, H., Saido, T.C., Suzuki, K. (1994). New era of Calpain research. Discovery of tissue-specific Calpains. *FEBS Lett.* **343**, 1-5.

Stennard, F., Zorn, A.M., Ryan, K., Garrett, N., Gurdon, J.B. (1999). Differential expression of VegT and Antipodean protein isoforms in *Xenopus*. *Mech. Dev*. **86**, 87-98.

Streit, A., Stern, C.D. (1999). Neural induction. A bird's eye view. *Trends Genet*. **15**, 20-24.

Struhl, K. (1998). Histone acetylation and transcriptional regulatory mechanisms. *Genes Dev*. **12**, 599-606.

Sun, B.I., Bush, S.M., Collins-Racie, L.A., LaVallie, E.R., DiBlasio-Smith, E.A., Wolfman, N.M., McCoy, J.M., Sive, H.L. (1999). derriere: a TGF-beta family member required for posterior development in *Xenopus*. *Development* **126**, 1467-1482.

Suzuki, K., Sorimachi, H. (1998). A novel aspect of Calpain activation. *FEBS Lett*. **433**, 1-4.

Tada, M., Smith, J.C. (2000). Xwnt11 is a target of *Xenopus* Brachyury: regulation of gastrulation movements via Dishevelled, but not through the canonical Wnt pathway. *Development* **127**, 2227-2238.

Takai, Y., Kishimot, A., Inoue, M., Nishizuka, Y. (1977). Studies on a cyclic nucleotide-independent protein kinase and its proenzyme in mammalian tissues. I. *J. Biol. Chem*. **252**, 7603-7609.

Takebayashi, K., Takahashi, S., Yokota, C., Tsuda, H., Nakanishi, S., Asashima, M., Kageyama, R. (1997). Conversion of ectoderm into a neural fate by ATH-3, a vertebrate basic helix-loop-helix gene homologous to Drosophila proneural gene atonal. *EMBO J*. **16**, 384-395.

Tan, C, Deardorff, M.A., Saint-Jeannet, J.P., Jing Yang, J., Arzoumanian, A., Klein, P.S. (2001). Kermit, a frizzled interacting protein, regulates frizzled 3 signaling in neural crest development. *Development* **128**, 3665-3674.

Thisse, C., Thisse, B. (1999). Antivin, a novel and divergent member of the TGFbeta superfamily, negatively regulates mesoderm induction. *Development* **126**, 229-240.

Thomsen, G.H., Melton, D.A. (1993). Processed Vg1 protein is an axial mesoderm inducer in *Xenopus*. *Cell* **74**, 433-441.

Torchia, J., Glass, C., Rosenfeld, M.G. (1998). Co-activators and co-repressors in the integration of transcriptional responses. *Curr. Opin. Cell Biol*. **10**, 373-383.

Tracey, W.D. Jr., Pepling, M.E., Horb, M.E., Thomsen, G.H., Gergen, J.P. (1998). A *Xenopus* homologue of aml-1 reveals unexpected patterning mechanisms leading to the formation of embryonic blood. *Development* **125**, 1371-1380.

Tsuda, H., Sasai, N., Matsuo-Takasaki, M., Sakuragi, M., Murakami, Y., Sasai, Y. (2002). Dorsalization of the neural tube by *Xenopus* tiarin, a novel patterning factor secreted by the flanking nonneural head ectoderm. *Neuron* **33**, 515-528.

Vincent, J.P., Gerhart, J.C. (1987). Subcortical rotation in *Xenopus* eggs: an early step in embryonic axis specification. *Dev. Biol.* **123**, 526-539.

Wallingford, J.B., Harland, R.M. (2001). *Xenopus* Dishevelled signaling regulates both neural and mesodermal convergent extension: parallel forces elongating the body axis. *Development* **128**, 2581-2592.

Wang, J., Hoshino, T., Redner, R.L., Kajigaya, S., Liu, J.M. (1998). ETO, fusion partner in t(8;21) acute myeloid leukemia, represses transcription by interaction with the human N-CoR/mSin3/HDAC1 complex. *Proc. Natl. Acad. Sci. USA* **95**, 10860-10865.

Wang, S., Krinks, M., Lin, K., Luyten, F.P., Moos, M. Jr. (1997). Frzb, a secreted protein expressed in the Spemann organizer, binds and inhibits Wnt-8. *Cell* **88**, 757-766.

Wells, J.M., Melton, D.A. (1999). Vertebrate endoderm development. *Annu. Rev. Cell Dev. Biol.* **15**, 393-410.

Wessely, O., De Robertis, E.M. (2002). Neural plate patterning by secreted signals. *Neuron* **33**, 489-491.

Wettstein, D.A., Turner, D.L., Kintner, C. (1997). The *Xenopus* homolog of Drosophila Suppressor of Hairless mediates Notch signaling during primary neurogenesis. *Development* **124**, 693-702.

Wilson, P.A., Hemmati-Brivanlou, A. (1995). Induction of epidermis and inhibition of neural fate by Bmp-4. *Nature* **376**, 331-333.

Wolford, J.K., Prochazka, M. (1998). Structure and expression of the human MTG8/ETO gene. *Gene* **212**, 103-109.

Wolpert, L., Beddington, R., Brockers, J., Jessell, T., Lawrence, P., Meyerowitz, E. (eds.) (1998). Principles of development. Oxford University Press.

Xanthos, J.B., Kofron, M., Wylie, C., Heasman, J. (2001). Maternal VegT is

the initiator of a molecular network specifying endoderm in *Xenopus laevis*. *Development* **128**, 167-180.

Yasuo, H., Lemaire, P. (1999). A two-step model for the fate determination of presumptive endodermal blastomeres in *Xenopus* embryos. *Curr. Biol.* **9**, 869-879.

Yasuo, H., Lemaire, P. (2001). Generation of the germ layers along the animal-vegetal axis in *Xenopus laevis*. *Int. J. Dev. Biol.* **45**, 229-235.

Yost, C., Torres, M., Miller, J.R., Huang, E., Kimelman, D., Moon, R.T. (1996). The axis-inducing activity, stability, and subcellular distribution of beta-catenin is regulated in *Xenopus* embryos by glycogen synthase kinase 3. *Genes Dev.* **10**, 1443-1454.

Zhang, J., Houston, D.W., King, M.L., Payne, C., Wylie, C., Heasman, J. (1998). The role of maternal VegT in establishing the primary germ layers in *Xenopus* embryos. *Cell* **94**, 515-524.

Zhang, J., Hug, B.A., Huang, E.Y., Chen, C.W., Gelmetti, V., Maccarana, M., Minucci, S., Pelicci, P.G., Lazar, M.A. (2001). Oligomerization of ETO is obligatory for corepressor interaction. *Mol. Cell Biol.* **21**, 156-163.

Zhang, J., King, M.L. (1996). *Xenopus* VegT RNA is localized to the vegetal cortex during oogenesis and encodes a novel T-box transcription factor involved in mesodermal patterning. *Development* **122**, 4119-4129.

Zhao, H., Cao, Y., Grunz, H. (2001). Isolation and characterization of a *Xenopus* gene (XMLP) encoding a MARCKS-like protein. *Int. J. Dev. Biol.* **45**, 817-826.

Zimmerman, K., Shih, J., Bars, J., Collazo, A., Anderson, D.J. (1993). XASH-3, a novel *Xenopus* achaete-scute homolog, provides an early marker of planar neural induction and position along the mediolateral axis of the neural plate. *Development* **119**, 221-232.

Zimmerman, L.B., De Jesus-Escobar, J.M., Harland, R.M. (1996). The Spemann organizer signal noggin binds and inactivates bone morphogenetic protein 4. *Cell* **86**, 599-606.

CURRICULUM VITAE (Lebenslauf)

Name:	CAO, Ying
Birthdate/place:	April 19, 1967/Jiangsu, China
Marital status:	married with MA, Haihua
Child:	CAO, Zirui
Parents:	LI, Quanying
	CAO, Shuchao

Education and research experiences

9/1974-7/1979, Shanhou Primary School, Pizhou, China;

9/1979-7/1981, Keyong Primary School, Pizhou, China;

9/1981-7/1985, Bayiji High School, Pizhou, China;

9/1985-7/1989, B.Sc. in marine fishery resources and management, Fishery School, Ocean University of Qingdao, China;

7/1989-9/1991, technician in Huangdao Marineculture Company, Qingdao, China;

8/1992-8/1993, research assistant in fish molecular biology, State Key Laboratory of Freshwater Fish Germplasm Resources and Biotechnology, China;

9/1991-7/1994, M.Sc. in fish genetics, Fishery School, Huazhong (Central China) Agricultural University, Wuhan, China;

8/1994-10/1998, assistant professor in fish molecular biology, Laboratory of Biotechnology, Freshwater Fishery Research Center of Chinese Academy of Fishery Science, China;

10/1998-present, PhD student in developmental biology of Xenopus laevis, Department of Zoophysiology, University of Essen, Germany.

Publications

Cao, Y., Zhao, H., Grunz, H. (2001). XCL-2 is a novel m-type Calpain and disrupts morphogenetic movements during embryogenesis in *Xenopus laevis*. *Dev. Growth Differ*. **43**, 563-571.

Cao, Y., Zhao, H., Hollemann, T., Chen, Y., Grunz, H. (2001). Tissue-specific expression of an Ornithine decarboxylase paralogue, XODC2, in *Xenopus laevis*. *Mech. Dev*. **102**, 243-246.

Zhao, H., **Cao, Y.**, Grunz, H. (2001). Expression of *Xenopus* L-arginine:glycine amidinotransferase (XAT) during early embryonic development. *Dev. Genes Evol*. **211**, 358-360.

Zhao, H., **Cao, Y.**, Grunz, H. (2001). Isolation and characterization of a *Xenopus* gene (XMLP) encoding a MARCKS-like protein. *Int. J. Dev. Biol*. **45**, 817-826.

ACKNOWLEDGEMENT

The completion of this study would have been not possible if not dependent on the steadfast support and encouragement of my wife and daughter. They hence paid equal contribution to the study for which I always feel profound gratitude in my heart.

I would like to express here the very thanks to my dissertation advisor, Prof. Dr. Horst Grunz, University of Essen, who provided me the opportunity to do such a research in his laboratory, ushered me in to the discipline of developmental biology, and instructed me the delicate embryological methodologies.

I also owe my special thanks

to Dr. Yonglong Chen, now a postdoc in Goettingen, for sharing his experimental experiences at the beginning of the research;

to my colleague Hui Zhao for his kind cooperation during the research;

to Sabine Effenberger for her dexterous preparation of histological sections and many other helps;

to Annette Klippstein for her effort in typing the manuscript of the dissertation and also many other helps during the research; and

to Drs. Yonglong Chen (Goettingen, Germany), Eddy M. DeRobertis (Los Angeles, USA), H. Beverley Osborne (Rennes, France), Tewis Bouwmeester (Heidelberg, Germany), Christof Niehrs (Heidelberg, Germany), Ralph Rupp (Munich, Germany), Chris Kintner (San Diego, USA), David J. Anderson (Pasadena, USA), Eric Bellefroid (Brussels, Belgium), Jacquiline Lee (New York, USA), J. Peter Gergen (Stony Brook, USA), Nancy Papalopulu (Cambridge, UK), Gerhard Schlosser (Bremen, Germany), and Kathy Zimmermann (New York, USA), for their generous gifts of plasmids.

Erklärung:

Hiermit erkläre ich, gem. §6 Abs. 2, Nr. 7 der Promotionsordnung der Fachbereiche 6 bis 9 zur Erlangung des Dr. rer. nat., dass ich das Arbeitsgebiet, dem das Thema „Screening and characterization of novel genes involved in the embryogenesis of *Xenopus laevis*“ zuzuordnen ist, in Forschung und Lehre vertrete und den Antrag von Herrn Ying Cao befürworte.

Essen, den 15. 4. 2002

Professor Dr. Horst Grunz

Erklärung:

Hiermit erkläre ich, gem. §6 Abs. 2, Nr. 6 der Promotionsordnung der Fachbereiche 6 bis 9 zur Erlangung des Dr. rer. nat., dass ich die vorliegende Dissertation selbstständig verfaßt und mich keiner anderen als der angegebenen Hilfsmittel bedient habe.

Essen, den 15. 4. 2002

Ying Cao

Erklärung:

Hiermit erkläre ich, gem. §6 Abs. 2, Nr. 8 der Promotionsordnung der Fachbereiche 6 bis 9 zur Erlangung des Dr. rer. nat., dass ich keine anderen Promotionen bzw. Promotionsversuche in der Vergangenheit durchgeführt habe und dass diese Arbeit von keiner anderen Fakultät abgelehnt worden ist.

Essen, den 15. 4. 2002

Ying Cao